Synthesis of Sewage Sludge-based Biochar and Alum Sludge Composite Adsorbent for the Removal of Methylene Blue Dye from Industrial Wastewater

Tsedeniya Emishaw Estifanos

A Thesis Submitted to

The Department of Applied Chemistry

School of Applied Natural Science

Presented in Partial Fulfillment of the Requirement for the Degree of Master's in Applied Chemistry (Industrial Chemistry)

Office of Graduate Studies

Adama Science and Technology University

November, 2022

Adama, Ethiopia

Synthesis of Sewage Sludge-based Biochar and Alum Sludge Composite Adsorbent for the Removal of Methylene Blue Dye from Industrial Wastewater

Tsedeniya Emishaw Estifanos

Advisor: Eshetu Bekele (Ph.D.)

A Thesis Submitted to

The Department of Applied Chemistry

School of Applied Natural Science

Presented in Partial Fulfillment of the Requirement for the Degree of Master's in Applied Chemistry (Industrial Chemistry)

Office of Graduate Studies

Adama Science and Technology University

November, 2022

Adama, Ethiopia

DECLARATION

I hereby declare that this Master Thesis entitled "**Synthesis of Sewage Sludge-based Biochar and Alum Sludge Composite Adsorbent for the Removal of Methylene Blue Dye from Industrial Wastewater**" is my original work. That is, it has not been submitted for the award of any academic degree, diploma or certificate in any other university. All sources of materials that are used for this thesis have been duly acknowledged through citation.

_____	_____	_____
Name of the Student	Signature	Date

RECOMMENDATION

I, the advisor of this thesis, hereby certify that I have read the revised version of the thesis entitled "**Synthesis of Sewage Sludge-based Biochar and Alum Sludge Composite Adsorbent for the Removal of Methylene Blue Dye from Industrial Wastewater**" prepared under my guidance by Tsedeniya Emishaw Estifanos submitted in partial fulfillment of the requirements for the degree of Masters of Science in Applied Chemistry (Industrial Chemistry). Therefore, I recommend the submission of revised version of the thesis to the department following the applicable procedures.

Major Advisor	Signature	Date

APPROVAL SHEET

I, the advisor of the thesis entitled "**Synthesis of Sewage Sludge-based Biochar and Alum Sludge Composite Adsorbent for the Removal of Methylene Blue Dye from Industrial Wastewater**" and developed by Tsedeniya Emishaw Estifanos, hereby certify that the recommendation and suggestions made by the board of examiners are appropriately incorporated into the final version of the thesis.

Major Advisor	Signature	Date

We, the undersigned, members of the Board of Examiners of the thesis by Tsedeniya Emishaw Estifanos have read and evaluated the thesis entitled "**Synthesis of Sewage Sludge-based Biochar and Alum Sludge Composite Adsorbent for the Removal of Methylene Blue Dye from Industrial Wastewater**" and examined the candidate during open defense. This is, therefore, to certify that the thesis is accepted for partial fulfillment of the requirement of the degree of Master of Science in Applied Chemistry (Specialization in Industrial Chemistry).

Chairperson	Signature	Date
Internal Examiner	Signature	Date
External Examiner	Signature	Date

Final approval and acceptance of the thesis is contingent upon submission of its final copy to the Office of Postgraduate Studies (OPGS) through the Department Graduate Council (DGC) and School Graduate Committee (SGC).

Department Head	Signature	Date
School Dean	Signature	Date
Office of Postgraduate Studies, Dean	Signature	Date

DEDICATION

This M.Sc. thesis is dedicated to the glory of God, to my beloved families, especially to my Mother Asamenech Ashine, to my father Emishaw Estifanos and to my two brothers, whose advice, support, and prayers, helped me all along the right way. They will always be in my heart.

ACKNOWLEDMENT

At the very beginning, I would like to express my deepest gratitude to almighty God for giving me strength and the composure to finish my study on safe and sound mind. Words actually will never be enough to express how grateful I am, but nevertheless I will try my level best to express my gratefulness towards some people from the very deep of my heart.

Although this study work eventually represents my achievements, I have profited significantly from many people that I would like to recognize. First and foremost, I am thankful to my hard-working advisor: Dr. Eshetu Bekele, for his excellent supervision and scientific input in this research work. I am lucky to be guided by him, and it is an incredible benefit and honor for me to be advised by him. Then I would like to express my genuine appreciation to Adama Science and Technology University wastewater treatment plant and Adama drinking water treatment plant workers for giving me all the necessary help to conduct my research work. I never forgot their incredible contribution.

I greatly acknowledge Ato Tilahun Zeleke from (Sugar corporation research and development main center) for UV-Vis measurement, Ato Tsegaye Markos from Jimma University (JU), Department of Material Science and Engineering for FT-IR and XRD characterization, Ato Leta from Adama Science and Technology University (ASTU), Department of Applied Biology for SEM characterization, Ato Aseged Bekele from Addis Abeba Science and Technology University (AASTU), Department of Chemical Engineering for his assistance in BET characterization, and Ato Alebel Abebaw from Bahirdar University (BDU), Department of Chemistry for TGA-DTA characterization.

Last but not the least, I want to express my deep gratitude to my families, all well-wishers whose helps assist me to complete this thesis.

TABLE OF CONTENTS

LIST OF TABLES

TABLE PAGE

LIST OF FIGURES

FIGURE PAGE

LIST OF ABBREVATIONS AND ACRONYMS

AlS	Alum sludge
ASTU	Adama Science and Technology University
BC	Biochar
BET	Brunauer-Emmett-Teller
EDS	Energy Dispersive Spectroscopy
EIZ	East Industry Zone
EPA	Environmental Protection Agency
FT-IR	Fourier Transform Infra-red
MB	Methylene blue
SEM	Scanning Electron Microscopy
SS	Sewage sludge
SSBC	Sewage Sludge-Based Biochar
USEPA	United States Environmental Protection Agency
UV-Vis	Ultraviolet-Visible Spectroscopy
XRD	X-ray Diffraction

ABSTRACT

Development of a low cost and efficient adsorbent from waste materials is a genuine practice to ensure environmental sustainability. This study investigates the synthesis and application of sewage sludge-based biochar (SSBC)-alum sludge (AlS) composite adsorbent (SSBC-AlS) on methylene blue (MB) dye removal from industrial wastewater. The synthesis is based on the idea that combining the high carbon content of SSBC with high surface area, and suitable functional groups with rough and highly porous surface properties of AlS have a synergetic to increase the composite's efficiency on MB dye removal. To this end, locally available sludges, Sewage sludge (SS) and AlS samples collected from water treatment plants were used. The samples were sun-dried and ground to a sieve size of 0.18 mm. Then, the SS samples were pyrolyzed at temperatures of 350 °C, 450 °C and 550 °C for 2 h at a heating rate of 10 °C ·min $^{-1}$ to produce SSBC and labeled (SSBC350, SSBC450, and SSBC550). The SSBC, and AlS as well as SSBC-AlS composite adsorbent prepared by mixing selected SSBC with AlS, were characterized for physicochemical and thermal characteristics using FT-IR, TGA-DTA, XRD, SEM, and BET. The SSBC-AlS composite adsorbent MB removal efficiency was investigated using a batch adsorption technique, and the effect of experimental parameters such as temperature, pH of the solution, contact time, initial MB concentration, and adsorbent dosage were studied carefully. Using the optimized parameters, the kinetics and adsorption isotherm as well as reusability of the adsorbents were also investigated. The result revealed that, the adsorption efficiency reached maximum at pH 7, adsorbent dose of 1 g, contact time of 30 minutes, initial MB dye concentration of 100 mg/L and at room temperature. The maximum MB removal efficiency of the composite at optimized condition from aqueous solution and wastewater was 99.96% and 96.9%, respectively. The maximum adsorption capacity of the composite at optimized condition was found to be 19.98 (mg/g). The kinetics of the adsorption process fitted well with the Pseudo-second-order kinetic model and from the tested isotherm models, the Langmuir isotherm model was found to be the best fit. From the regeneration study, it is possible to conclude that SSBC-AlS adsorbent was recyclable and reused as MB dye adsorbent for 6 successive cycles without that much significant efficiency loss. The result clearly indicated the SSBC-AlS composite (with composition of 75wt% SSBC and 25wt% AlS) at optimized condition can be utilized to effectively remove MB dye from wastewater.

Keywords: Alum sludge, Sewage sludge-based biochar, Composite, Regeneration.

1. INTRODUCTION

1.1. Background of the Study

A large amount of sewage sludge (SS), produced as by product of wastewater treatment process, has increasingly become a challenge in the field of environmental protection (Zeng et al., 2021). This waste sludge comprised of organic compounds, macro- and micronutrients, trace elements, micro-organisms and micro pollutants has been classified as hazardous semi-solid waste. Its vast output and high treatment cost also significantly challenge the follow-up treatment (Kumar et al., 2017). At present, commonly used SS disposal methods mainly include incineration, landfill, composting, ocean discharge, and so on (Jafari & Botte, 2021). However, these methods have certain limitations, and exploring new methods for SS disposal and new ways for comprehensive utilization of resources is of great significance in solving the problem of SS disposal (Shang, 2019). Therefore, the development of closed-loop technologies has emerged as a contemporary way to convert trash into treasure (Russo et al., 2019).

When compared to traditional landfilling procedures, SS pyrolysis treatment is simple, inexpensive, robust, and safe besides of it can be used for transforming biomass into useful products such as bio-oil, syngas and biochar (BC) (Yi et al., 2020; Mao et al 2020; Zhu et al., 2018). The preparation of BC from SS through pyrolysis is a clean and efficient SS handling method since it can effectively reduce the volume of sludge, stabilize heavy metals in sludge under inert gas atmosphere without causing excess secondary pollution (Zhou et al., 2017), remove or passivate harmful substances, and kill pathogenic bacteria in the SS (Tan et al., 2014; Ameri et al., 2020). The most appealing feature of BC is that it is an inexpensive, sustainable and easily-produced stable material with potentially relevant application in environmental pollutant removal (Yi et al., 2020). However, its effectiveness in the removal of pollutants depend on the surface area and complex pore structure as well as other physicochemical properties of the BC, which in turn varies with raw materials used and pyrolysis conditions (Tan et al., 2015). Sewage sludge-based biochar (SSBC) possesses unique properties such as good surface area, good porosity, oxygen functional groups and stable carbon structure which make it suitable adsorbent material for different inorganic and organic contaminants from polluted wastewater (Ho et al., 2017).

The severe water contaminations by natural and anthropogenic causes have become one of the major environmental challenges of the 21st century (Mironyuk et al., 2019). More than 2000 chemical pollutants, mostly organic pollutants, have been discovered in wastewater (Tatarchuk et al., 2019). Organic dyes, widely employed in a variety of areas, are among the organic contaminants that cause substantial water pollution (Sonal et al., 2018). Some of the commonly used organic dye removal methods from wastewater includes, coagulation, flocculation, ion-exchange, advanced oxidation, and membrane separation (Yuan et al., 2019). Other than these techniques, adsorption is also used using eco-friendly and low- cost adsorbents such as zeolite, banana peel activated carbon, bagasse fly ash, and clay minerals (Zhou et al., 2019).

Among the different types of organic dyes, Methylene blue (MB), a cationic thiazide redox dye, is abundant in wastewater and surface water due to its use in several industries. It contains organic groups, such as phenyl and amino groups, and has a complex structure. It will be more stable and difficult to degrade after entering the water bodies (Qi et al., 2020). Even though MB is essential and widely used in many industries, excessive discharge of it from various sources into aquatic systems is a matter of concern because of its toxic, mutagenic or carcinogenic properties (Mashkoor et al., 2020). Due to its hostility, it will cause serious adverse effects on the environment and human health. As a result, Environmental Protection Agency (EPA) recommends a limit value of 0.2 mg/L of MB in wastewater (Environmental Protection Agency, 2001). For that reason, treating MB effluent before discharging it into the environment is critical in order to meet the EPA limit and for limiting its negative effects. From the different MB dye removal methods from contaminated water, adsorption is one of the most often utilized methods in dye wastewater remediation and it is quite effective for removing dyes in water (Bulgariu et al., 2019). However, commercial adsorbent materials are both very expensive and non-renewable, which limits their practical utility. To address this issue, production of low-cost adsorbent material from locally available resources such as SS, have been investigated (Fan et al., 2016; Leng et al., 2015; Wei et al., 2018). Related to this, in the treatment of MB contaminated wastewater, adsorbents like SSBC adsorbent is a current research hotspot (Fan et al., 2016; Leng et al., 2015).

Even though MB adsorption using SSBC adsorbent material appears promising (Fan et al., 2017; De Gisi et al., 2016), its solitary application as an adsorbent is insufficient (Tang et

al. 2018). The adsorption efficiency of BC derived from SS can be improved by adopting various activation processes. The most commonly used activation methods are physical activation and chemical activation. Several studies reported that adding or mixing additives (surfactants, metals, catalysts, agriculture based residues and industry waste) in the fresh SS or after carbonization, enhanced the adsorption capacity of SSBC (Leng et al., 2015). Aside from these modifications, to further increase the MB adsorption capacity of SSBC, forming a composite adsorbent with alum sludge (AlS) is a promising approach due to the chemical nature, high surface area, and amorphous structure of the AlS from waterworks residuals. All of such characteristics of AlS make the SSBC to be a superior adsorbent material (Ippolito et al. 2011; Geng et al., 2018; Yusuff et al., 2018).

AlS generation is rapidly increasing, its disposal, as well as the accompanying costs and environmental impacts, remains a global concern (Hidalgo et al., 2017). Recent lifestyles require more water consumption per capita, so fresh water demand is increasing. Further, the urgent need for clean water is a prerequisite. In such context, drinking water treatment plants produce massive waste by-product, so-called waterworks sludge. Aluminum sulfate is usually used as a primary coagulant in drinking water treatment plants, the result is that aluminum ions were hydrolyzed into aluminum hydroxide that is precipitated, and the so-called AlS is generated (Basri et al., 2019). Insoluble water impurities and organic substances are absorbed by aluminum hydroxide through raw water processing (Zhao et al., 2018).

In the available literature, there are numerous research studies on proper handling and reuse of huge amounts of AlS in an economical and environmentally friendly manner which include environmental applications, for example, use in building and construction materials, re-use as a coagulant in wastewater; and use in agricultural or forest sectors (Dassanayake et al., 2015). Beside from these, the reuse of AlS as low-cost alternative adsorbent for strongly-adsorbing oxyanion, organic pollutants as well as heavy metals removal in the environment have been studied (Shen et al., 2019; Kim et al., 2020). AlS have promising result in removing MB from wastewater (Nasser et al., 2017, Yusuff et al., 2018), the present study tries to improve MB removal efficiency of SSBC by making composite adsorbent with AlS as low cost adsorbent. This is because the composite combine the best qualities between the two materials, resulting in adsorbent with multiple-pore structures, better durability, stability, surface area and compatibility. Moreover, the use of composite

adsorbent made up of SSBC and AlS adsorbent materials would lower the cost of disposal of the sludges, reduce the land pollution and aid in the protection of water resources and human health.

1.2. Statement of the Problem

Water usage is continuing to rise worldwide, accompanied by a growth in the development of vast volumes of waste effluents every day, which contain dangerous compounds that are damaging to both human and aquatic life. Industrial effluents, which contain various inorganic and organic contaminants, constitute a significant source of water pollution in the environment (Rudi et al., 2020). Industries that utilize MB dye for dyeing purpose produce MB contaminated wastewater, resulting high risks to public health, the surrounding environment and socioeconomic activities (Karaer et al., 2016; Hassan et al., 2017). This is because of its non-biodegradability and recalcitrant nature, as exhibited by its stability against sunlight, temperature, oxidizing agents, and microbial attack (Sham & Notley 2018). Consuming MB contaminated water has significant consequences for the human cardiovascular, gastrointestinal, and central nervous systems, as well as a variety of respiratory, digestive, and cardiovascular illnesses such as dyspnea, diarrhea, and tachycardia (Ataei et al., 2016). It also causes convulsion, cyanosis, sweating, confusion, and short periods of difficult breathing on inhalation. Its degradation products in the body, such as toluidine, benzidine, and other aromatic components, may cause cancer and mutations (Reddy et al. 2016).

Many methods including flocculation, electrolysis, biodegradation, ion-exchange, and adsorption have been applied for removing of MB dye in wastewaters (Bhatnagar et al., 2010; Salleh et al., 2011). Except adsorption, these procedures are costly and lead to the generation of large quantities of sludge or the formation of derivatives. Among the processes for treating dye contaminated liquid discharges, adsorption remains a relatively used and easy to implement technique. In recent years, studies have shown that using low-cost adsorbents for MB dye decontamination from wastewater is a major development trend with high efficiency and economy (Ragab et al., 2019).

On the other hand, associated to rapid population growth, development of urbanization and industrialization, wastewater treatment plant generates unavoidable and increasing amount of SS (Mateo-Sagasta et al., 2019). The SS which is produced in the wastewater treatment

plant of developing countries, specifically Ethiopia is stockpiled in open environments and produce secondary pollution. The presence of pathogenic organisms, volatile organic compounds, heavy metals in the SS results in serious adverse effects for the surrounding locality and this sludge is becoming the problematic waste item to handle and the demand of standardized treatment of SS has paid much attention. So, in order to give remedy on how to handle this sludge in a way that is economically, environmentally, and socially acceptable manner- a way that is sustainable, an adsorbent development using thermal treatment technology and then applied to the wastewater treatment process is a sustainable management option (Ho et al., 2017). As an emerging sludge treatment technology, pyrolysis minimizes the organic contaminant characteristics of the sludge, fixes and immobilizes the heavy metals in the BC matrix so that the risk of leaching is minimized compared to the direct application of the sludge as an adsorbent (Agrafioti et al., 2013; Yi et al., 2020).

SSBC possesses unique properties such as good surface area, good porosity, oxygen functional groups and stable carbon structure which make it suitable adsorbent material for different inorganic and organic contaminants from polluted wastewater (Ho et al., 2017). As a result, SSBC adsorbent material has been practiced for treating MB-contaminated wastewater (Sierra et al., 2017). However, the application of it alone has a limited MB adsorption capacity (Liu et al., 2013). In order to further increase adsorption efficiency, researchers have activated SSBC before utilizing it as an adsorbent (Devi & Saroha, 2017; Wu et al., 2018). Researchers have studied the adsorption capacity of SSBC activated by NaOH, H_2SO_4, KOH, and $ZnCl_2$ as an adsorbent for MB (Tang et al., 2018). SSBC prepared by impregnation with K_2CO_3 followed by activation with CO_2, exhibits removal ability of 56.1 mg/g. On the other study, activated SSBC by NaOH removes 20.1 mg/g of MB from polluted ecosystems. The high mesoporous volume of activated SSBC by NaOH removes MB from different ecosystems (Gomez-Pacheco et al., 2012). Leng et al. (2015) also uses the complex mixture of inorganic and organic activating agents for the activation of SSBC for dye removal from wastewater (Leng et al., 2015). The activation of sludge with the mixture of zinc chloride and citric acid increases the BET surface area and pore volume ratio as well. However, with an increase in activation temperature, citric acid breaks down into carbon dioxide and water, which lead to the widening of macropore in the SSBC. The activation by using steam also produces SSBC with high porosity and surface area. At a particular temperature, SSBC produced by steam activation method possesses high

adsorption efficiency and larger pore size distribution but if the activation temperature exceeded 800 ^{o}C, there will be loss of fixed carbon and led to a reduction in BET surface area (Wang et al., 2017). Beside these modifications, creating a composite adsorbent with other sludge residue can be considered. Composite making with other waste sludge material is good activation method since it is relatively economically feasible, cheap and eco-friendly than the chemical or physical based activation method.

With an estimated global output surpassing 100,000 tons per year, AlS is one of the most extensively produced and locally available water treatment residual in the world (Zhao et al., 2018). In Ethiopia, several tons of AlS produced from raw water treatment plant, is generally thrown away outside of the treatment plant causing secondary contamination in surface water, soil and atmospheric environments of the surrounding area. At Adama drinking water plant, Oromia Regional State, Ethiopia, AlS is manufactured in large quantities. This has piqued curiosity in how to handle this residual in a way that is both ecologically friendly and sustainable manner. An adsorbent development based on this cheap and abundant residue sludge can effectively remove organic pollutants particularly dyes from wastewater (Yusuff et al., 2018). Creating a composite adsorbent of SSBC and AlS could help to boost the adsorption capacity of the SSBC. This is because the loading of poorly crystalline metal oxides/hydroxides ($Al(OH)_3$) from AlS onto the SSBC adsorbent surface is important because their chemical nature is suitable to attract cations, the amount of surface active sites and oxygen-containing functional groups, including Al-O-Si, Si-O, OH, and others, will be increased after addition of AlS, the modification by AlS will enhance surface polarity and changed the surface electrical properties of the adsorbent material, also AlS have high surface area with macro and micro-porous structure, and amorphous structure better than SSBC, which will make the modification fruitful.

1.3. Objective

1.3.1. General objective

The general objective of this study was to synthesize and characterize SSBC-AlS composite adsorbent and evaluate its performance in removing MB dye from wastewater.

1.3.2. Specific objectives

- ✓ To prepare AlS and SSBC prepared at pyrolysis temperature of 350 °C, 450 °C and 550 °C.
- ✓ To synthesize SSBC-AlS composite adsorbent from SSBC and AlS.
- ✓ To study the physicochemical characteristics, surface functional groups, structural crystallinity, surface morphology, thermal stability, and surface area of the prepared adsorbents.
- ✓ To investigate the optimal adsorption parameters (temperature, pH, adsorbent dose, contact time, and initial MB concentration) for efficient removal of MB dye from an aqueous solution.
- ✓ To study the adsorption mechanism through adsorption isotherm and kinetics.
- ✓ To remove MB dye from the real textile wastewater sample by SSBC-AlS composite adsorbent.
- ✓ To evaluate regeneration of SSBC-AlS composite adsorbent.

1.4. Significance of the Study

This study can be used to provide a method to remove MB dye that pose serious health and environmental hazard using a simple, cost-effective, and environmentally friendly adsorption method.

- ✓ The prepared composite adsorbent can be used for the removal of the MB dye from wastewater of different industries before the dye-contaminated wastewater is discharged into the environment.
- ✓ The research will assist in demonstrating insight on how to develop simple, cost-effective, environmentally friendly, and easily available composite adsorbent that can be used to replace imported activated carbon or other commercially available expensive adsorbent materials.

- ✓ The conversion of SS biomass into a valuable SSBC supports the reduction of greenhouse gases, decrease the amounts of residuals accumulated in the environment and reduce the environmental stress.

- ✓ Using the described by-products as adsorbents could be a good solution for huge quantities of these wastes in terms of sustainable development and green projects, as well as a means of cutting disposal costs.

- ✓ The research will be essential for other researchers and academicians to perform additional investigation by expanding this examination.

2. LITERATURE REVIEW

Comprehension of related literature from previous studies is critical for any research in order to develop appropriate methods that will serve as a guiding force as the research progresses. Literature can be used to infer new study areas. The review of literature related to the current study is organized and presented in this chapter.

2.1. Municipal Sewage Sludge

In available literatures, municipal SS is defined as SS from the treatment of municipal wastewater, which includes a range of organic and inorganic compounds (Demirbas et al., 2016). Expanding urbanization contributes to increased wastewater volume in both developing and industrialized nations, which in turn causes a rise in SS generation because of wastewater treatment (Kumar et al., 2017). In addition to this, the output of SS is increasing internationally because to environmental protection legislation that mandate wastewater treatment before reintroducing it to the environment (Lu et al., 2012). Each cubic meter of wastewater is thought to contain 0.25 kilogram of sludge (Grosser et al., 2013). The amount of SS is anticipated to increase because of more homes being connected to centralized wastewater treatment facilities, stricter regulations on effluent discharges, and advances in wastewater efficiency technologies. Due to widespread SS production, careful management of this organic waste is necessary to prevent harm to human health and the environment (Kumar et al., 2017; Liu et al., 2020; Yang et al., 2019).

2.1.1. Composition of sewage sludge

The techniques used in the wastewater treatment facility, the season, and other factors all have an impact on the composition of SS, making it highly changeable. Examples of these factors include the specificity of the sludge source area (Rorat et al., 2019). The sources of the SS significantly affect the composition of the overall SS, particularly in terms of the amount of organic and inorganic substances present. The type of sewage system, whether it is exclusively for dry weather flow of wastewater or also for rainfall, when inorganic parts from roads are flushed into sewage system, and wastewater is diluted with rain and underground water, is another crucial indicator of SS composition (Racek et al., 2020).

Despite the fact that depending on the aforementioned circumstances, the composition of the SS generated varies, it is typically a heterogeneous mixture of undigested organic waste

(paper, plant residues, oils, etc.) water, inorganic substance, and microbes (Lasaridi et al., 2018). Proteins, peptides, lipids, polysaccharides, phenolic and aliphatic structures comprising macromolecules, polycyclic aromatic hydrocarbons, etc. are among the hydrocarbons that make up the SS's undigested organic matter. Different types of nitrogen and phosphorus are also present in dry SS. SS also contains inorganic salts including ions (CO_3^{2-} , PO_4^{3-}, SO_4^{2-}, and NO_3^-), heavy metals (e.g., Zn, Pb, Ni, Cd, Cr, Cu, As, and Hg), and other elements (e.g., Si, Al, K, Na, Ca, and Mg) (Wang et al., 2019).

2.1.2. Characteristics of sewage sludge

The purified water is separated from the SS, which resembles a slurry and contains a sizable amount of water, at water treatment plants. SS contain a high water content (below 10% in thermally dried SS and between 55% and 80% in dewatered SS). This moisture content must be brought down to a minimum before the SS is used, either for disposal or for reuse. Several drying process options are available to do this. These drying techniques include mechanical dewatering, fry drying, and thermal drying (including thermal drying and typical air drying) (Hugo et al., 2016). Other than this, the undigested organic constituents consist of an exceedingly complex mixture of fragments obtained from proteins, peptides, lipids, polysaccharides, plant macromolecules with phenolic structures or aliphatic structures along with organic toxins (Lucia et al., 2018; Paula et al., 2015) are about (from 75 % in raw sewage sludge to 45 % - 55 % in stabilized sludge). SS also contains heavy metals, for example, zinc, copper, chromium, nickel, lead and cadmium. The sewage treatment process of conditioning might alter the chemical species distribution of heavy metals, which could result in the immobilization of some heavy metals like Pb (Qiao et al., 2018). Additionally, the nitrogen component level of SS is high (2-7%), and its phosphorus content is minimal (Ak & Dumrul, 2017). Table 2.1 summarizes the physical and chemical features of municipal SS.

Table 2. 1: Physical and chemical characteristics of municipal SS (Werle & Dudziak, 2014; Bharathiraja et al., 2014).

Characteristic	
pH	7.1-8.2
Bulk density (Kg/L)	1.26-2.56
Particle density (Kg/L)	2.40-2.56
Organic matter (g/Kg)	418-592
Ash (g/Kg)	345-440
Higher heating value (MJ/kg)	11.3-14.2
Organic carbon (g/Kg)	205-403
Oxygen (g/Kg)	185-219
Nitrogen (g/Kg)	45-49
Hydrogen (g/Kg)	40-46
Iron (g/Kg)	24-38
Phosphorus (g/Kg)	22-30
Calcium (g/Kg)	21-29
Aluminium (g/Kg)	16-22
Sulfur (g/Kg)	11-17
Magnesium (g/Kg)	3.2-4.8
Barium (g/Kg)	2.8-4.2
Zinc (g/Kg)	2.4-3.6
Silicon (g/Kg)	2.2-2.7
Potassium (g/Kg)	1.2-1.6
Copper (g/Kg)	0.7-1.2
Chromium (g/Kg)	0.5-0.9
Nickel (g/Kg)	0.3-0.5
Manganese (g/Kg)	0.1-0.2
Lead (g/Kg)	0.1-0.3
Sodium (g/Kg)	0.1-0.2
Tin (g/Kg)	01-0.2

Concentration values in dry mass basis.

2.1.3. Sewage sludge treatment and disposal

Concerns over SS disposal have grown as a result of increased industrialization, urbanization, and the massive growth of modern areas (the fourth industrial revolution). Traditional means of treatment and disposal include filling, incineration, paving, dumping into bodies of water, and converting it into building materials, but these processes can easily lead to secondary pollution. Due to socioeconomic and environmental problems, there is interest in the creation of alternate methods to treat and dispose of SS in order to get around this (Sung et al., 2015). Nowadays, there are two main types of SS treatment: biochemical and thermochemical. Anaerobic fermentation and hydrolysis are part of the biochemical treatment process, sometimes known as the wet treatment process. The biosolids' organic substance is broken down by fermentation using microorganisms. Water and enzymes are delivered to the biosolids, where they are hydrolyzed and decomposed. The temperature is used in thermochemical treatment, also known as a dry treatment technique, to dissolve chemical bonds in biosolids (Ran et al., 2019).

2.1.4. Thermal treatment of sewage sludge

As it is shown in Figure 2.1, there exist many thermochemical treatment processes, which can be classified into two main categories such as thermochemical oxidative processes and thermochemical reductive processes. Combustion is one of the thermochemical oxidative treatment methods when oxygen is present in stoichiometric or higher levels. Gasification, hydrothermal carbonization, and pyrolysis are examples of thermochemical reductive reactions where oxygen is absent or present in very small amounts (Kumarathilaka et al., 2016). Classes of thermochemical reductive treatment process of SS are reported in Table 2.2, focusing on the process temperature, residence time and products in weight %.

Table 2. 2: Thermochemical reductive treatment process of biosolids (Thangarajan et al., 2016; Capodaglio et al., 2016; Callegari et al., 2018).

Thermochemical treatment	Process temperature	Residence time	Products of thermochemical treatment (weight %)		
			Gases	Liquid	Solid
Pyrolysis	100-1300 ^{0}C	0.05 s-4 h	Pyrolysis gas (2-29%)	Pyrolysis oil (5-20%)	Biochar (10-80%)
Gasification	800-1200 ^{0}C	10-20 s	Syngas (>85%)	Bio-oil (<5%)	Char (10%)
Hydrothermal carbonization	175-295 ^{0}C	5 min-12 h	Gas product (2-5%)	Liquid product (5-25%)	Hydrochar (45-70%)

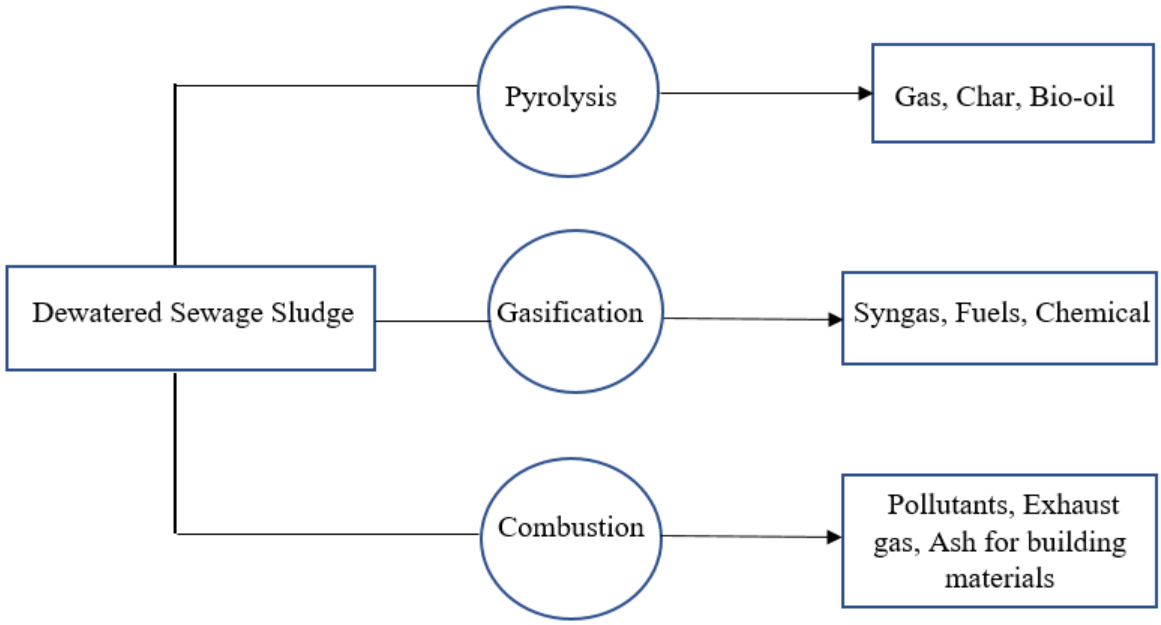

Figure 2.1: Schematic diagram of thermochemical processes for SS (Gao et al., 2020).

2.1.4.1. Pyrolysis of sewage sludge

Depending on the desired end product, there are three different categories of SS pyrolysis. Group 1 includes thermal degradation of SS for the preparation of solid adsorbent (BC), Group 2 includes pyrolysis of SS for the preparation of syngas and bio-oil, Group 3

comprises thermo-gravimetric analysis of SS to identify reaction kinetics (Bonfiglioli et al., 2014). The primary factors affecting pyrolysis product quality are pyrolysis temperature, dwell duration, heating rate, ambient gases, pressure, and raw material properties. Process variables vary according to the expected ultimate product quality (Fan et al., 2016). Depending on the residence time, the pyrolysis temperature of the process might range from 350 to 1000 ^{0}C. Figure 2.2 shows the steps of SS degradation during pyrolysis.

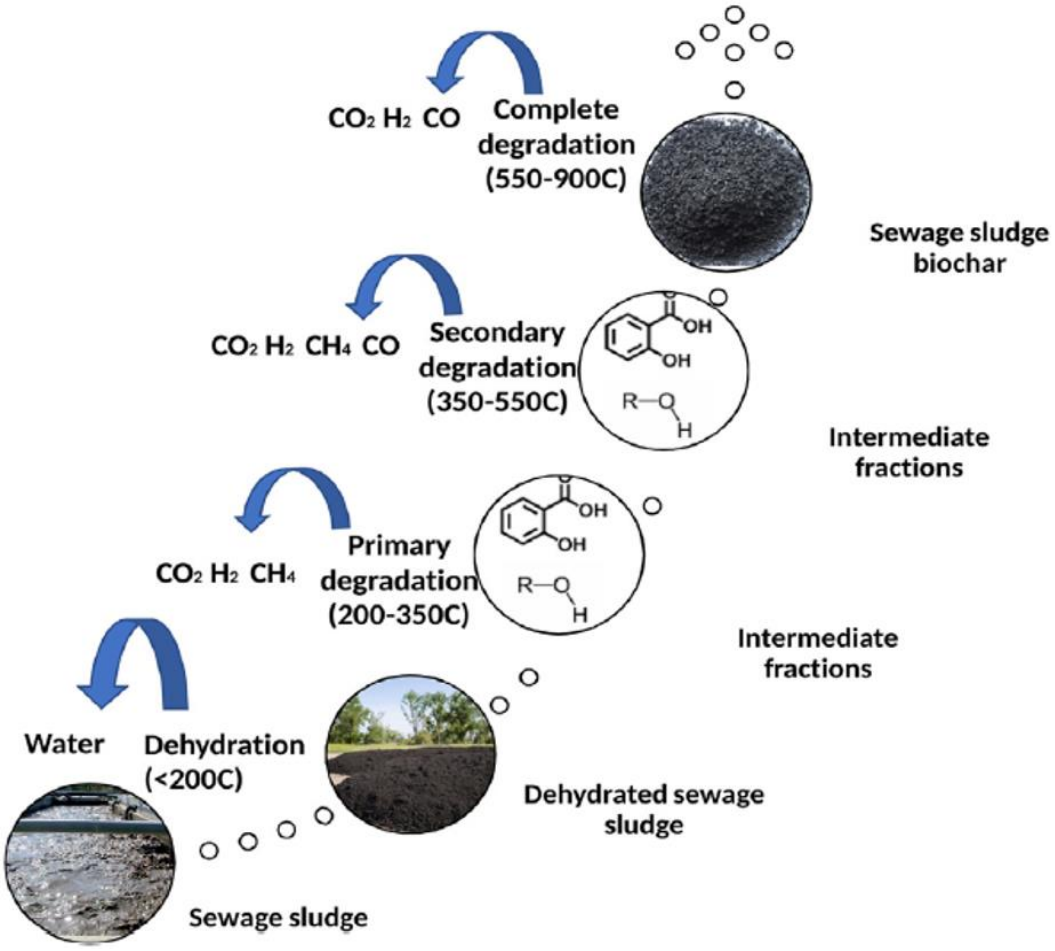

Figure 2.2: Different stages of pyrolysis of SS (Singh et al., 2020).

Dehydration at an average temperature of 200 ^{o}C, which releases water, initiates the thermal disintegration of SS (primary, secondary and complete). The dehydrated SS first undergoes primary degradation at temperatures ranging from 200 to 300 ^{o}C, producing alcohols and hydrocarbons while releasing CO_2, CH_4, and H_2. After primary degradation, the intermediate fractions are subjected to secondary degradation, which occurs at temperatures between 350 and 450 ^{o}C and results in the production of alcohols and hydrocarbons. Following secondary degradation of sewage sludge at an average temperature of 550 ^{o}C, the

intermediate fractions completely degrade, producing biochar and emitting CO_2, CH_4, and H_2. Almost majority of the biodegradable organic matter in sludge is volatilized during the earliest stages of pyrolysis between 150 ^oC and 400 ^oC, and then nonbiodegradable organic matter is volatilized between 400 ^oC and 550 ^oC. (Bonfiglioli et al., 2014). Pyrolysis is a promising treatment method for SS because it results in pathogen neutralization, organic pollutant degradation, and waste volume reduction. Compared to raw sludge, SSBC concentrates heavy metals while having less microorganisms and odor (Luque et al., 2012).

2.1.4.1.1. Preparation of sewage sludge-based biochar

The creation of BC from SS is proven to be a viable approach for managing SS, which is typically considered to be waste (Mehta et al., 2015). A carbon-rich solid product called BC is produced by the thermal breakdown of biomass, which includes solid wastes like municipal sludge, shells, and manure as well as green wastes, primarily agricultural biomass (Nanda et al., 2016).

Preprocessing, pyrolysis, and characterization are the main steps in the process of making SSBC (Zhu et al., 2019). Preprocessing and pyrolysis in general are crucial for getting high quality SSBC. Sludge is preprocessed through drying, filtering, and activation. Drying is typically done to lessen the amount of sludge and lower the energy needed for pyrolysis (Lin et al., 2016). SS can be dried to eliminate moisture content using two techniques: oven drying, which is done in a hot air oven at 100 ^0C for 24-48 h, and the sun-drying method, which is done by exposing the wet sludge to direct sunshine (Gao et al., 2017). In line with this, the goal of sieving is to produce sludge powder that is homogeneous and has a large specific surface area. The objective of activation is to produce high-quality BC, and the activation process comprises both physical and chemical activation (Wu et al., 2018). The physical or chemical activation of sewage sludge can be done before or after the carbonization (Devi & Saroha, 2017). In general, the heating technique used in pyrolysis methods such as microwave pyrolysis and resistance tube furnace pyrolysis differs from one another. In order to increase the collision and friction of the particles already existing in the material, a process known as microwave pyrolysis is used, producing a high thermal efficiency (Zhang, 2013). The sample's surface temperature is higher than its interior temperature due to the transfer of heat during pyrolysis in a resistance tube furnace from the sample's surface to its inside (Gong et al., 2018). Microwave pyrolysis is superior than

resistance tube furnace pyrolysis because it heats materials quickly, uniformly, efficiently, and selectively (Zaker et al., 2019).

2.1.4.1.2. Effect of physical conditions on pyrolysis of sewage sludge

Effect of pyrolysis temperature

The properties and quality of SSBC are significantly influenced by the temperature at which the pyrolysis of SS is carried out. It has been noted that while the yield of BC falls as the pyrolysis temperature rises, the ash content and cationic exchange capacity rise (Xu et al., 2015). The acidic and basic nature of SSBC's surface characteristics are also impacted by the pyrolysis temperature. Low-temperature BC is often acidic in nature, whereas high temperature BC is alkaline. The release of sodium oxide, which raises the pH of BC, is the cause of the alkaline nature of BC at high temperatures (>500 ^{0}C). The surface appearance and structure of the SSBC are influenced by the pyrolysis temperature as well (Hadi et al., 2015). BET surface area and pore volume surface area both rise with warmth. However, the BC's porosity was reduced by the high temperature, which also improved the smoothness of the surface structure and overall aromaticity (Gao et al., 2017). Additionally, it was noted that high moisture content in the sludge results in steam-enriched conditions at high temperatures, which causes BC to partially gasify and accelerate the formation of micropores (less than 2 nm) (Rajapaksha et al., 2016).

Effect of dwell time

Shorter dwell time at high carbonization temperatures are reportedly necessary when pyrolyzing SS (Hadi et al., 2015). The recommended dwell periods are 240 minutes at 500 °C and 120 minutes at 650 °C (Mendez et al., 2009). Furthermore, Montoya et al. (2015) proposed that the ideal dwell time is 60 minutes at 950 ^{0}C. Smith et al. (2009) also noted that at 650 ^{0}C, mesopores and BET surface area decrease while micropore development is consistent with an increase in residence time. According to Mohan et al. (2014), increasing dwell time at the same carbonization temperature resulted in a decrease in the micropore volume of BC.

Effect of heating rate

The primary factor that enables us to distinguish between the different forms of pyrolysis is the heating rate of SS during pyrolysis (slow or fast pyrolysis). The time it takes to reach

the temperature for the biomass reaction is called the heating rate (Hadi et al., 2015). Heating rates on the order of 1 ^{0}C/min-100 ^{0}C/min are needed for slow pyrolysis processes, whereas heating rates of more than 1000 ^{0}C/min are needed for fast pyrolysis processes (Montoya et al., 2015). Higher heating rates result in an increase in BC yield and carbon content while a decrease in hydrogen content. He et al. (2013) showed that the prolonged residence time during the carbonization process led to an increase in surface area with a decrease in heating rate.

2.1.4.1.3. Characterization of sewage sludge-based biochar

As it is shown in Figure 2.3, high pH, good water holding capacity, porosity, and moderate surface area are only a few of the physical and chemical characteristics of SSBC. We can measure the physical shape and micro-porosity of SSBC produced at various temperatures using a Scanning Electron Microscope (SEM). Due to the presence of various inorganic and organic contaminants in the sludge, SSBC appeared as a plate-like layer with a sparse, smooth, and compact structure when observed under SEM (Breulmann et al., 2018). Additionally, it was discovered that the surface area of the SSBC grew with rising pyrolysis temperature. Low pyrolysis temperatures result in the condensation of organic volatiles, which clogs the pore and reduces the surface area available for absorption. The creation of voids in the BC matrix by high-temperature pyrolysis and volatilization, which increase the porosity of SSBC, are crucial processes. Specific surface area of SSBC grew at high pyrolysis temperature, 500 ^{0}C, whereas it decreased at low temperature, 300 ^{0}C, and was very low (20.2 m^2 g^{-1}) (Figueiredo et al., 2018). The large difference in the physical properties of SSBC suggests that BC produced at higher temperatures can imitate activated carbon and be utilized for environmental remediation, whereas BC produced at lower temperatures can be used to control the nutrients released from fertilizers. Additionally, it has been noted that the hydrophobic property of SSBC surfaces created at low temperatures is what causes them to have a low capacity to absorb contaminants and water. Additionally, electrical conductivity, for example, increases until the temperature reaches 500 ^{0}C, at which point it decreases to half, as a result of the extreme temperature range (Faria et al., 2018). The majority of academics have focused on SSBC because of its unique features and ability to clean wastewater effectively. Because SSBC is porous, there is more surface area available for increased adsorption of phenols, metals, and colors from wastewater (Capodaglio & Callegari, 2017; Liu et al., 2015).

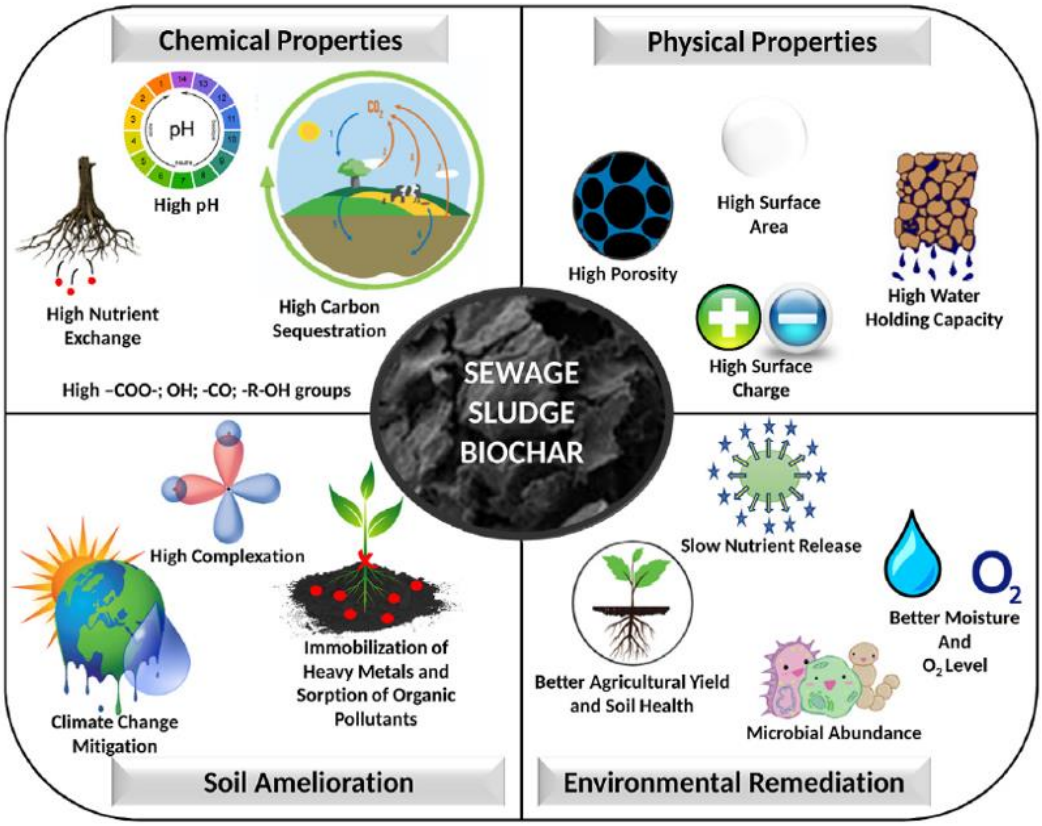

Figure 2. 3: Properties and applications of SSBC (Singh et al., 2020).

2.1.4.1.4. Activation of the sewage sludge-based biochar

Physical activation

Two steps are involved in the physical activation of SSBC: (a) carbonization at low pyrolysis temperatures (400–750 ^{0}C) in the presence of heat, gases (carbon dioxide, helium, and nitrogen), and steam to break down the cross-linkages between the C atoms; and (b) activation in a gaseous environment at relatively high pyrolysis temperatures (typically 800-1200 ^{0}C) to further increase the porosity of the BC. Various activating agents are reported in the literature, which includes carbon dioxide, air, nitrogen, steam, oxygen etc (Wang et al., 2017). For the thermal activation of BC, mild oxidizing agents like steam and carbon dioxide are typically utilized because they encourage a delayed oxidation process that results in the development of new pores and the widening of existing pores (Contescu et al., 2018). Compared to chemical-based activation methods, physical activation methods are more economically viable, inexpensive, and environmentally friendly. The main variables that determine the quality and distinguishing characteristics of BC during the

physical activation process are the activation duration, temperature, and gas flow rate. According to reports, BC's surface area and porosity grow as gas flow rate and process temperature rise, however activation time has adverse effects after a certain amount of time (Devi & Saroha, 2017).

Steam activation

Steam activation is a cost-effective technique for preparing BC that has a high porosity and surface area. In comparison to carbon dioxide activation method-produced BC, steam activation method-produced BC has higher adsorption efficiency and a wider range of pore sizes. According to Ncibi et al. (2009), steam activation tempts the development of mesopores and micropores. The expansion impact of steam causes the mesopores of the BC to widen as a result of water molecules diffusing to the interior surface, increasing the BET surface area. However, if the activation temperature was higher than 800 ^{0}C, fixed carbon would be lost, which would reduce the amount of BET surface area (Wang et al., 2017).

Carbon dioxide, nitrogen and air activation

The functional moieties of the BC are likewise impacted by the carbon dioxide and nitrogen activation. In contrast to the activation by nitrogen, which requires a significantly higher activation temperature, the activation based on the use of carbon dioxide could boost the creation of micropores only at a lower activation temperature (600–650 ^{0}C). According to earlier research, the distortion of the acidic functional groups on the surface of SSBC causes the acidity of the BC to drop and the basicity to increase as the activation temperature rises (Gao et al., 2014). Additionally, due to the production of metal oxides within the inorganic matrix of BC, SSBC produced by carbon dioxide activation are more basic in character. At 270-280 ^{0}C, air activation of SSBC increases the surface with acidic oxygenated functional groups such (- COOH, -R-O-R-), which enhances BC's ability to adsorb (Bagreev & Bandosz, 2004).

Chemical activation

The different inorganic (zinc chloride, sulphuric acid, potassium, sodium, potassium carbonate, phosphoric acid, ferric nitrate, and hydrogen peroxide) and organic (citric acid) agents are used in the chemical activation process (Devi & Saroha, 2017). The most popular and efficient activating agent for creating BC with a large surface area and greater

adsorption capacity is zinc chloride. By removing the hydrogen and oxygen atoms from the SS, zinc chloride acts as a dehydrating agent and triggers a condensation process, increasing the BC's BET surface area and pore volume. The adsorption efficiency of SSBC increases as zinc chloride concentration rises up to 3 mol/L (Wang et al., 2017). A further rise in concentration slabs the BC's meso- and micropores and reduces its surface area. The SSBC preparation process uses less energy since the zinc chloride activation method is effective in reducing the activation time and temperature. The fraction of sludge activated with zinc chloride at lower activation temperature (600-650 ^{0}C) requires less activation time (20-30 min) in contrast to the non-zinc chloride activated sludge requires more activation time (1-2 h) at higher activation temperature (800-850 ^{0}C). When compared to alternative activating agents, the advantages of using phosphoric acid as an activating agent are its low activation temperature and economic viability. The effects of phosphoric acid during SS activation were mentioned in several papers (Pokorna et al., 2009). By encouraging depolymerization and dehydration, it transforms aliphatic carbon into aromatic carbon, increasing BC production and cation exchange capacity in the process. The significance of a combination of activating agents for the creation of BC from SS was highlighted by Zhai et al. (2014). For the activation of SS, they utilized a solution of zinc chloride and sulfuric acid. It was discovered that the two compounds had synergistic effects and that a combination of activators works more effectively than a single activator. The combination of activating agents promotes the condensation and dehydration reactions, which improves the BC's ability for adsorption. Similar to this, it was reported by that the complex mixture of organic and inorganic activating agents for the activation of SS (Leng et al., 2015). The BET surface area (867 m^2 g^{-1}) and pore volume ratio are both increased when zinc chloride and citric acid are added to sludge. Citric acid helps the production of macropores, while zinc chloride starts the formation of micro and mesopores. However, as the activation temperature rises, citric acid decomposes into carbon dioxide and water, causing the macropore in the SSBC to enlarge. The surface area and adsorption effectiveness of SSBC are also influenced by the activation agent concentration (Pokorna et al., 2009). Adsorption capacity and pore volume surface area both rise with concentration, but they decrease when activation agent concentrations are over the optimal level (Trinh et al., 2013).

Addition of binder agents

It has been observed that various binder agents, such as humic acid, polyvinyl acetate, and clay soil, are typically added to the SS before chemical activation, which improves the granulometry of SSBC (Zhai et al., 2014). Humic acid and clay soil are said to reduce the meso and macropores of SSBC (Wang and Jia, 2012). The hardness of the BC produced by physical activation (steam) and the addition of a binder agent (polyvinyl acetate) is 90-93%, compared to the hardness of the BC produced without the addition of a binder agent, which is between 57% and 70% (Xu et al., 2015).

2.1.4.1.5. Composites of sewage sludge-based biochar

Mian et al. (2018) have created a novel TiO_2/Fe/Fe_3C-BC composite that functions as a heterogeneous catalyst. The substance was made in a way that included SS and various nanoparticle dosages impregnated with chitosan utilizing coagulation and flocculation methods for later thermal decomposition at 800 ^oC and use in MB degradation experiments. The highest MB removal capacity in neutral pH was determined to be 376.9 mg L^{-1} (Mian et al., 2018). Other researchers studied three different MnO_2 polymorphs, α-MnO_2, β-MnO_2, and δ-MnO_2, with K^+-tuned tunnel structures loaded on sludge-based BC. Then MnO_2-loaded BCs served as the catalyst for ciprofloxacin removal. Results showed that as-prepared materials exhibited better catalytic activity than raw BC, among which BC-α-MnO_2 achieved superior ciprofloxacin removal. Additional to adsorption desorption experiments confirmed that both adsorption and degradation contributed to the ciprofloxacin removal by MnO_2-loaded BCs. Compared with the raw BC, the contribution of degradation increased 27.87%, 19.87%, and 14.19%, respectively, for BC-α-MnO_2, BC-β-MnO_2, and BC-δ-MnO_2 (Xu et al., 2018).

2.1.4.1.6. Adsorptive properties of sewage sludge-based biochar

Adsorbent for the removal of contaminants from wastewater, SSBC is characterized by its medium specific surface area, enriched functional groups, mineral composition, and porous structure. Adsorption by SSBC often involved one of several different processes, including physical adsorption, chemical adsorption, electrostatic interaction, precipitation, ion complexation, and ion exchange (Chen et al., 2015). Due to its many sorption sites, SSBC can effectively remove both inorganic and organic contaminants (Wei et al., 2018). Adsorption by BC is the most effective technique of heavy metal removal when compared

to other treatment options because it combines electrostatic interaction, ionic exchange, chemical precipitation, and complex formation with BC surface functional groups (Braghiroli et al., 2018). Additionally, SSBC is said to be more effective at removing colors from various liquid solutions than commercial activated carbon. The surface chemistry and pore structure of SSBC have a significant impact on the adsorption of cationic and anionic dyes on SSBC (De Gisi et al., 2016).

2.2. Water Pollution

Polluted water is a major ecological issue that affects both the human health and the environment across the world, resulting in considerable economic and social consequences. Water quality has deteriorated over time as a result of human activity, population growth, fast industrialization, and unskilled use of natural water resources, among other factors (Launary et al., 2016; Chowdhary et al., 2018). Contaminants in wastewater, which come from a variety of sources and in varying amounts, reach the environment either directly or indirectly, causing harm (Emongor et al., 2015).

Water contamination is caused by a variety of organic and inorganic contaminants, which are primarily discharged from industrial and agricultural activities (Bartolomeu et. al., 2018). Disposal of organic compounds arising from various industries such as cosmetics, leather, plastics, paper, pharmaceuticals and textiles industries, has attracted much attraction in recent years because of those effluents, contain a broad types of highly toxic and carcinogenic contaminants (Sahoo et al. 2019). Heavy metals, excess nutrients, and chemical fertilizers, on the other hand, come in various amounts of toxic inorganic contaminants (Alssgeer et al., 2018).

Over 100,000 commercial dyes are estimated to be utilized in industry, and more than 700,000 tons of dyestuff are produced each year (Markandeya et al., 2017). The environmental problems associated with residual dye content or residual color in treated textile effluents are always a concern for every textile operator that directly discharges, sewage treatment plants, and commercial textile operations to fulfill the color and residual dye requirements imposed on the treatment and disposal effluent (Zaharia et al., 2011). In watercourses higher than 1.0 mg/L, dye concentrations induced by direct discharges of textile effluents, treated or not, can give rise to public enforcement. Among plenty of dyes, MB is common type of dye used in the textile industry. Not only in textile industry MB is

also used in many areas such as staining paper, leather, rubber, plastics, etc. The aromatic nature of MB makes it tough to breakdown (Markandeya et al., 2017).

2.3. Methylene Blue Dye

MB ($C_{16}H_{18}N_3SCl$) is a basic cationic dye with a molecular mass of 319.87 g/mol. The molecular structure and physical and chemical properties of MB is presented in Figure 2.4 and Table 2.3, respectively. It is a cationic dye that gives a net positive charge when mixed with aqueous solutions due to the presence of chemical groups such as amine or sulfur. At room temperature, MB is solid, odorless, dark green powder and gives a blue solution if dissolved in water (Laysandra et al., 2017). It is used to several applications like the coating and coloring of paper, hair, cotton, and wool; it is also used as an indicator of oxidation-reduction and as a disinfectant, besides its many other medical usages in medicine, in pharmaceutical formulations, in pesticide production, varnish, and lacquer manufacturing, among others (Zaghbani et al., 2007).

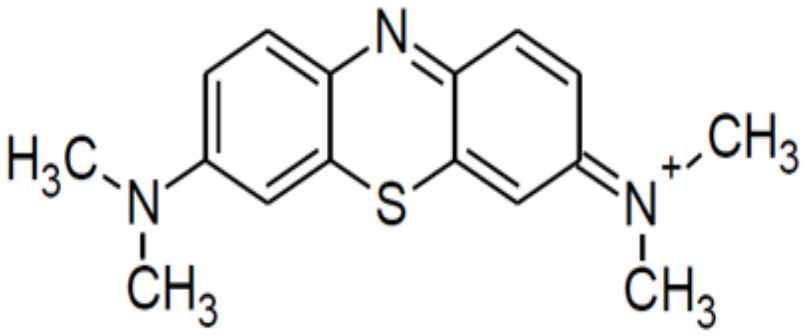

Figure 2. 4: Molecular structure of MB.

Table 2. 3: Physical and chemical properties of MB

Chemical and physical properties	Values
Family	Basic dye
Chemical formula	$C_{16}H_{18}N_3SCl$
Chemical name	3, 7-bis-(dimethylamino)phenazathionium
Melting Temperature	180 ^oC
Solubility in water	35.5 g/L
Molecular weight	319.09 g/mole
Color	Blue-green in oxidized form, colorless in reduced form

2.3.1. Industrial and medicinal uses of methylene blue

MB is one of the most commonly utilized organic compound. It is used to color paper, hair, cottons, and wools, as well as for biological staining. Cottons, wools, and silks were frequently dyed using this dye in the textile business (Miraboutalebi et al., 2017).

In particular, methemoglobinemia and urinary tract infections are treated with MB injection. MB is also used to treat chronic urolithiasis, cutaneous viral infections, and manic-depressive psychosis, among other things. In a patient with septic shock, MB is also used to improve vascular tone and myocardial function. In general, MB is a safe medication that has a dose-dependent hemolytic effect (Tronsmo et al., 2016).

2.3.2. Methylene blue dye in industrial effluents

Textile, painting, rubber, leather, cosmetics, pharmaceuticals, food, paper, and plastics are just a few of the industries that produce dye effluents. The global textile industry is estimated to be worth around $1 trillion USD and its contribution towards total world exports is around 7%, employing 35 million people worldwide. The most prominent and destructive form of

pollution, caused by the textile industry, is the water pollution due to the usage of dyes (Desore & Narula, 2018).

Textile effluents are both aesthetically polluted, and have high salinity, chemical oxygen demand, and ecotoxicity (Liang et al., 2020), and due to their increasing ubiquity in surface water, can lead to adverse effects to human and wildlife health and to aquatic ecosystems in general. Of the different types of dyes, MB, which is commonly used in textile dyeing, paper printing, and other sectors, can eventually build up in industrial effluents and be discharged into receiving streams and other water sources (Shakoor et al., 2016).

2.3.3. Adverse effects of methylene blue dye in the environment

Dye pollution is a hazard to ecological balance and human health because of its mutagenic, carcinogenic, and teratogenic effects when inhaled or absorbed via the skin. Massive and illegal releases of MB-contaminated wastewaters from textile mills into lakes and rivers have caused a severe threat to ecosystems, as the lack of dissolved oxygen in the water limits the growth of aquatic life (Guo et al., 2017). High concentrations of MB dye in aquatic environment stop the absorbing water's reoxygenation potential and cut off sunlight, interrupting biological activity in aquatic life as well as the photosynthesis cycle of aquatic plants and algae (Zaharia et al., 2011).

MB is also directly hazardous to human health, as it is poisonous, mutagenic, and carcinogenic. Dyspnea, diarrhea, and tachycardia are just a few of the respiratory, digestive, and cardiovascular disorders it can induce (Sham & Notley 2018). This dye can cause eye burns, which may be responsible for permanent injury to the eyes of human and animals. So, the treatment of wastewater contaminated by MB dye is the focus of considerable water treatment research (Khatri et al., 2015).

2.4. Adsorption of Dyes

Adsorption is defined as the attachment or adherence of particles to the surface of a solid substance. On the surface of the adsorbent material there are active adsorptive sites, which bind molecules (gas or liquid) from the adsorbate solution (Figure 2.5).

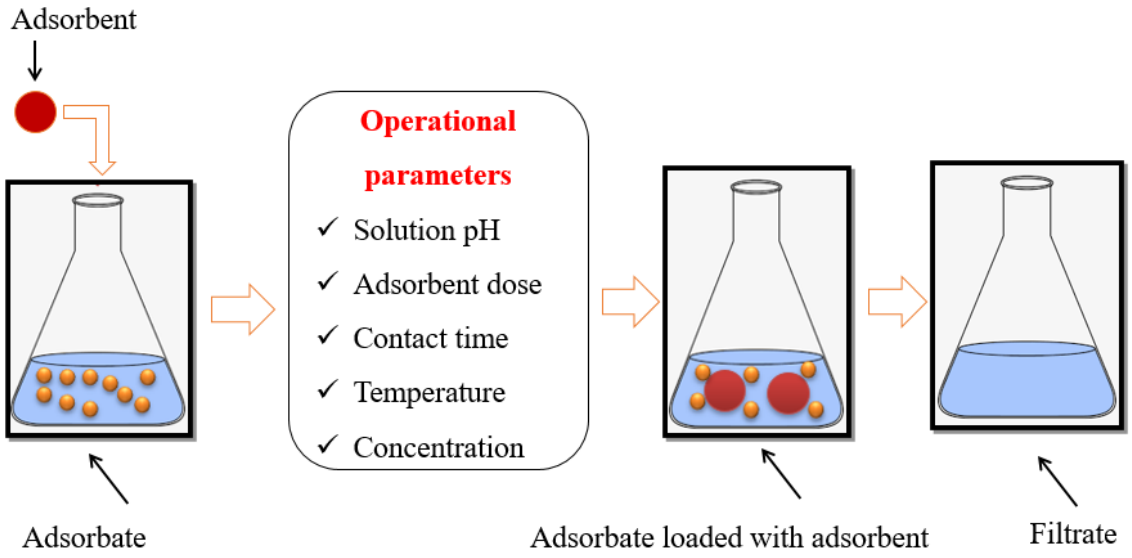

Figure 2. 5: Schematic diagram of batch adsorption (Khalid et al., 2020).

Molecules can be adsorbent either physically or chemically (Ceini et al., 2019) (Figure 2.6). The mass transition, in which gaseous or liquid molecules are moved to a solid phase, might take the form of migration, diffusion, or convection. Physisorption is defined by interactions such as Lewis acid-base, van der Waals, and Columbic, whereas chemisorption is distinguished by the formation of new adsorbate-adsorbent bonds (Yan et al., 2015). Due to the nature of the substance, the adsorptive sites may have the same or different energy. Adsorption has sparked attention for use in hydrogen storage, sensing, medication delivery, gas capture, and water treatment due to its concept (Monama et al., 2018).

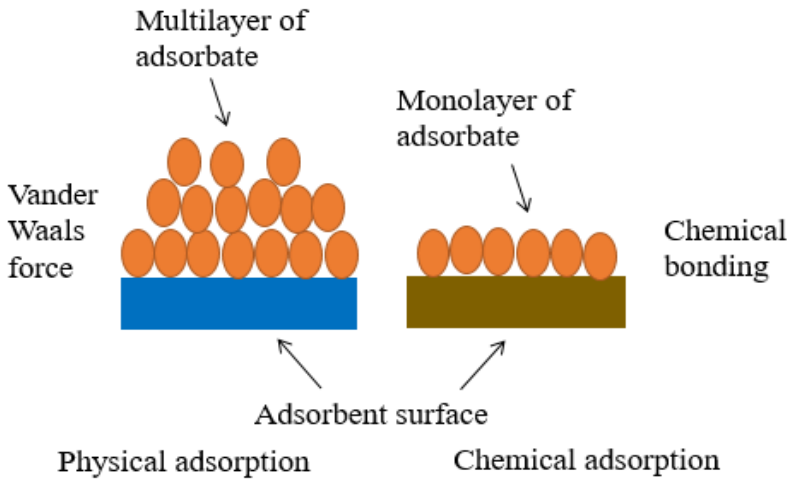

Figure 2. 6: Physical and chemical adsorption (Sarkar & Paul, 2016).

Adsorption for the treatment of dyes from wastewater has recently sparked attention due to its cheap operating costs, ease of design, efficiency, and speed of dye removal (Ji et al., 2018). As shown in Figure 2.7, different adsorbent materials can be used for the removal of dye contaminants from wastewater (Singh et al., 2018).

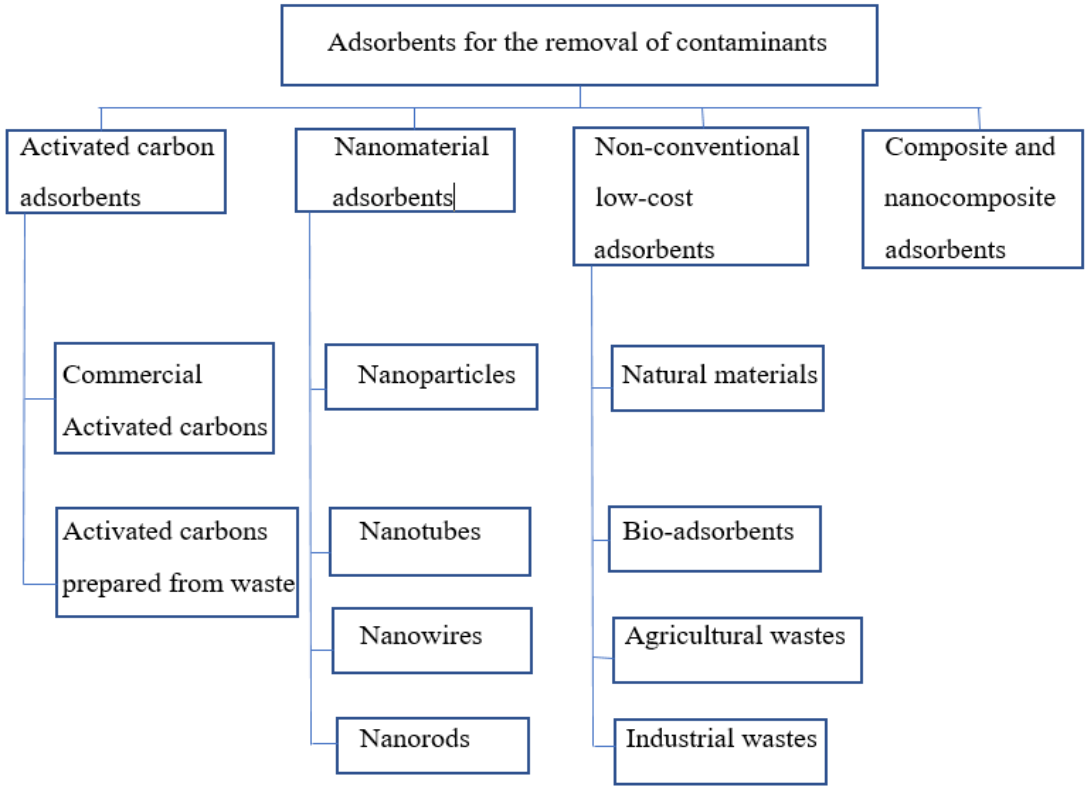

Figure 2. 7: Adsorbents for removal of dye contaminants from wastewater (Singh et al., 2018).

2.4.1. Applications of sewage sludge-based biochar as an adsorbent of methylene blue dye

Due to its exceptional physico-chemical characteristics, large quantities of SS generated as a by-product of municipal wastewater treatment processes, can be turned into an appealing adsorbent for the treatment of dye-containing wastewaters (Rashed et al. 2016). The adsorption of cationic dyes on SSBC is greatly influenced by surface chemistry and pore structure of SSBC. The adsorption of cationic dyes like MB was solely related to the bonding forces between negatively charged functional groups and the dye (Xu et al., 2018).

2.4.1.1. Mechanism and efficiency of dye adsorption by sewage sludge-based biochar

As shown in Figure 2.8, electrostatic interaction, hydrogen bonding, functional group interaction and π-π interaction can all be used as adsorption mechanisms for BC to remove organic contaminants (Qiu et al., 2009). This is dependent on the BC's physiochemical properties, such as dose, pyrolysis temperature, and medium/ effluent pH. Increased aromatic groups in the BC can result in π-π interactions with aromatic groups in organic contaminants. The adsorption of organic molecules is often found to be influenced by surface area (Ahmed et al., 2018). Sorption of organic contaminants from water onto BC occurs due to the latter's high surface area and microporosity; electrostatic attraction/repulsion between organic contaminants and BC has been indicated as another possible adsorption mechanism (Ahmad et al., 2014).

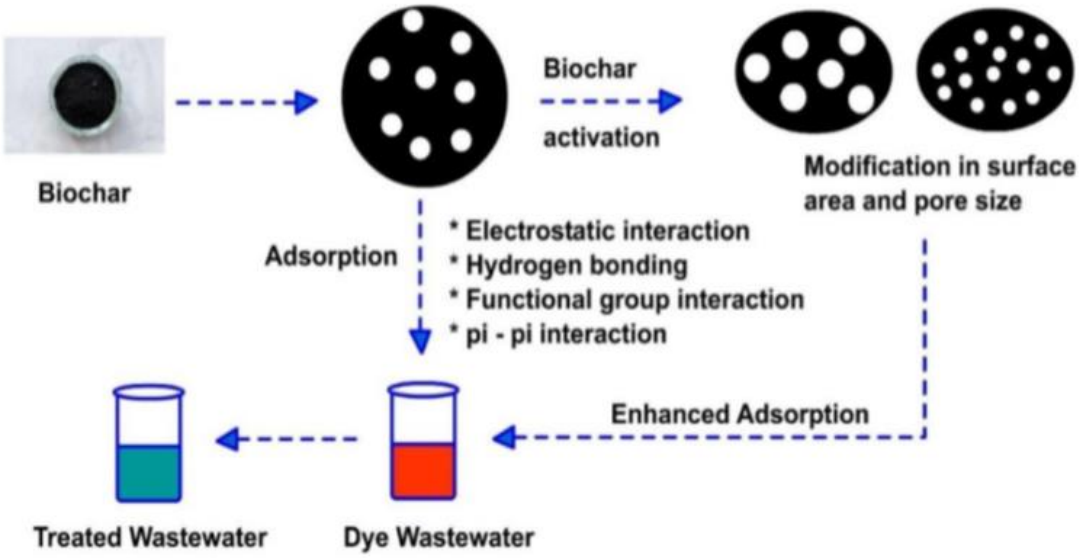

Figure 2. 8: Dye adsorption mechanism using BC (Qiu et al., 2009).

Since BC surfaces, in fact, are normally negatively charged, the main mechanism for cationic dye for instance MB adsorption onto SSBC is electrostatic interaction in which carboxyl, phosphate and anionic functional groups act as binding sites for cationic dyes (Rio et al., 2005; De Gisi et al., 2016).

Fan et al. (2017) used SSBC to remove MB from aqueous solution and nearly 90% of the dye was adsorbed within 10 h. This might be attributed to its coarse and porous texture

structure (Fan et al., 2017). Liu et al. (2013) used calcium as a binder to make granular activated carbon (4 mm in diameter and 9 mm long) from SS and its adsorption of MB reached 131.9 mg/g which was dominated by physisorption (Liu et al., 2013). This adsorption mechanism significantly differed from that in Fan's study (Fan et al., 2017). They declared that the MB adsorption process was well described by the pseudo-second-order kinetic model and the MB diffusion in micropores was the potential rate-controlling step. On the other study, the high mesoporous volume of activated SSBC by NaOH removes MB from different ecosystems. The adsorption depends on surface chemistry and the degree of meso porosity (Gomez-Pacheco et al., 2012). As we can see from the aforementioned research works, the adsorption efficiency of SSBC can be improved by adopting various activation processes. The most commonly used activation methods are physical activation and chemical activation. But other than these most commonly used activation methods, we can also mix SSBC with other sludge material like that of AlS to enhance the adsorption capacity of the biochar since AlS is widely available efficient adsorbent material for MB (Yusuff et al., 2018; El-Tokhy et al., 2020).

2.5. Alum Sludge

Water treatment residuals, sometimes referred to as water treatment sludge or waterworks sludge, are by-products generated by water treatment plants. Water treatment residuals are typically made up of naturally-occurring colloidal and other particulate matter (e.g. silt, clay, algae), dissolved natural organic matter (e.g. humic acids, fulvic acids), precipitated water treatment chemicals, oxide precipitates of inorganic species dissolved in the raw water (e.g. iron, manganese) and filter media flushed out during backwashing (Wolowiec et al., 2019; Quinones et al., 2016).

The coagulation and flocculation process, which removes suspended particles, dissolved inorganics, and organic matter, is an important stage in achieving clean water supply (Ahmad et al., 2017). Most water treatment plants in the world use aluminum sulphate, or just alum (Al_2 $(SO_4)_3.14H_2O$), for water clarification because alum is the cheapest and simplest Al-based flocculent available (Odimegwu et al., 2018). Al ions were hydrolyzed into aluminum hydroxide ($Al(OH)_3$) when alum salts were introduced to raw turbid water sources during the water purification process, as illustrated in Equation 1 (Ippolito et al., 2011).

$$Al_2(SO_4)_3 . 14H_2O + 3Ca(HCO_3)_2 \longrightarrow 2Al(OH)_3 (S) + 3CaSO_4 + 6CO_2 + 14H_2O \ldots \text{Eq. 1}$$

In the water treatment plant, when the chemical coagulant combines with suspended particles in the water, it will result in the formation of bigger heterogeneous aggregates known as flocs. Flocs settle from suspension to the bottom of settling basins. The settled WTR solids are collected and removed from the settling basins (Ippolito, 2015; Litaor et al., 2019). As an outcome, both the sedimentation process (after coagulation and flocculation) and the reverse washing process during the filtering stage produce AlS in water treatment plants. Before being dewatered, these two streams of sludge are thickened and treated to make cakes for final disposal (Xu et al., 2020). The settled AlS sediments are then collected from the settling basins, air-dried, and landfilled or beneficially used.

Wet sludge accounts for up to 5% of total processed water volume and is complex and costly to handle (Litaor et al., 2019). The volume of WTRs produced is dependent on a number of factors, including the volume of water or wastewater treated, the quality of the water or wastewater, color intensity, coagulant dosages, and many more (Szerzyna, 2013).

2.5.1. Alum sludge treatment and disposal

Many water purification stations discharge AlS into local drains, which eventually meet the water source on the downstream side of the intake. The wastes were deemed toxic to aquatic life owing to the inherent high amounts of Al and so, lately they have been landfilled or incinerated after drying (Ahmad et al., 2016). Landfilling is also constrained by land use, public concerns and more stringent environmental regulations. The simple method of final disposal, although a less expensive, is not a proper solution due to the possibility of contamination of water bodies and soil from the chemical products used in the treatment (Zhao et al., 2018). Incineration is very costly, emits greenhouse gases as well as other harmful substances such as dioxins and furans. Ash contains heavy metals, and its disposal incurs additional expenditures. In addition, burning is often unpopular with the public, and it only works for sludges with low moisture content (Devi et al., 2017).

2.5.2. Characteristics and composition of alum sludge

The quality of AlS is greatly reliant on the source of water quality, quality and purity of the alum and additional treatment chemicals employed, such as powdered activated carbon for taste and odour control, and polymers used to aid flocculation (Maiden et al., 2015). From

available literatures, AlS is generated with a variety of pollutants and contaminants, including clay minerals, sandy and loamy particles, organic matter, microorganisms, and Al-salt residual, depending on the source water (Li et al., 2018).

2.5.2.1. Physical structure

Although the quality of sludge varies from plant to plant, the core elements remain the same (Ackah et al., 2018). AlSs are bulky and gelatinous, especially before they've been dewatered. The surface of dewatered AlS is rough and amorphous. Observations utilizing powder X-Ray Diffraction (XRD) and SEM techniques have confirmed this (Chittoo et al., 2014). Oxalate aluminium is a characteristic that represents amorphous-structured aluminium hydroxide. Other researches have confirmed that the amorphous form of AlS is due to the presence of non-crystalline aluminium hydroxide, which increases the specific surface area of AlS (Yang et al., 2008). The median of the surface area results in literature, using the standard nitrogen Brunauer-Emmett-Teller (BET) surface area, revealed an average specific surface area of 121.895.3 m^2/g (Norah et al., 2020). A non-porous structure has a surface area of less than 10 m^2/g (Boyer et al., 2011). The specific surface area of AlS is directly related to the number of hydroxide sites available. This means that increasing AlS hydroxide sites is a significant way to increase specific surface area. Haynes et al. (2015) stated that particle size, shape and porosity determine surface area, and the larger the surface area, the more active sites there are.

2.5.2.2. Chemical composition

Elemental analysis of AlS is commonly performed using Inductively Coupled Plasma-Atomic/Optical Emission Spectrometer (ICP-AES/OES) as well as X-Ray Energy Dispersive Spectroscopy (X-Ray EDS) (Gao et al., 2013; Ackah et al., 2018). Total Al in AlS makes up about 16% of the chemical composition, with values ranging from 118,700 ± 24,260 mg/kg in different investigations (Table 2.3). Other components found in AlS include; Ca, SiO_4^{2-}, Fe, Cl^-, SO_4^{2-} and humic acids measured as total organic carbon. These organic and inorganic elements are those that have been extracted from raw the water and those that are present in the coagulants. Table 2.4 summarizes the literature's physicochemical composition of AlS.

Table 2. 4: Biophysico-chemical composition of AlS (Ahmad et al., 2016; Ippolito et al., 2011; Sales et al., 2011).

Parameter	Units	AlS	Parameter	Units	AlS
Al	mg/Kg	118,700 ± 24,260	Cd	mg/Kg	0.12 ± 0.02
Ca	mg/Kg	10,360 ± 4,299	Cr	mg/Kg	20 ± 7
Fe	mg/Kg	37,000 ± 19,740	Cu	mg/Kg	624 ± 581
K	mg/Kg	3547 ± 582	Hg	mg/Kg	0.46 ± 0.11
Mg	mg/Kg	2407 ± 572	Mn	mg/Kg	2998 ±1122
Na	mg/Kg	355 ± 142	Ni	mg/Kg	28 ± 10
S	mg/Kg	6763 ± 2955	Pb	mg/Kg	22 ± 12
pH	-	6.5 ± 0.3	Zn	mg/Kg	98 ± 31
Total solids	mg/L	3800 ± 1385	TOC	g/Kg	120.0 ± 33.8

2.5.3. Utilization of alum sludge in different areas

Over time, strategies for dealing with AlS have evolved. The reuse techniques were primarily created to target AlS as a usable material in many fields, so transforming AlS from a waste to a useful raw material and bolstering the sustainable principle. In a review by Babatunde and Zhao, three major types of previous and present AlS applications were recognized: wastewater treatment, engineering and construction materials, and land application (Babatunde et al., 2007). Dassanayake et al. (2015) primarily concerned on the use of AlS in agriculture rather than wastewater treatment. Babatunde et al. (2008) and Yang et al. (2018) addressed the usage of dewatered AlS as a substrate and filter in constructed wetlands, as well as how such types of emergent constructed wetlands can be a long-term wastewater treatment solution.

In recent years, potential reuse of AlS has been studied as a low-cost adsorbent because of their amorphous nature and large surface area. Aluminum hydroxide, the major component of AlS, can successfully adsorb anionic pollutants such as arsenate, fluoride, and phosphate, as well as organic and other inorganic pollutants, for the rehabilitation of many contaminated waters (Hua et al., 2018).

2.5.4. Application of alum sludge as an adsorbent for various pollutants

Regardless of the difference in source water composition, AlS commonly share two characteristics of interest: physically, AlS typically have both macro- and micro-porous structure within larger aggregates; and chemically, AlS contain substantial quantities of poorly-crystalline aluminum hydroxide. These properties make AlS a suitable option for reuse as a sorbent, especially with regards to controlling strongly-sorbing oxyanion, organic pollutants as well as heavy metals (Shen et al., 2019). A large number of studies have demonstrated AlS ability and considerable capacity as a low-cost adsorbent (Ahmad et al., 2016; Xu et al., 2020). Zhao et al. (2015) used AlS for arsenic immobilization and found that whenever the pH of the arsenic solution was changed from 9.0 to 4.0, the highest adsorption capacities ranged from 0.61 to 0.96 mg-As/g (Zhao et al., 2015). Li et al. (2018) examined modified AlS (pyrolysis and hydrochloric acid treatment) for fluoride immobilization and discovered that the maximal adsorption capacity could be 0.14 mg/g, with an 81.2% fluoride removal rate (Li et al., 2018). In some other work, Shakya et al. (2019) employed AlS to remove fluoride from a starting concentration of 5.0 mg/L to an 80% reduction in 2 hours (Shakya et al., 2019). Dias et al. (2021) have looked at the removal of two endocrine disrupting chemicals, 17-estradiol and 17-ethinylestradiol, from water treatment plant sludge without any modifications (Dias et al., 2021). Meanwhile, investigations on a variety of scales have looked into the ability and capability of AlS to adsorb a variety of heavy metals and semimetals, including Cd, Cr, Co, Cu, Pb, Hg, Ni, Zn, Mo, V, Ga, As, Se, and others. Shen et al. (2019) conducted a comprehensive review on this aspect, with adsorption capacities being reported (Shen et al., 2019). These studies have shown that AlS is a cost-effective sorbent that can reduce the concentration of toxic heavy metals in aqueous solutions. Similar research has shown that AlS is an excellent low-cost adsorbent for removing phosphate and nitrate from wastewater, broadening the scope and benefits of the water treatment sludge reuse regime. Using AlS, Nair and Ahamed were able to remove 95% of phosphorus (Nair et al., 2015).

2.5.4.1. Alum sludge as an adsorbent for methylene blue

Studies showed that AlS can be employed as dyes adsorbent (Rashad et al.,2016; Sarioglu & Atay et al., 2006). Most researchers agree that adsorption reactions in general as well as adsorption capacity and removal efficiency of AlS depends on the chemical and physical characteristics of the adsorbent used as well as external conditions of the experiments. Physical and chemical characteristics of the sorbent itself include its particle size, surface functional groups, specific surface area, metal content and stability. External or environmental conditions are those that surround the adsorption components and these comprise the solution pH, temperature, presence of competitors, as well as dosage of sorbent (Ali et al., 2012).

MB adsorption capacities of AlS that have been recorded in literature includes, chemically and physically treated AlS based adsorbent where the maximum adsorption capacity of AlS was 85.4 mg/g (Rashed et al., 2016), and other study used AlS as a starting material and immobilized by sodium alginate (SA) to develop low cost adsorbent for the removal of MB from aqueous solutions and removal efficiency of MB was 92.5% under the optimum conditions (Poormand et al., 2017). These differences were attributed to variations in the qualities of the AlS used in the studies as well as external conditions.

The removal of MB dye onto AlS adsorbent were due to the formation of physical and chemical bonds including van der Waals forces, hydrogen bonding, and hydrophobic interactions (Agarwal et al., 2016). The electrostatic interactions were identified as main mechanisms for dye removal (Devi et al., 2017). The application of Langmuir model which proved its ability in the description of sorption data and pseudo first-order model which represent the kinetic data indicate that the removal process of MB by AlS was governed by chemisorption and physical forces (Al Juboury et al., 2020; Yusuff et al., 2018).

2.6. Adsorption Equilibrium Isotherm Models

The adsorption isotherm depicts the interaction between the adsorbent and the adsorbate at a constant temperature under equilibrium conditions and also represents the effect of initial adsorbate concentration as a function of adsorbent dosage. Additionally, they provide information about the mechanisms of adsorption, adsorption capacity and surface properties. Basically the models employed are Langmuir, and Freundlich isotherm models (Singh et al., 2018).

In 1916, the Langmuir isotherm was established by Irving Langmuir. According to the model theory, all active sites on a solid surface have the same energy, resulting in homogenous adsorption of adsorbate molecules (monolayer coverage) (Li et al., 2017). Graphically, adsorption equilibrium is observed by a plateau, which is a point where all active sites are fully occupied and no further adsorption can occur (State et al., 2012). The Langmuir isotherm assumes that homogeneous monolayer adsorption occurs on the surface of the adsorbent can be expressed as set out in the Equation 2.

$$\frac{C_e}{q_e} = \frac{1}{q_m} c_e + \frac{1}{q_m K_L} \quad \text{.....Eq. 2}$$

where, the K_L (Lg^{-1}) is the Langmuir equilibrium constant and q_m (mg g^{-1}) is about the maximum monolayer saturation capacity obtained from the theoretical Langmuir model. Whilst, q_e (mg g^{-1}) is the adsorption capacity of MB and C_e is the MB concentration remaining in solution at equilibrium respectively.

On the other hand, the Freundlich isotherm model described the adsorption on the heterogeneous surface of the adsorbent and this through a multilayer adsorption mechanism. It is one of the oldest models which is extensively used, it was developed by Freundlich in 1932**.** In this model, it is described that during the adsorption process different sites of the adsorbent are involved with several adsorption energy (Bilgic, 2019). The equation for Freundlich isotherm model can be described as Equation 3:

$$\log q_e = \frac{1}{n} logC_e + logK_F \quad \text{.....Eq. 3}$$

where, K_F and $\frac{1}{n}$ are Freundlich constants and the characteristics of the system, q_e is the amount of adsorbate per unit weight of adsorbent in equilibrium with a solution concentration C_e in mg/L.

2.7. Adsorption Kinetics Models

Both the rate of adsorption and the amount adsorbed are necessary to attain an acceptable optimal performance. A good adsorbent should have quick adsorption kinetics in addition to porosity, polarity, and high surface area. For practical application, it is critical that the highest amount of adsorbate be removed in the quickest time possible (Gupta et al., 2009).

Lagergren's pseudo-first-order equation or pseudo-second-order equation can be used to investigate the mechanism of adsorption. The first-order model is believed to be the earliest model and it was developed by Lagragren in 1898 (Qiu et al., 2009). To describe the kinetic process of liquid-solid phase adsorption he presented the first-order model as presented in Equation 4. On the other hand, now a days the pseudo-second-order rate equation is probably the most widely used model for adsorption kinetics (Bullen et al., 2021). Equation 4 and 5 express the liner form of pseudo-first-order rate equation and pseudo-second-order rate equation, respectively.

$$\log(q_e - q_t) = \frac{-K_1 t}{2.303} + \log q_e \quad \text{..... Eq. 4}$$

$$\frac{t}{q_t} = \frac{t}{q_e} t + \frac{1}{k_2 q_e 2} \quad \text{..... Eq. 5}$$

where, q_e and q_t (mg/g) are the adsorption capacities at equilibrium and time t (min), respectively, K_1 (min^{-1}) is the pseudo first order rate constant for the kinetic model and k_2 is the equilibrium rate constant of pseudo-second order sorption.

2.8. Parameters that Affects Dye Adsorption Process

Solution pH

One of the most critical parameter determining adsorption process has been identified as the pH of the aqueous solution. It affects dye chemistry in the solution as well as the degree of ionization of the solute, the surface charge of the adsorbent, and dissociation of functional groups on the active sites of the adsorbent. Protonation of the dye occurs at a low pH, resulting in reduced dye adsorption in acidic media. At low pH, dye removal is inhibited, owing to greater competition between protons and dye molecules for the same binding sites. The dye gets more deprotonated as the pH of the solution rises, increasing the negative charge density on the adsorbent's surface. As a result, effective dye removal is observed as the pH of the solution rises (Pathania et al., 2017).

For MB, when the MB dye solution's starting pH was raised from 4 to 11, the percentage of dye removed increased from lower to greater. The type of the adsorbent influences the increasing trend of MB removal with increasing pH. At lower pH, the percentage of MB removed decreased, whereas at higher pH, the trend of MB removal increased (Rahman, et al., 2012).

Adsorbent dose

Adsorbent dosage is an important parameter because adsorbents provide the binding sites for dye adsorption. Therefore, adsorbent dosages determine the capacity of an adsorbent for a given initial concentration, separation cost and consequently the overall water treatment cost (Fan et al., 2017). The amount, size, and pore volume of adsorbent significantly influence the capacity of adsorption toward various molecules. The adsorbent's pore size and unoccupied site limit the rate and amount of dye molecules that can migrate to the surface. The removal effectiveness grew significantly when the amount of adsorbent was raised until it reached a set amount of adsorbent, after which it dropped beyond the fixed adsorbent dose. Then, as the amount of adsorbent was increased, the removal efficiencies did not change considerably (Menya et al., 2018).

Adsorbate concentration

The adsorbate concentration is another crucial factor that influences the adsorption process. With increasing starting concentrations, the clearance effectiveness decreases. At low concentrations, most of the MB in a solution may come into contact with the adsorbent's active sites, but as the concentration rises, all MB species will be unavailable to contact the active surface due to active sites already being occupied (Rahman et al., 2012).

Contact time

Another crucial characteristic that has been discovered to have a major impact on the adsorption process is contact time. According to certain studies, dye removal efficiency increases fast up to 60 minutes, after which the adsorption rate gradually drops. This demonstrates that when the dye and adsorbent have enough contact time, the removal efficiency is higher until the equilibrium time is attained (Subramaniam & Ponnusamy, 2015).

Ho et al. (2005) demonstrated that as the dye concentration was increased, the adsorption capacity rose, and the rate of adsorption on the surface of the adsorbent had to be proportional to the driving force times the area. Within 30 minutes of contact time, a rapid initial dye removal was achieved, and adsorption capacity at equilibrium increased, but percent removal declined from 100 to 61 % as the MB dye concentration was varied. The equilibrium state was obtained with a further increase in contact time (Ho et al., 2005). The

quick removal of dye molecules was owing to solute transfer, as there were only adsorbate-adsorbent interactions with little interference from solute-solute interactions (Kaczmarski & Bellot, 2013).

3. MATERIALS AND METHODS

3.1. Materials

3.1.1. Chemicals and reagents

All chemicals and reagents used in this study were analytical grades. Hydrochloric acid, HCl (LOBA CHEMIE PVT.LTD, 35.4%) and Sodium hydroxide, NaOH (LOBA CHEMIE PVT.LTD, 98%), were used for pH adjustment and desorption experiments, Ethanol (SAMIR TECH-CHEM, 96%) was used as a solvent for SSBC-AlS composite adsorbent preparation, Potassium Chloride, KCl (LOBA CHEMIE PVT.LTD) was used as electrolyte for determination of zero point charge (pH_{pzc}) of adsorbent and Methylene blue, $C_{16}H_{18}ClN_3S$ (SAMIR TECH-CHEM, Mw = 319.87 g/mol) was used for stock MB solution preparation. In addition, Sulfuric acid, H_2SO_4 (LOBA CHEMIE PVT.LTD, 96%) and detergents were used for equipment cleaning and distilled water was used to prepare aqueous solutions and to rinse equipments.

3.1.2. Apparatus and equipments

The apparatus and equipments used for characterization of adsorbents during this research work were, Fourier Transform-Infrared Spectrometer (FT-IR) (model FT/IR6600, JAPAN), X-Ray Diffractometer (XRD) (XRD-7000), Scanning Electron Microscope (SEM) (JCM-6000PLUS Bench Top SEM, JEOL, Japan), Brunauer-Emmett-Teller (BET) (SA-9600 Series Surface Area Analyzer), Thermogravimetric Analysis-Differential Thermal Analysis (TGA-DTA) (Shimadzu co., DTG-60H, South Korea Japan), and UV-Vis spectrometer (UV-Vis-2000 AUG, USA). Other than these sample collection materials (buckets, glass bottles and plastic bottles), digital electronic balance (FA2104, German), muffle furnace (MF2015, India), pH and conductivity meter (model Mettler-Toledo GmbH), oven, orbital shaker (OS-500OS), ultrasonic instrument, centrifuge (LC-O4C), filter paper (Whatman 42), mortar and pestle, glass rod, pipettes, spatulas, Erlenmeyer flask, filter cloth, shovels, volumetric flask, and different sizes of beakers were used for different activities.

3.2. Methods

3.2.1. Collection and analysis of real textile wastewater

The wastewater samples were collected from the Eastern Industrial Zone (EIZ) in Dukem, Ethiopia. It is located, 35 km southeast of Addis Ababa, 10 km to North West of Bishoftu Town, and 63 Km Northwest of Adama Town. EIZ is the first and largest-scale industrial park for Ethiopia and numerous Chinese-based companies in textile, apparel, building materials (including east steel, cement factory), mechanical manufacturing, and agricultural processing were found. The literatures (Bahiru et al., 2019; Dagne, 2020) reported that 26 Chinese companies are working and manufacturing different products for export markets having an agreement with EIZ in all targeted areas. In addition, to the present 26 manufacturing industries, more than 20 other manufacturing industries are about to join the Eastern Industrial Zone. This suggests that more wastewater from the various industry of EIZ is discharged to the surrounding through one wastewater channel; this wastewater is used as a source of irrigation water by the farmers around this industry's area.

The MB dye contaminated textile wastewater sample was collected from discharging points of Dongfang Spinning, Printing and Dyeing PLC textile industry after the dyeing process. During the sample collection period, the textile industry used MB as dyeing agent. Using a plastic bottle, a sample volume of 1 L was collected during the month of August 2022. The bottle used for collecting MB dye contaminated textile wastewater samples was previously washed carefully with detergent and rinsed with distilled water at the point of collection. Sample collection, preservation and storage were performed according to standard procedures recommended by United States Environmental Protection Agency (USEPA) guide to water sample collection. Then, measurement of physicochemical parameters of real textile wastewater sample including, color, pH, temperature, and electrical conductivity was performed according to experimental procedures descried by Zazou et al. (2019) and kept for adsorption experiment.

3.2.2 Preparation of methylene blue stock and working solutions

At room temperature, 1 g of MB dye was added to distilled water to prepare a stoke solution of 1000 $mg \cdot L^{-1}$ in a 1000 mL volumetric flask. Then, the solution storage bottle was wrapped with aluminum foil to prevent de-colorization of the solution as MB is naturally very sensitive to light. The standard series solutions were prepared from the previously

prepared stock solution by using the dilution method. UV-Vis spectrometer was used to measure the concentrations of MB dye solutions at the maximum absorbance of λmax 665 nm (Utomo et al., 2015).

3.2.3. Adsorbent preparation

3.2.3.1. Alum sludge collection and adsorbent preparation

Fresh AlS sample was collected from Adama drinking water plant, Oromia Regional State, Ethiopia, using the composite sampling method in every two days for two-week in March 2022. The sludge was placed into clean buckets using clean shovels. Once filled, the buckets were sealed and transport to the laboratory. The semi-liquid AlS was settled for 24 h to separate the liquid part from the sludge. The AlS cake was sun-dried for 3 days till complete dryness. The sun-dried AlS was then ground using a mortar and pestle then sieved to provide the testing adsorbent with particle size of 0.18 mm (Rashed et al., 2016).

3.2.3.2. Sewage sludge collection and preparation

SS sample was collected from Adama Science and Technology University wastewater treatment plant located at Adama in March 2022. The sample was collected when the sludge was pumped from an open ducts by clean buckets and for better results, the SS was carefully mixed by pouring it repeatedly from one bucket into another. The sludge was washed three times with distilled water to remove dust and surface impurities. Then, liquid sludge was settled for 24 h to separate the liquid part from the sludge in unsealed, partly filled polyethylene buckets. The sample for measuring of volatile compounds was stored in sealed glass bottles (Lacorte et al., 2012). The sample has a dark black color.

After 24 h the sludge was filtered using clean filter cloth then after the filtered SS was sun-dried in a clean yard for 4 days to remove the moisture (Tripathi et al., 2016). The sun-dried SS sample was then crushed and sieved to obtain 2 mm particle size using gravimetric sieve. This was because apart from the drying process, the dewatered sludge must be crushed to small sizes to attain high heating rate (Gopinath et al., 2021). Finally, the treated sample was stored inside an air-tight plastic bag and subjected to the process of pyrolysis.

3.2.3.3. Sewage sludge-based biochar preparation

The sun-dried SS samples were pyrolyzed at temperatures of 350 °C, 450 °C and 550 °C in muffle furnace for 2 h (Fan et al.,2017). The muffle furnace temperature was programmed to increase at a rate of 10 °C ·min^{-1} then the produced SSBC was cooled for 24 h in a dissector (Fan et al., 2017). The SSBC was washed with plenty of distilled water to remove any non-adhesive impurities and small particles, and dried at 105 ^{o}C in an oven to constant weight. The dried SSBC was grind and passed through 0.18 mm sieve to attain same particle size as AlS-based adsorbent labelled as SSBC350, SSBC450, and SSB550. Then, the SSBC was stored inside a sealed plastic container until use (Ferreira et al., 2017).

3.2.3.4. Composite adsorbent preparation

After preparing the individual adsorbent materials, five different ratios of SSBC and AlS (100:0, 75:25, 50:50, 25:75, and 0:100, respectively) were first physically mixed and then the mixtures were dispersed by sonicating in 30 ml of ethanol in beakers for 1.5 h to obtain uniform dispersions. Then, the dispersions were stirred using magnetic stirrer for 1 h at room temperature to form a homogenized solutions. The obtained precipitates were centrifuged and washed with distilled water and ethanol several times. The prepared SSBC-AlS composite adsorbents were dried at 80 °C until constant weight and grind and passed through 0.18 mm sieve to attain suitable particle size. Finally, the prepared SSBC-AlS composite adsorbents were stored for characterizations and batch adsorption experiments (Affam, 2020).

3.2.4. Physicochemical analysis of sewage sludge, sewage sludge-based biochar and alum sludge

All the physicochemical characteristics of SS, SSBC, and AlS analysis were conducted in ASTU wastewater treatment plant laboratory.

Moisture content

The moisture content of SS (ASTM D3173), SSBC (Enders & Lehmann et al., 2017) and AlS (ASTM D1102-56) samples were determined by the weight loss of the sample as it was heated to 105 °C for 24 h. The moisture content was calculated using Equation 6.

$$\text{Moisture (\%)} = \frac{(W_1 - W_2)}{W_1} \times 100 \quad \ldots\ldots\ldots\ldots\ldots\ldots\ldots\ldots\ldots \text{Eq. 6}$$

where, w_1 and w_2 are weight of sample before and after drying (gm), respectively.

Ash content

Ash content of SS sample was determined by taking 1 g of dried sample and then incinerated at 800 ^{o}C for 3 h. The crucible was cooled in desiccators and reweighed (ASTM D3174). As for the determination of the ash content of the SSBC, sample of SSBC was heated at 800 ^{o}C in muffle furnace for 1 h (Sierra et al., 2017). To determine the ash content of AlS, 1 g of sample was taken and kept in a muffle furnace for 2 h at a temperature of 550 °C. Then, it was taken out and kept in desiccators for half an hour to cool down and then again the weight was measured (ASTM D1102-56). The percentage weight of the remaining samples was considered as ash content Equation 7.

$$\text{Ash (\%)} = \frac{W_2}{W_1} \times 100 \ldots\ldots\ldots\ldots\ldots\ldots\ldots\ldots\ldots\ldots\ldots\ldots\ldots \text{Eq. 7}$$

where, w_1 and w_2 are the weight of sample before and after incineration (gm), respectively.

Volatile matter content

For volatile matter determination of the SS and SSBC samples, about 1 g of dried sample was weighed and incinerated at 950 ^{0}C for 7 min in muffle furnace. The crucible was cooled in desiccators and reweighed. The percentage weight loss was regarded as the percentage of volatile matter (ASTM D3175). The volatile matter content was calculated using Equation 8.

$$\text{Volatile Matter (\%)} = \frac{(W_1 - W_2)}{W_1} \times 100 \ldots\ldots\ldots\ldots\ldots\ldots\ldots\ldots\ldots\ldots \text{Eq. 8}$$

where, w_1 and w_2 are weight of sample before and after incineration (gm), respectively.

Fixed carbon

The fixed carbon content of SS and SSBC is a calculated value, and it is the resultant of summation of percentage of ash content and volatile matter content subtracted from 100 (ASTM, 1989). The fixed carbon content was calculated using Equation 9.

$$Fixed\ Carbon\ (\%) = 100 - (Moisture\ content\ (\%) + Ash\ content\ (\%) + Volatile\ matter\ (\%))$$ ……. Eq. 9

SSBC yield

The yield of the BC is one of the essential parameters used to evaluate the efficiency of the BC preparation method. The yield of SSBC was determined as the ratio of the weight of the produced BC to the dry weight of the SS subjected to pyrolysis. SSBC yield was calculated using Equation 10 (Stella Mary et al., 2016).

$$Yield_{SSBC}(\%) = \frac{Mass\ of\ BC(gm)}{Mass\ of\ dried\ SS(gm)} \times 100$$ …….. Eq. 10

Bulk density

The bulk density of SSBC was evaluated by placing 5 g of SSBC in a 10 mL graduated cylinder to a volume of 2-4cm^3. Then, the cylinder was tapped against a hard surface about 50 times to "compact" the SSBC and the volume (cm^3) was read (ASTM D2854-09 2014). Whereas for AlS, 50 g of the dried sample was transferred to 100 mL graduated cylinder. Then, the cylinder was tapped four times to settle the material (ASTM D1102-56). The bulk density was evaluated using Equation 11.

$$\rho = \frac{M_s}{V_p}$$ ……Eq. 11

where, ρ is the bulk density (g/cm^3), is the sample mass (g), and is the volume of the sample in cm^3.

Particle density

To determine the particle density of AlS, 60 ml distilled water was measured and transferred to 100 ml cylinder. On this, 50 gm of dried sample was weighed and transferred into the cylinder with water. Then, it was stirred to remove trapped air (ASTM D1102-56). The volume was read and the particle density was calculated using Equation 12.

$$p = \frac{D}{S}$$ ……. Eq. 12

where, p is particle density (gm/cm^3), D is mass of dry sample (gm), and S is volume of sample.

Porosity

Porosity is the fraction of the total powder volume that is taken up by the pore. The porosity of the sludge powder was determined based on the particle density and bulk density of the sludge using Equation 13. (ASTM D1102-56).

$$P = 1 - \left(\frac{B_d}{P_d}\right) \quad \text{Eq. 13}$$

where, P is Porosity (%), B_d is bulk density and P_d is particle density.

pH

The pH value of fresh SS sample was measured directly after sample collection using a glass electrode pH meter. The pH of SSBC and AlS was determined using the 24 h equilibrated solution of sample and distilled water with a solid/liquid ratio of 1:10 (w/w) (Fan et al., 2017, ASTM (D1102-56). Before each measurement, the pH meter was calibrated and corrected for temperature.

3.2.5. Structural and surface characterization of sewage sludge-based biochar, alum sludge, and sewage sludge based biochar-alum sludge composite adsorbent

The adsorption rate is specific to the adsorbent and largely depends on the characteristics of the adsorbent (Alatalo et al., 2013). In this study, the structural characteristics of the adsorbent were studied by detecting FTIR, TGA-DTA, XRD, SEM, BET and pH_{PZC}.

3.2.5.1. Fourier transform-infrared spectroscopy (FT-IR) analysis

The FT-IR technique was used to qualitatively estimate the functional groups on the surface of the SSBC pyrolyzed at different pyrolysis temperature, AlS and SSBC-AlS composite adsorbent. FT-IR spectroscopy (model FT/IR6600, JAPAN) recorded the spectra in the wavelength range of 400-4000 cm^{-1} using the potassium bromide (KBr) pellet method. For FT-IR characterization, 1 mg of the sample and 100 mg of KBr were mixed with mortar and pestle. Then a small amount of powder from the mixture was pelletized using a mechanical presser. Finally, the pellet was analyzed using a FTIR spectrometer to determine the structural elucidation of the analyte (Ravulapalli & Kunta, 2018). Then, in this study the FT-IR analysis results of SSBC pyrolyzed at different pyrolysis temperature were considered as one of parameter to select the best pyrolysis temperature to prepare SSBC.

The FTIR analysis was carried out in Jimma Institutions of Technology, at the Department of Material Science and Engineering.

3.2.5.2. Thermogravimetric analysis (TGA)-Differential thermal analysis (DTA) analysis

TGA coupled with DTA by a (Shimadzu co., DTG-60H, South Korea Japan) analytical instrument, was used to determine the thermal stability and percentage weight loss of the SSBC350, SSBC450, SSBC550, and SSBC-AlS as a function of temperature under a constant rate of heating. An oven-dried adsorbent samples were heated from room temperature to 700°C in a Platinum/alumina cup with a heating rate of 10 °C/min, and an empty Platinum/alumina cup as control. 700 °C was taken as final temperature, because SSBC at this temperature is mostly stable implying no more degradation to take place (Ali et al., 2021). The analysis was performed in Bahirdar University, at the Department of Chemistry.

3.2.5.3. X-ray diffraction (XRD) analysis

The XRD patterns SSBC550, AlS and SSBC-AlS were recorded using an X-ray diffractometer (XRD-7000) in Jimma Institutions of Technology, at the Department of Material Science and Engineering to study the oxides composition as well as the amorphous or crystalline nature of the adsorbent materials. Small amount of adsorbent was taken for each adsorbent from already prepared samples for XRD characterization and filled in a sample holder. Then the sample was analyzed by using an X-ray diffractometer with Cu-Kα radiation source at λ= 1.54 Å and operating at 40 kV and 30 mA. X-ray diffractograms were obtained for the 2θ angles scan range from 10˚ to 80˚ with scans step 0.02˚. All the experiments were done at room temperature, with a scans speed of 3˚/ min, and a counting time of 0.40 sec.

3.2.5.4. Scanning electron microscope (SEM) analysis

The SSBC550, AlS and SSBC-AlS composite adsorbent surface morphology were characterized by a SEM (JCM-6000PLUS Bench Top SEM, JEOL, Japan) using a high-energy electron, and the outcoming electrons are analyzed (by applying a 10 kV electron acceleration voltage) in Adama Science and Technology University, at the Department of Applied Biology. For SEM characterization, 30 mg sample were taken from

each previously prepared samples and characterized by using SEM were the resulting images provides information about the surface features and texture, shape, size, and arrangement of the particles on the sample's surface (Gregorio et al., 2018; Sharma et al., 2018).

3.2.5.5. Brunauer-Emmett -Teller (BET) analysis

Since adsorption is surface phenomenon, the SSBC-AlS composite adsorbent specific surface area was characterized by the BET instrument (SA-9600 Series Surface Area Analyzer) in Addis Abeba Science and Technology University at the department of Chemical Engineering. For BET characterization, the empty sample cell was weighed using an electronic balance and 0.1 g of the sample was placed in the empty samples cell. Then, the sample was degassed at temperature 300 ˚C for 9 h to remove impurity in the degas station of surface area analyzer according to the International Union of Pure and Applied chemistry (IUPAC). After degassing, 0.05 g of the sample was placed in the analysis station in the range of 0.1 to 0.99 relative pressures and 10 psi of nitrogen gas using Brunauer-Emmett-Teller (BET) (Ngan et al., 2019).

3.2.5.6. Point of zero charge (pH_{pzc}) analysis

The values of pH_{pzc} for SSBC-AlS composite adsorbent was determined by contacting the 0.025 g sample with 0.1 M KCl solution (25 mL) at different initial pH (2-10). The initial pH of the mixture solution was adjusted to the range using either 1 M HCl or 1 M NaOH solutions. Each tube was vigorously agitated in a shaker for 24 h at ambient room temperature. After that, the suspensions were settled down and the final pH was measured immediately. The differences between final and initial pH values (Δ pH) were calculated and plotted against the initial pH values. Therefore, the initial pH at which Δ pH is zero is the pH_{pzc} (Zeng et al., 2021).

3.2.6. Batch adsorption experiments

Prior to batch adsorption experiments to optimize the factors that affect the adsorption process, pre-test adsorption experiments at optimized working condition was performed. The pre-test experiment was conducted to selected the best adsorbent material among the five different proportion of SSBC and AlS (100:0, 75:25, 50:50, 25:75, and 0:100, respectively). As indicated in (Appendix 1) the pre-test experiment was conducted based on available literature by performing batch adsorption experiment at pH 7, dose of 0.5 g/100ml,

contact time of 60 minutes, initial concentration of 100 mg/L, shaking speed of 100 rpm at room temperature. The criterion utilized to specify the best proportion is the highest value of adsorption capacity to remove MB from contaminated water (Appendix 1).

All adsorption experiments were carried out in batch mode because of the simplicity and reliability of the technique for small-scale investigations (Sharma et al., 2018). Batch mode adsorption studies for individual parameters were carried out using a 250 mL beaker and the parameters such as solution temperature, MB initial concentration, SSBC-AlS adsorbent dose, contact time, and pH were studied by adjusting the pH of the solution by 0.1 N HCl and 0.1 N NaOH solutions (Raposo et al., 2009). After each batch adsorption experiment was completed using selected SSBC-AlS composite adsorbent, the resulting suspension was taken and filtered using a Whatman filter paper (42) then the filtrate was analyzed for the corresponding MB dye concentration using UV-Vis spectrophotometer (UV-Vis-2000 AUG, USA) at the maximum wavelength of 665 nm (El-Tokhy et al., 2020). All experiments were repeated for three times, and additional analysis was performed when the difference between the two measurements was greater than 5%. Then, the percent adsorption efficiency (% R) and the adsorption capacity (milligram of dye adsorbed per gram of adsorbent (q_e)) were calculated using Equations 14 and 15, respectively.

$$\% R = \frac{(C_o - C_f)}{C_o} \times 100 \quad \text{..... Eq. 14}$$

where, % R is percent removal, C_o is initial dye concentration (mg/L), and C_f is concentration after adsorption (mg/L).

$$q_e = \frac{(C_o - C_e)V}{m} \times 100 \quad \text{..... Eq. 15}$$

where, q_e is the MB dye quantity adsorbed at equilibrium (mg/g), C_o is initial concentration of MB dye (mg/L), C_e is the equilibrium MB concentration in solution after adsorption, m is adsorbent mass in gram and V is volume of MB dye solution (L) used during the experiment (Petrova et al., 2017).

Effect of solution temperature

The effect of temperature towards adsorption efficiency of SSBC-AlS was studied by varying the solution temperature and keeping other variables constant. The temperature range (15-55 ^oC by 10 ^oC difference) was taken based on the study reported by Dordevic et

al. (2016). 0.5 g of adsorbent dose was added to a 100 ml volume of 100 mg/L MB dye solution for 60 minutes contact time at stirring rate of 100 rpm and pH 7. Then after the completion of the experiment, the filtrate concentrations of MB dye were analyzed using a UV-Vis spectrophotometer.

Effect of pH

The effect of initial pH of the solution was investigated at various pH (5, 6, 7, 8, and 9) and making other parameters fixed. 0.5 g of AlS-SSBC composite adsorbent was added to 100 ml volume of 100 mg/L MB dye aqueous solution. The experiment temperature was 25 ^{o}C and stirred at 100 rpm for a constant sorption time of 60 minutes. The pH range (5-9) was selected because, most literature reported that the maximum MB removal efficiency was obtained on this pH range (El-Tokhy et al., 2020; Al Juboury et al., 2017). Within this pH range, acidic substances on adsorbents surface are gradually neutralized, and negative surface charge of adsorbents are continuously increased. Finally, the residual MB dye concentration which remains in the filtrate was measured by UV-Vis spectrophotometer.

Effect of adsorbent dose

100 ml volume of 100 mg/L MB dye solution was mixed with various dosages of SSBC-AlS composite adsorbent (0.25, 0.5, 0.75, 1, 1.25, and 1.5 g) at a contact time of 60 minutes, stirring rate of 100 rpm, temperature of 25 ^{o}C and pH 7. The adsorbent dose (0.25, 0.5, 0.75, 1, 1.25, and 1.5 g) was selected and studied based on the literature (Fan et al., 2017). After this, the residual MB dye concentration which remains in the filtrate was measured by UV-Vis spectrophotometer.

Effect of contact time

1 g of adsorbent was added to 100 ml of 100 mg/L MB dye solution for various contact times (15, 30, 45, 60, and 90 minutes) at a constant pH 7, stirring rate of 100 rpm and temperature of 25 ^{o}C. The contact time was selected and studied based on the literature reported by El-Tokhy et al. (2020). After the specified time, the residual MB dye concentration which remains in the filtrate was measured by UV-Vis spectrophotometer.

Effect of initial methylene blue dye concentration

1 g of adsorbent was placed in beaker with 100 ml volume of MB dye solution. The initial concentrations of the dye solutions were (10, 50, 100, 150 and 200 mg/L). The initial concentration range was selected based on the literatures reported that the concentration of MB present in wastewater is in this range (Yusuff et al., 2018; Liu et al., 2013). The pH was adjusted at 7, the contact time of experiment was fixed at 30 minutes, the stirring rate was 100 rpm and the temperature was 25 ^{o}C. The mixture was agitated and after the specified time the filtrate concentrations of MB dye were analyzed using a UV-Vis spectrophotometer.

3.2.7. Determination of adsorption models

After identifying the optimum conditions of adsorption parameters, isotherm and kinetics studies were carried out to differentiate the adsorption mechanism that occurred through the adsorption process and to describe the interaction of adsorbate and adsorbent.

To study the adsorption isotherm, since the initial concentration optimization was performed after optimization of the pH, adsorbent dose, and contact time, there is no need to perform additional batch adsorption experiment by varying initial MB dye concentration at optimum conditions of pH, adsorbent dose, and contact time. The adsorption isotherms were analyzed using the Langmuir and Freundlich isotherm models using the Equations (2) and (3), respectively. Equilibrium isotherm models equations were used to describe the experimental adsorption data which provide information about the capacity of the adsorbent (Uddin et al., 2017). Linear regression is frequently used to determine the best-fitting isotherm, and the applicability of isotherm equations is compared by judging the correlation coefficients (Tan et al., 2008).

Kinetic models were used to investigate the controlling mechanism of adsorption process (Wakkel et al., 2019). Once again, since pH and adsorbent dose was optimized prior to contact time optimization and the initial concentration used while optimizing pH and adsorbent dose was 100 mg/L, and the optimized initial concentration was 100 mg/L, there is no need to perform additional batch adsorption experiment by varying the contact time at optimized values of pH, adsorbent dose and initial MB concentration. Thus, the kinetics of MB adsorption onto SSBC-AlS was analyzed using pseudo-first-order and pseudo-second-order kinetic models using Equations (4) and (5), respectively. Satisfactory conformity

between experimental data and the model-predicted values was expressed by the correlation coefficient (R^2).

3.2.8. Adsorption experiment of methylene blue dye from real textile industrial wastewater

Adsorption experiment of MB dye from real textile industrial wastewater sample was done by SSBC-AlS composite adsorbent by applying the optimum conditions of adsorption process. The adsorbent dose was 1 g/100 ml of wastewater sample, pH was 7, fixed stirring rate at 100 rpm, contact time was 30 minutes at room temperature. After adsorption of MB, the composite adsorbent was filtered from the solution by a Whatman filter paper (42) then the residual MB dye concentration was measured by UV-Vis spectrophotometer (El-Tokhy et al., 2020).

3.2.9. Desorption and adsorbent regeneration study

To study the desorption of the MB dye and SSBC-AlS adsorbent regeneration, the optimized condition of the batch adsorption experiments were considered. The MB adsorbed on the SSBC-AlS composite adsorbent surface at an adsorbent dosage of 1 g/100 ml of dye solution, pH of 7, contact time of 30 minutes, initial dye concentration of 100 mg/L with a stirring rate of 100 rpm at room temperature were detached (desorbed) through washing the adsorbent several times using 0.1 N HCl and distilled water, then dried in an oven at 80 °C to constant mass. The recovery of the adsorbent using 0.1 N HCl and distilled was done six times and investigated the degree of adsorption (Zeng et al., 2021). To investigate the degree of adsorption of the recycled adsorbent after batch adsorption experiment, the filtrate was analyzed by UV-Vis spectrophotometer. The % R was calculated using Equations (14).

3.2.10. Data analyses and interpretation

All data generated from the previously performed experiments were analyzed using the Microsoft Excel, OriginPro 2021, X'Pert HighScore Plus and presented using tables, and graphs.

3.2.11. Data quality assurance

Since data quality is essential for the validity of the adsorption experiment, quality control and quality assurance procedures were used to ensure the validity of the results. For this

reason, a preliminary test was carried out on the adsorbent to identify the adsorption performance of the adsorbents ratio used for adsorption study.

In wastewater sampling, every attempt was made to minimize changes in the chemistry of the sample. To assist in maintaining the natural chemistry of the sample, preservation methods such as pH control, refrigeration and protecting from light was performed. Sampling equipments were cleaned before sampling and at the end of sampling, sampling equipments were labeled referring to the sampling point and date of sampling.

The sludge sampling equipment (plastic bucket) was cleaned properly using detergent and Sulphuric acid then rinsed with distilled water. After adsorbents preparation, the adsorbents were put in tightly closed plastic bag in a place free from any contamination for further analysis.

4. RESULTS AND DISCUSSIONS

4.1. Characteristics of Sewage Sludge, Sewage Sludge-based Biochar, Alum Sludge, and Sewage Sludge-based Biochar-Alum Sludge Composite Adsorbent

4.1.1. Physicochemical characteristics

The moisture content (wt.%) of fresh SS and AlS as received basis were 82.2%, and 46.1%, respectively (Table 4.1). After sun-dying, the moisture content of AlS was found to be 2.44%. This value is lower as compared to other adsorbents such as activated carbon from coffee husk where the moisture content was 19% (Dessalew, 2013). The high moisture content of fresh SS implied the need of pretreatment for elimination of water molecules to meet the minimum moisture content of SS before pyrolysis (Tripathi et al., 2016). Therefore, the moisture content of SS was removed by sun-drying. Low moisture is advisable for the BC production due to considerable reduction in the heat energy and time required for the pyrolysis, making the process economically viable compared to pyrolysis involving biomass with high moisture content (Tripathi et al., 2016). As shown in Table 4.1, the moisture content of SSBC decrease as the pyrolysis temperature increases. Such a phenomenon was mainly due to increment of the rate of drying as temperature increased. Hence, more water was being removed from the surface of BC as the pyrolytic temperature increased (Zhang et al., 2013). The lower the moisture contents of an adsorbent, the higher its adsorption efficiency. Adsorption efficiency decreases with an increase in moisture content of an adsorbent because water molecules can potentially affect the pores of an adsorbent by filling the adsorbent binding site before it contact with the solution (Silgado et al., 2014).

The raw SS sample had 31.5% ash content whereas SSBC ash content obtained was 36.17%, 44.42%, 50.24% at 350 ˚C, 450 ˚C and 550 ˚C, respectively (Table 4.1). The results indicated, the ash content follows an increasing trend with increase in pyrolysis temperature. This may be due to during pyrolysis, most inorganic components were condensed and kept in BC (Agrafioti et al., 2013, Chen et al., 2014). Comparable results were reported by Song et al. (2014) and Jin et al. (2016) during pyrolysis thermal treatment process to produce SSBC. The ash content in the BC obtained after pyrolysis of SS is generally higher than the ash content of BC obtained after pyrolysis of other biomass (Zielinska et al., 2015). This is principally due to the high mineral content of SS that is incorporated into the ash at higher

temperature. The investigations of Zhang et al. (2019) compared the features of BC obtained from SS with corn straw and coconut shell. The ash content obtained from SS was 42.2, 56.3, 67.3 % at 400 ˚C, 500 ˚C and 600 ˚C, respectively, which were much higher than those obtained for other biomass (Zhang et al., 2019). In this study, the ash content of AlS which was approximately 79%, represented other non-soluble compounds or minerals (not including heavy metals) that can be found in the sludge. The ash content value obtained in this study was higher than Awab et al. 2012 who reported 66.67% (Awab et al., 2012).

As indicated in Table 4.1, the volatile matter content in the SS was 60.2 %, and the SSBC had volatile matter content of 45.91%, 37.1%, 30.43% at 350 ˚C, 450 ˚C and 550 ˚C, respectively. This shows an increase in pyrolysis temperature from 350 ˚C to 550 ˚C leads to decreased content of volatile matter. Similar trend was also found by Crombie et al. (2013); Tag et al. (2016), during pyrolysis of biomass (Crombie et al., 2013; Tang et al., 2016). Zhao et al. (2017) also reported that an increase in the pyrolysis temperature decreased the content of volatile matter (from 60.8 to 14.9%) for BC obtained from apple tree branches. This may be due to the increasing temperature resulted in further cracking of the volatile fractions into low-molecular-weight liquids and gases. Pyrolysis temperature has an influence on the structure of BC due to the release of volatiles and the formation and volatilization of intermediate melts (Shaaban et al., 2014). On the other hand, an increase in the pyrolysis temperature from 350 ˚C to 550 ˚C led to increase in the fixed carbon content from 17.92% to 19.33%. The FC content represented the efficiency of the pyrolytic conversion of ash-free organic matter in the sludge to a relatively pure, ash-free carbon (Antal et al., 2003).

The sludge yield decreased in the following order as the temperature increase: 70.4% > 64.2% > 60.8% at 350 ˚C, 450 ˚C, 550 ˚C, respectively (Table 4.1). The observed results are in agreement with a general trend in which, BC yield reduces when pyrolysis temperature is increased. Upon elevation in pyrolytic temperature, the decrease in SSBC yield is attributed to the loss of chemically bound H_2O content, destruction of organic matter, and loss of CO, and CO_2 accompanied by the development of the aromatic structure (Gopinath et al., 2021). This result was analogous to Hossain et al. (2011) who reported the pyrolysis of dried secondary SS under different temperatures ranging from 300 ˚C to 700 ˚C, in which the BC yield decreased in the following order: 72.3% > 63.7% > 57.9% > 52.4 % at 300 ˚C, 400 ˚C, 500 ˚C and 700 ˚C, respectively (Hossain et al., 2011).

The bulk density of SSBC derived at different pyrolysis temperature indicates a decreasing trend in value as pyrolysis temperature increase. As pyrolysis temperature increase from 350 ˚C to 550 ˚C, the bulk density follows the decreasing order from 0.91 g/cm^3 to 0.64 g/cm^3 (Table 4.1). On the other hand, the bulk density of AlS that was found in this study was 0.71 g/cm^3. The particle density that is found in this study also shows the particles are medium which in return results in high porosity of 69.2%. The result that is reported in this study is somehow similar with what was reported by Awab et al. 2012. The results confirmed, the AlS that is used in this study is expected to provide a relatively high adsorption capacity. Low bulk density and an increase in porosity enhance adsorption, means the adsorbent has relatively large potential of adsorbing the adsorbate (Jae et al., 2002).

The fresh SS had pH of 6.7 and the pH of SSBC was 7.2, 7.6, 8.1 at pyrolysis temperature of 350 ˚C, 450 ˚C and 550 ˚C, respectively (Table 4.1). The pH value is in agreement with the value that was reported by Zeng et al. (2021). Upon rise in pyrolytic temperature, the SSBC pH value changed from near neutral (pH 6.7) to alkaline (pH 8.1). The biomass was nearly neutral then becomes alkaline after the formation of SSBC due to the reduction in the quantity of acidic groups at higher temperatures and the cleavage of alkali metal salts from the organic matrix of the biomass (Zielinska et al., 2015). At higher pyrolysis temperature, the alkali salts in SS were liberated out of the structure, and the oxygen-containing functional groups decomposed, resulting in a decrease in the number of acidic functional groups (Zheng et al., 2012, Wang et al., 2019). There was also report that the BC pH value was more significantly influenced by its high aromatization (Khan et al., 2020). The higher values reported by Zhang (2019), for the BC derived from SS which varies from 8.7 to 11, may be due to the impact of the initial pH of SS on the final BC pH (Rehman et al., 2018). The AlS had a pH value of 7.3 and the result that was found in the pH range of AlS reported by Putra et al., (2011), 5.12-8.0.

Table 4. 1: The physiochemical characteristics of the SS, SSBC produced at different pyrolysis temperatures (350 °C, 450 °C , and 550 °C), and AlS.

Parameter	SS	SSBC350	SSBC450	SSBC550	AlS
Moisture (%)	82.2[a]	2.3[b]	1.9[b]	1.5[b]	46.1[a]
Ash (%)	31.5[b]	36.17[b]	44.42[b]	50.24[b]	79[b]
Volatile matter (%)	60.2[b]	45.91[b]	37.1[b]	30.43[b]	-
Fixed carbon (%)	8.3[c]	17.92[c]	18.48[c]	19.33[c]	-
SSBC yield (%)	-	70.4[b]	64.2[b]	60.8[b]	-
Bulk density (g/cm^3)	-	0.91[b]	0.78 [b]	0.64[b]	0.71[b]
Particle density (g/cm^3)	-	-	-	-	2.3[b]
Porosity (%)	-	-	-	-	69.2[c]
pH	6.7	7.2	7.6	8.1	7.3

a= received basis, b= dry basis, c= calculated value.

4.1.2. Functional groups analysis

The functional moieties present on the adsorbent surface can be determined from FT-IR, and a molecule's spectra are considered to be an important physical property (Gopinath et al., 2021). FT-IR spectra of SSBC350, SSBC450, SSBC550, AlS and SSBC-AlS are shown in Figure 4.1.

As shown in Figure 4.1$_{a\text{-}c}$, a vibrational band formed between 3700-3200 cm^{-1} which is represented by yellow shadow in this study, represent –OH stretching (Tang et al., 2019). The peak decreased rapidly as the pyrolytic temperature rose from 350 ^{0}C to 450 ^{0}C, showing that a large number of free and associate hydroxyl bond and structure hydroxy (-COOH and COH) associated with water, alcohols and carboxylic were decomposed in pyrolysis (Keiluweit et al., 2010). The peak for SSBC350 and SSBC450 at approximately 2925 cm $^{-1}$ was generated by asymmetrical and symmetric -CH_x stretching vibration,

indicating that the aliphatic structures existed in SS. The peak of -CH_x vanished as the temperature rose to 550 °C, indicating that aliphatic hydrocarbons were broken down into gases such as carbon dioxide, methyl hydride or converted to aromatic annulus (Gao et al., 2017). The bands at 2830-2810 cm $^{-1}$ of SSBC550, AlS, and SSBC-AlS respond to N-CH_3 (aromatic) bonding whereas the bands at 2750-2730 cm $^{-1}$ respond to N-CH_3 (aliphatic) bonding (Wang et al., 2021). The bands at 1605–1660 cm $^{-1}$ respond to aromatic annulus stretching (C=C) and amino links stretching (-CO-NH-), which are due to the existence of acids, aldehydes and esters in proteins in SS (Lu et al., 2013). The bands at 1430 cm $^{-1}$ for SSBC450 and the bands at 1450 cm $^{-1}$ for SSBC350 correspond with fatly chain (CH_2) bending (Zhao et al., 2016). The bands at 1385 cm $^{-1}$ for SSBC550, AlS, and SSBC-AlS correspond with CH_3 bending. The intensity between 600–800 cm $^{-1}$ attributed to the existence of aryl and heterocyclic aromatic components, which were mainly unchanged, indicating that the aryl C groups were fairly stabilized in pyrolysis (Lu et al., 2013). The reservation of the structure suggests the creation of condensed aryl structure in BC (Wang et al., 2021). The bonds below 600 cm $^{-1}$ which are mainly seen for SSBC at pyrolysis temperature of 350 ^{o}C and 450 ^{o}C were induced by metal–halogen (M–X, M for metal and X for halogen) stretch vibration, which is the primary feature between the FTIR spectra of BC derived from sludge and plant materials (Zhang et al., 2014).

The observed changes that occur on the BC surfaces prepared at different pyrolysis temperature confirmed impacts of pyrolytic temperatures on the conversion of functional group types. This includes the transformation of one functional group to another, decomposition of existing functional groups in the SS, and formation of new functional groups when the biomass is pyrolyzed at different temperatures (Gopinath et al., 2021). For instance, the C–N–C bending vibration at 1544 cm^{-1}, was observed only in SSBC550 samples and absent in the BC samples developed at 350 and 450 ^{0}C. And also, only SSBC550 shows strong band at 1100 cm^{-1} corresponding to C–O stretching. A strong C–H bending at 875 cm^{-1} is found only on SSBC550. Bands appeared at 780 cm^{-1} corresponding to Si–O vibrations is appeared for SSBC550 .The same result was obtained by Srinivasan et al. (2015). Therefore, as describe above and shown in Figure 4.1$_c$, SSBC550 contains suitable functional groups for MB adsorption than SSBC350 and SSBC450.

As it is shown in Figure 4.1$_d$, the broad band at 3340cm^{-1} of the AlS, is due to OH^- bonds of structural water present in $Al(OH)_3$ (Sembiring et al., 2014). The intense Si-O stretching

bands at 1030 cm^{-1} and 532 cm^{-1}, the bending band at 465 cm^{-1}, as well as the shoulder at 912 cm^{-1} are typical for smectite minerals (Danner et al., 2018). The band at 912 cm^{-1} is attributed to Al-O-H deformation of the octahedral sheet in such structures. Peaks at ~532 and 465 cm^{-1} are assigned to Al-O-Si and Si-O-Si, the latter characteristic of amorphous silica. The presence of quartz is also confirmed by the band at 793 cm^{-1} (Rodriguez et al., 2010).

The SSBC-AlS composite adsorbent then contain functional groups for instance (-OH), (C-N), (C-O), and (Si-O), and (Si-O-Si) bonds from the precursor material SSBC550 and AlS (Figure 4.1e. These functional groups are suitable to attach $–CH_3$ and aromatic nitro groups from MB to adsorbent surface (Xiong et al., 2010).

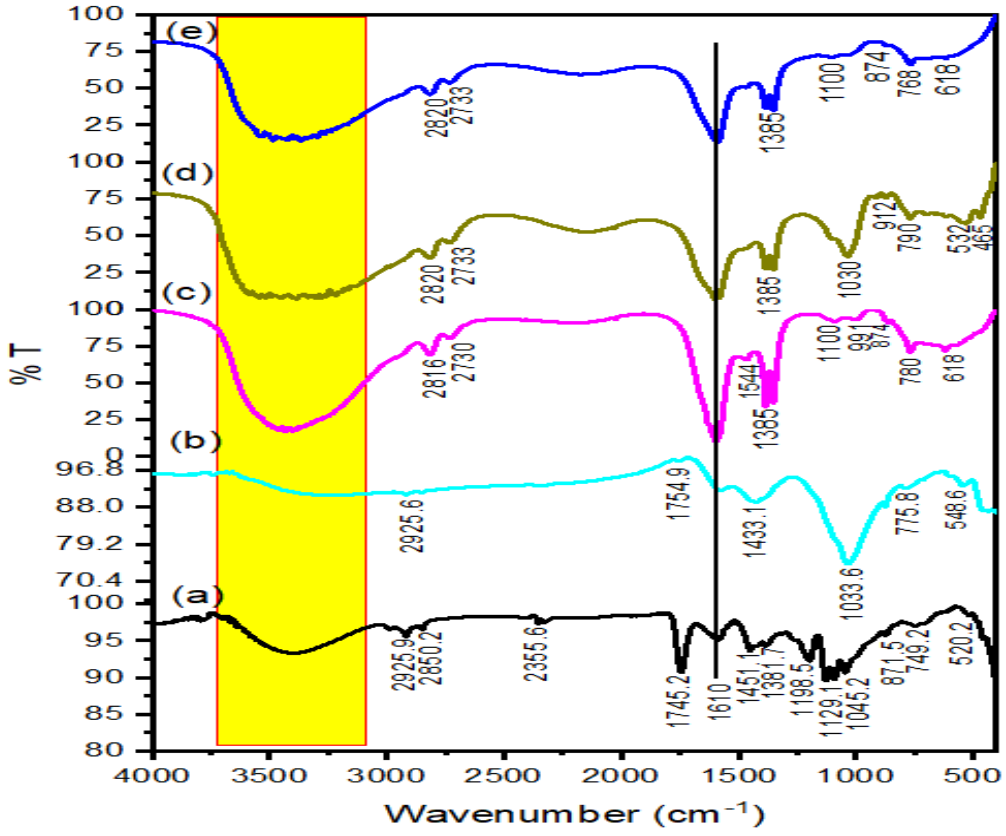

Figure 4.1: FTIR spectra for a) SSBC350, b) SSBC450, c) SSBC550, d) AlS and e) SSBC-AlS.

4.1.3. Thermal stability analysis

TGA-DTA of SSBC350, SSBC450, SSBC550 and SSBC-AlS were studied to evaluate the thermal stability of the materials and the results were shown in Figure 4.2. The process

involves heating samples of the adsorbent materials at high temperature at a constant rate and then monitoring the change in weight.

As shown in TGA-DTA Figures of 4.2, the weight loss in first stage was due to elimination of moisture. Then, the weight loss at higher temperatures is from degradation of inorganic compounds as well as dehydrogenation and aromatization of SSBC (Oja et al., 2016). The TGA-DTA curve of SSBC350 shows, the endothermic peak at 410.20 ^{o}C and exothermic peaks at 50.07, 370.33, and 446.41 ^{o}C, and the total mass loss associated with these peaks were about 5.37 mg (53.7%) (Figure 4.2). As shown in Figure 4.2, SSBC450 had exothermic peak at 452.79 ^{o}C and total weight loss of 3.21 mg (32.1%). SSBC produced at 550°C exhibited exothermic peak at 447.52 ^{o}C with an overall weight loss of only 3.09 mg (30.9%) (Figure 4.2). In this study it has been found that changes in temperature have a great impact on the thermal stability of the SSBC materials. The results clearly showed that when pyrolysis temperature were increased from 350 to 550 °C, the thermal stability of the products were improved since comparatively low loss of weight was recorded and this is good for a stable BC with strong carbon-carbon and hydrogen-carbon bonds remaining (Mohanty et al., 2013). Accordingly, the SSBC from SS biomass pyrolyzed at 550 °C were thermally more stable than those from 350 °C or 450 °C, and would be highly efficient and effective for water treatment applications as an adsorbent (Lehmann et al., 2017). The results found in this study is similar to Kim et al. (2012), who conclude that with increased pyrolysis temperature, BC from pitch pine woodchips become more stable. To further support the results in this study, according to literature pyrolyzing the SS at 550 ^{o}C is suitable temperature because transformation reaction of aliphatic compounds, protein, and carbohydrate compounds in the sludge, the breaking of peptide bonds and branched chains, and the release of a large number of volatiles is completed at this temperature (Magdziarz & Wilk, 2013). In addition, compared to low pyrolysis temperature, SSBC formed at high temperatures has a greater surface area and carbon content due to the rising micro-pore volume caused by the elimination of volatile organic molecules (Wang et al., 2019).

As shown in Figure 4.2, the SSBC-AlS had exothermic peak at 449.28 ^{o}C and more thermal stability than SSBC550 since the weight loss of the composite (2.3 mg (23%)) is lower than that of SSBC550 (3.09 mg (30.9%)) at the temperature under investigation, and this gives an indication of the lower amount of the volatile content in the composite sample. A thermally stable material sample has less volatile matter (Mimmo et al., 2014). The thermal

stability of composite adsorbents is an important parameter, since the thermal stability of these materials can be a limiting factor in both processing and end-use applications (Kalderis et al., 2014).

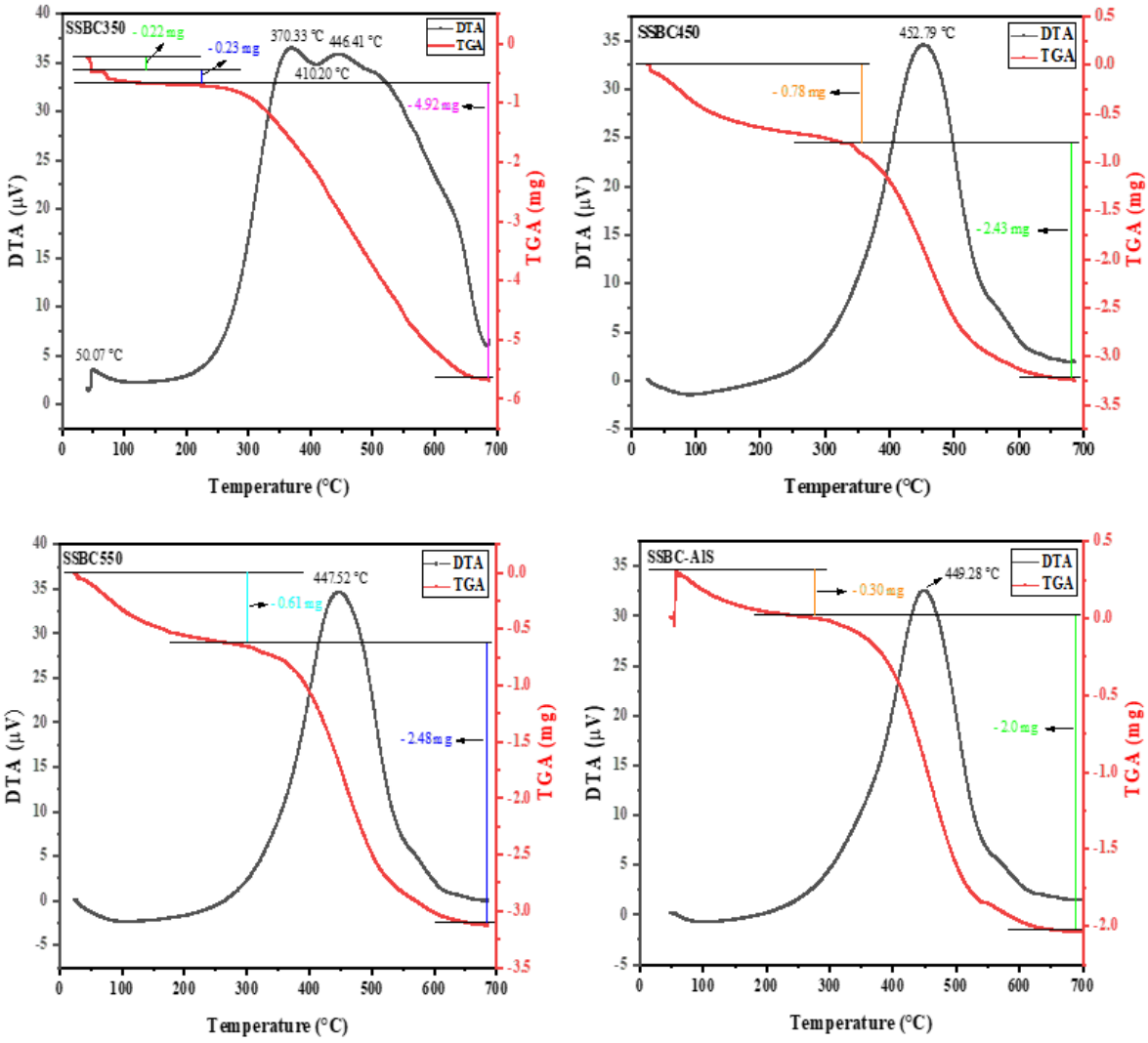

Figure 4. 2:TGA-DTA analysis results of SSBC350, SSBC450, SSBC550, and SSBC-AlS

Depending on physiochemical characteristics, FT-IR, and TGA-DTA results, as well as on the available literature on conversion of SS to SSBC to be used as an adsorbent for MB dye from wastewater (Fan et al., 2017), SS pyrolyzed at 550 ^{0}C (SSBC550) was selected to prepare composite adsorbent with AlS.

4.1.4. Mineralogical analysis

The XRD pattern of the selected SSBC (SSBC550 which possess suitable functional group, good thermal stability as well as low bulk density for MB adsorption), AlS and SSBC-AlS

composite were shown in Figure 4.3. The XRD patterns of SSBC550 were primarily amorphous and only few crystalline phases were detected. Such as, SSBC550 exhibits a crystalline peak, at around 25° and 42° 2θ which is indicative of carbon materials (ICDD Card No: 00-018-0311). Peaks associated with SiO_2 (ICDD Card No: 01-078-1255) were obtained at 26.98° 2θ, indicating the presence of quartz in the SSBC. The $CaCO_3$ (ICDD Card No: 00-029-0305) peaks were shown at 2θ value of (29.77°, 39.82°, and 48.97°). This is in match to the results of Yin et al. (2019). In the XRD patterns of AlS the peak at (20.08°, 26.8°, and 39.58° 2θ) indicates crystalline structure that corresponds to SiO_2 (ICDD Card No: 01-083-2466) as one of the major oxides in the dewatered sludge. Fe_2O_3 (ICDD Card No: 01-073-0603) peaks were also shown at (35.47°, and 49.66° 2θ), and $Al(OH)_3$ (ICDD Card No: 00-015-0136) peaks were shown at 2θ value of 21.07°, 27.64° and 53.35°. The results were consistent with Chen et al. 2017 work who applied modified waterworks sludge particles with poly aluminum chloride as a coagulant for the treatment of slightly polluted source water. SiO_2 was the major crystalline solids identified in numerous XRD analyses (Chiang et al., 2009; Yang et al., 2008). SiO_2 is mainly from the raw water and accounts for a significant part of the composition of the AlS, followed by $Al(OH)_3$ and Fe_2O_3 (Yang et al., 2006; Ahmad et al., 2016). The SSBC-AlS composite adsorbent possess the dominant peaks which were also shown in the precursor materials. Additionally the XRD of SSBC-AlS shows two peaks at 2θ value of 28.12 and 31.24°, which were shown on XRD pattern of SSBC but more intensified in the composite. This may be due to the precursor materials undergo physical and chemical process to form the composite adsorbent.

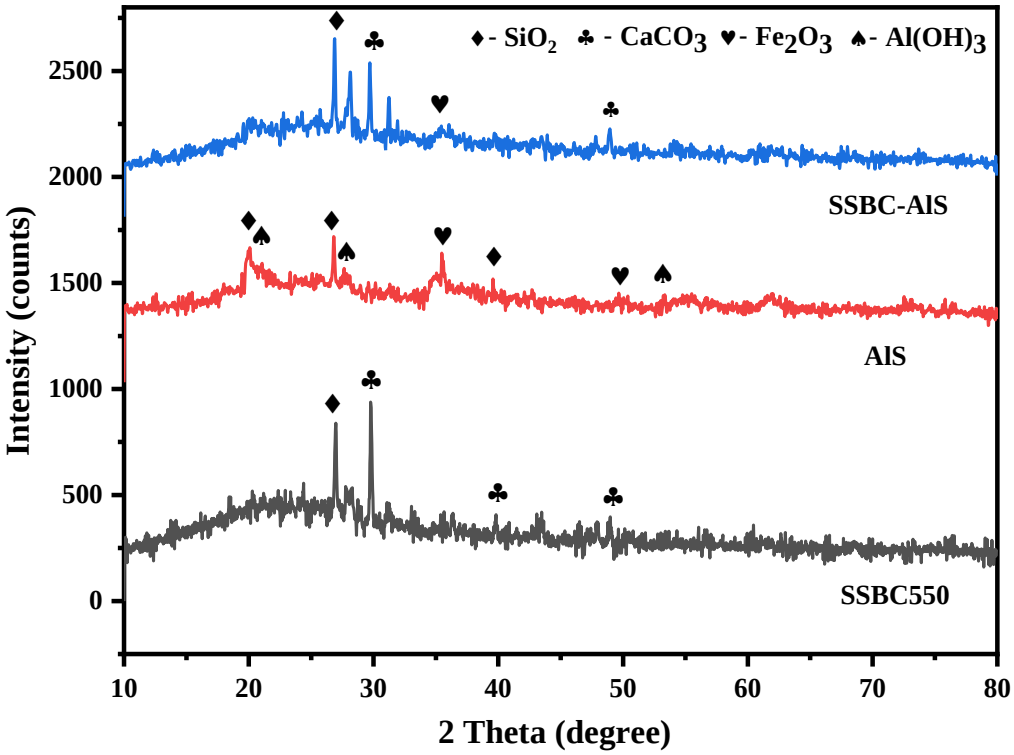

Figure 4. 3: XRD pattern of SSBC550, AlS, and SSBC-AlS.

4.1.5. Morphological features analysis

SEM is one of the most widely used methods that helps to visualize the morphological properties of the materials. Therefore, SEM micrographs were acquired to observe the surface morphologies of the SSBC550, AlS and SSBC-AlS (Figure 4.4$_{a-c}$). The micrograph of SSBC550 looks like, flakes of smooth surface micrograms with small pores. The pyrolysis temperature (550 ^{0}C) make volatilization more suitable, making the SSBC slightly porous and creating small voids within the SSBC matrix. Similar kind of SEM result was obtained by Breulmann et al. (2018) who prepared BC from SS.

The SEM result of AlS shows that the adsorbent developed from AlS had high porous structure (Figure 4.4$_{b}$). The micrograph also clearly show that the surface of the AlS was rough, therefore they are good candidates as adsorbents. The SEM result of AlS obtained in this study agreed with the previously reported SEM results (Chittoo & Sutherland, 2014).

The SEM results of the composite SSBC-AlS clearly showed surface pore enhancement of small pores of SSBC after composite making with AlS (Figure 4.4$_{c}$). The composite

adsorbent developed honeycomb-like structures and had irregular rough surface structure, which indicates that the material exist good characteristics to be employed, as an adsorbent for MB dye uptake.

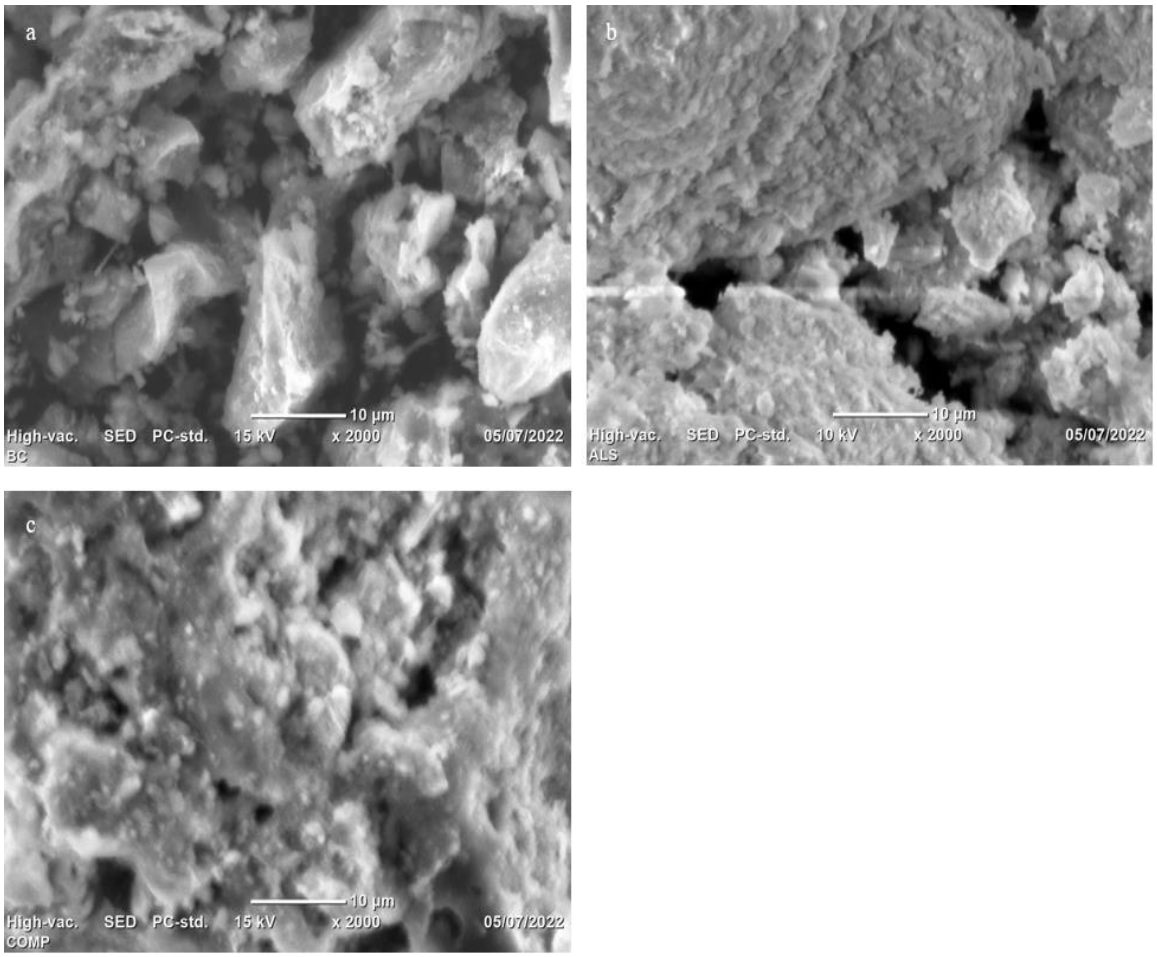

Figure 4. 4: SEM micrographs for a) SSBC550, b) AlS, and c) SSBC-AlS..

4.1.6. Surface area analysis

SSBC-AlS composite adsorbent prepared in this study have surface area of 55.97 m^2/gm (Appendix 2). The SSBC prepared by Fan et al. 2017 as an adsorbent for MB, has surface area of 25 m^2/gm. It can be seen that the specific surface area of SSBC-AlS is higher than that of the SSBC. This is because AlS combined well with BC, resulting in a rougher surface and an increased specific surface area. Similar result was obtained by Xiao et al. (2020).

The degree of adsorption is proportional to the specific surface area, where the larger the surface area the greater the surface for adsorption to take place (Haynes, 2015; Ambroz et al., 2018). In this manner the composite adsorbent prepared in this study have better

performance in removing MB from solution than the sole use of SSBC. Similar to this study, Chen et al. (2019) also stated that composite making of SSBC with other potential waste material helps to increase the surface area, which is a crucial parameter required for environmental remediation.

4.1.7. Point of zero charge (pH_{pzc}) analysis

The solution pH circumstance in which the surface charge density equals zero is termed the pH point of zero charges (pH_{pzc}). Figure 4.5 indicates the pH_{pzc} of the SSBC-AlS and its value was 6.5. From the plot, it is possible to deduce that the adsorbent surface is positively charged at pH <6.5 and becomes negatively charged at pH >6.5. Thus, the high uptake capacity was observed at pH >6.5. For pH values of pH <6.5 uptake process is delayed by the repulsive electrostatic force of attractions between adsorbent and adsorbate (Ben-Ali et al., 2017).

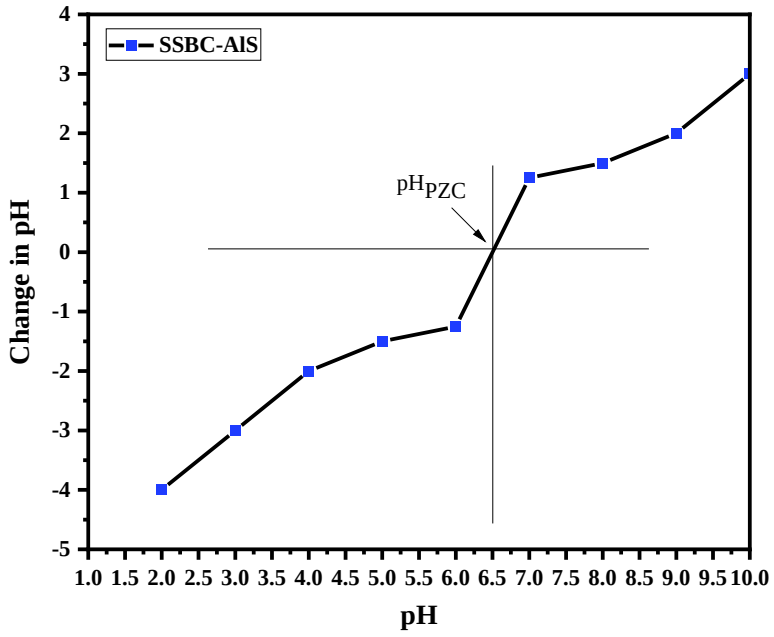

Figure 4. 5: Point of zero charge (pHpzc) of SSBC-AlS

4.2. Batch Adsorption Experiments

The FT-IR, TGA-DTA, XRD, SEM, and BET results of adsorbents as well as the pre-test conducted at selected adsorption working condition (Appendix 1) showed, SSBC-AlS

composite (75:25) developed better structure and provide better removal efficiency than the precursor materials. This implies that the preparation of the composite was achieved successfully and it was used for subsequent adsorption optimization experiments.

4.2.1. Optimizations for removal of methylene blue dye from aqueous solution

4.2.1.1. Effect of temperature

In order to determine the optimal temperature of the adsorption process, the adsorption of MB onto SSBC-AlS was studied by varying the solution temperature at 15, 25, 35, 45, and 50 °C while keeping other variables constant per 100 mL volume of adsorbate solution, and the results of the experiments are shown in Figure $4.6_{A,B}$. It was observed that as the temperature increased, both the % R and q_e shows no change in adsorption of MB onto SSBC-AlS from aqueous solution. Therefore, the optimal temperature was taken at room temperature (25 °C) with % R of 99.92% and q_e of 19.98 mg/g. Dissimilar to this study, in the literature (Liu et al., 2013), granular activated carbon made from SS for MB removal from aqueous solution, the MB adsorptive capacity of the adsorbent at higher temperature was higher than the lower temperature. The variation from previously reported result could result from, the SSBC-AlS composite adsorbent prepared in this study is thermally stable showing no change in adsorption capacity on the temperature range studied.

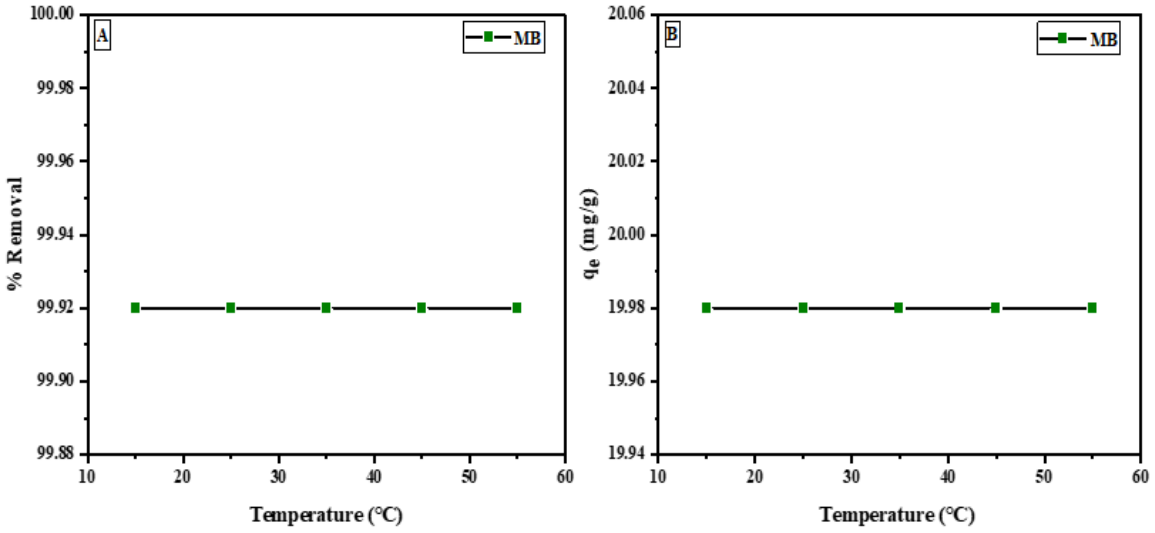

Figure 4. 6: Effect of solution temperature on MB adsorption onto SSBC-AlS using pH of 7, 100 mg/L initial concentration of MB, at an adsorbent dose of 0.5 g, contact time of 60 minutes, agitation speed 100 rpm. A) % R, B) q_e (mg/g).

4.2.1.2. Effect of pH

In adsorption, pH is one of the significant parameters affecting the adsorption efficacy. Figure $4.7_{A,B}$, shows the MB % R and q_e, respectively of SSBC-AlS composite adsorbent under different solution pH (5-9) and other parameters kept constant. Other parameters were kept constant per 100 mL volume of adsorbate solution. The results showed that the % R of MB by the SSBC-AlS composite adsorbent increased (from 99.87% to 99.93%) with an increase in pH from 5 to 7. Then the % R of MB by SSBC-AlS decreased with the increase in pH from 7 to 9. This implies pH 7 is found to be the optimum pH in which the maximum uptake of MB dye was obtained (Figure 4.7_A). The maximum q_e at the specified pH is 19.98 mg/g. (Figure 4.7_B).

The low adsorption of MB at an acidic pH was suggested to be due to the presence of excess H^+ ions that compete with the MB dye cation for adsorption sites. The number of positively charged sites decreases while the number of negatively charged sites increases, favoring the adsorption of MB due to electrostatic attraction. The decrease in the dye % R as the pH value increased from 7 to 9 is due to the formation of a hydroxyl complex between the adsorbent and the dye (El-Tokhy et al., 2020). This phenomenon was similar to previous result reported by Mian & Liu. (2018).

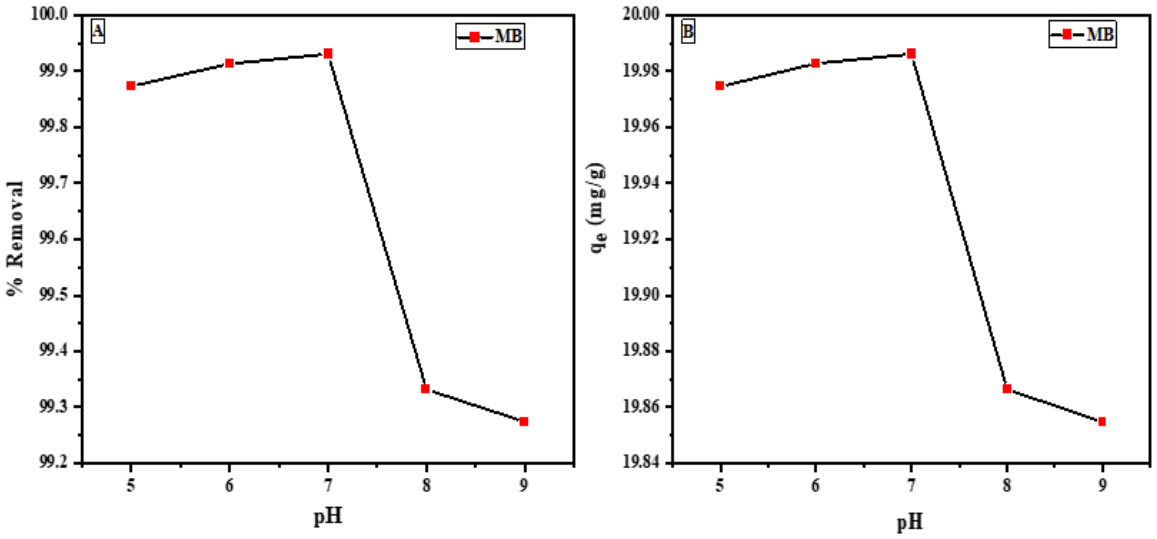

Figure 4. 7: Effect of pH on MB adsorption onto SSBC-AlS using 100 mg/L initial concentration of MB, at an adsorbent dose of 0.5 g, contact time of 60 minutes, agitation speed 100 rpm, and at room temperature. A) % R, B) q_e (mg/g).

4.2.1.3. Effect of adsorbent dose

Optimization of the adsorbent dosage is very significant to determine the capacity of an adsorbent for a certain adsorbate. Figure $4.8_{A,B}$, shows the % R and q_e, respectively of MB adsorption onto SSBC-AlS composite adsorbent under different adsorbent dosage (0.25, 0.5, 0.75, 1, 1.25, and 1.5 g). Other parameters were kept constant per 100 mL volume of MB dye solution. The results showed that the % R of MB by the SSBC-AlS composite adsorbent increased (from 90.90% to 99.97%) with an increase in SSBC-AlS dosage from 0.25 to 1 g. This is because as the adsorbent dosage increases, the surface area of the adsorbent will increase, and more adsorption sites are available to absorb the MB from the water sample and attain a value at equilibrium (Masresha & Enyew, 2017). Then the % R of MB by SSBC-AlS decreased with the increase in SSBC-AlS dosage from 1 to 1.5 g. The adsorption amounts decreased, and the adsorption amount per unit mass of adsorbent decreased even when the initial concentration of MB solution was constant. This implies 1 g is found to be the optimum SSBC-AlS dosage in which the maximum uptake of MB dye was obtained. The maximum q_e at 1 g is 9.99 mg/g. (Figure 4.8_B). Similar results were reported by Fan et al. (2017) in the adsorption of MB by SSBC, indicating that the % R increased with increasing dosage until optimum dose.

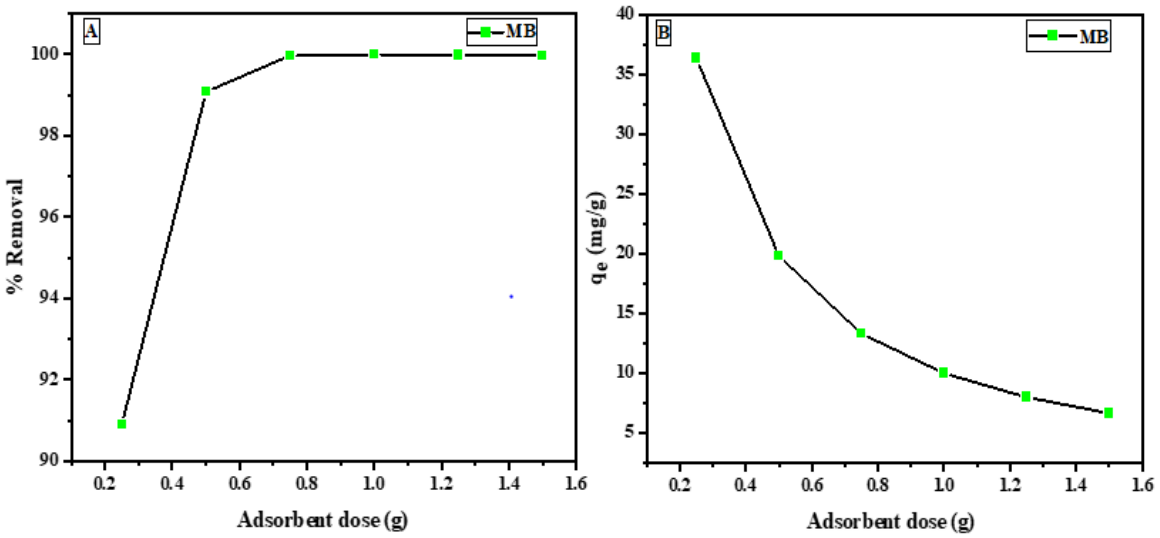

Figure 4. 8: Effect of adsorbent dose on MB adsorption onto SSBC-AlS using pH 7, 100 mg/L initial concentration of MB, contact time of 60 minutes, agitation speed 100 rpm, and at room temperature. A) % R, B) q_e (mg/g).

4.2.1.4. Effect of contact time

The contact time is also an important influencing factor for MB adsorption. Figure $4.9_{A,B}$, shows the % R and q_e, respectively of MB adsorption onto SSBC-AlS composite adsorbent under different contact time (15, 30, 45, 60, and 90 minutes) and other parameters kept constant. Other parameters were kept constant per 100 mL volume of adsorbate solution. The results showed that the % R of MB by the SSBC-AlS composite adsorbent increased (from 99.95% to 99.97%) with an increase in contact time from 15 to 30 minutes. An increase in % R up to 30 minutes is due to strong forces of attraction between the positive sites of cationic dyes and the adsorbent surface. Comparable result was found by Leng et al. (2015). Then the % R of MB by SSBC-AlS decreased with the increase in contact time from 30 to 90 minutes. After the equilibrium contact time (30 minutes), a decrease in the amount of adsorbed was observed. This phenomenon is attributed to the fact that a large number of vacant surface sites are available for adsorption at the initial stage, and after a lapse of time, the remaining vacant surface sites are difficult to be occupied due to repulsive force between the solute molecules on the solid and bulk phase (Nasr et al., 2017). Therefore, 30 minutes contact time is found to be the optimum value in which the maximum uptake of MB dye was obtained. The maximum q_e at the specified contact time is 9.99 mg/g. (Figure 4.9_B). Fan et al. (2017) demonstrated the adsorption of MB on SSBC and the optimum contact time was in the range of 8-10 h (Fan et al., 2017). The SSBC-AlS used in this study created a rapid reaction, indicating that the prepared adsorbent material had good dispersion and can fully contact with MB aqueous solution and complete adsorption in a short time.

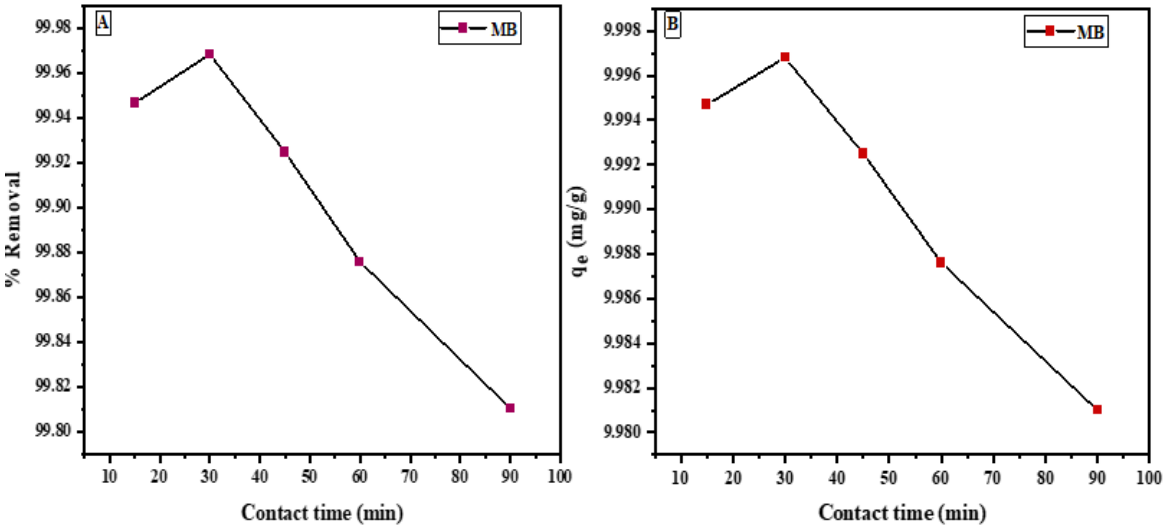

Figure 4. 9: Effect of contact time on MB adsorption onto SSBC-AlS using pH 7, 100 mg/L initial concentration of MB, at adsorbent dose of 1g/100 ml, agitation speed 100 rpm, and at room temperature. A) % R, B) q_e (mg/g).

4.2.1.5. Effect of initial methylene blue dye concentration

Figure 4.10$_{A,B}$, shows the % R and q_e, respectively of MB adsorption onto SSBC-AlS composite adsorbent under different initial MB concentration of 10, 50, 100, 150, and 200 mg/L. Other parameters were kept constant per 100 mL volume of adsorbate solution. The results showed that the % R of MB by the SSBC-AlS composite adsorbent increased (from 99.94 % to 99.96 %) with an increase in initial MB concentration from 10 to 100 mg/L. Then the % R of MB by SSBC-AlS decreased with the increase in initial MB concentration from 100 to 200 mg/L. Further increase in MB concentration results a decrease in % R due to the lack of active sites of SSBC-AlS adsorbent (Ismail et al., 2020). This implies initial MB concentration of 100 mg/L is found to be the optimum initial concentration in which the maximum uptake of MB dye was obtained. The maximum q_e at the specified initial MB concentration is 9.98 mg/g (Figure 4.10$_B$). q_e in mg/g showed different trends than % R. As the MB concentration of aqueous solution increases, the q_e of SSBC-AlS for MB enhances from (0.9994 to 19.63) mg g^{-1}. The result may be due to that MB concentration gradient between solution and adsorbent surface and mass transfer driving force are higher at high MB concentration (Roy et al., 2012). The results obtained in this study is consistent with the results obtained by (Liu et al., 2013).

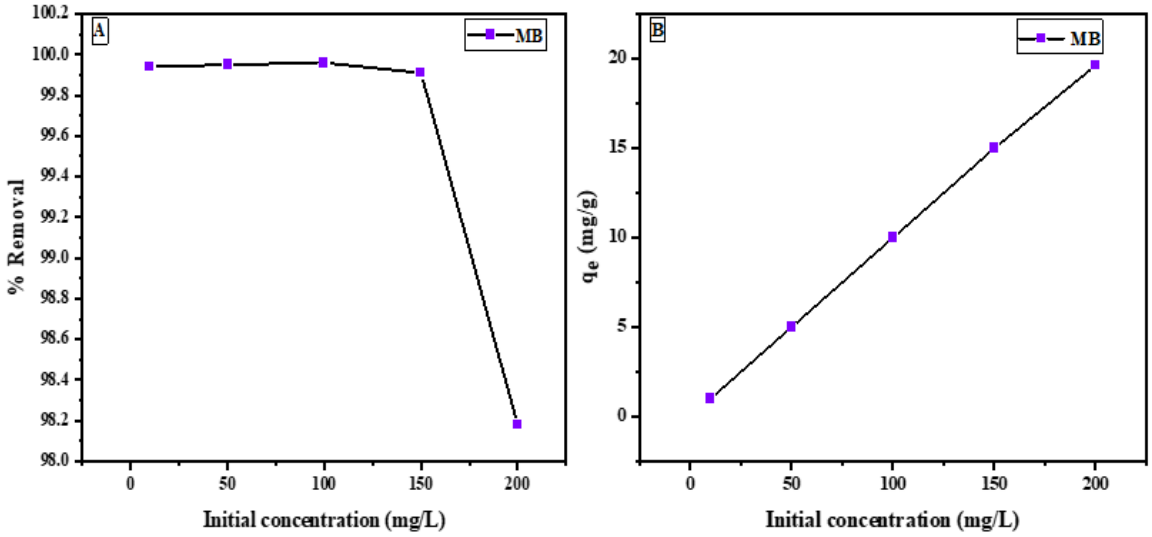

Figure 4. 10: Effect of initial concentration on MB adsorption onto SSBC-AlS using pH 7, at adsorbent dose of 1g/ 100 ml, contact time of 30 minutes, agitation speed 100 rpm, and at room temperature. A) % R, B) q_e (mg/g).

4.2.2. Adsorption equilibrium isotherm models

Adsorption isotherm is used in order to evaluate the behavior of molecules of MB with the adsorbent surface (Singh et al., 2018). The data generated from this study provides important physicochemical data for evaluating the applicability of the adsorption process as a unit operation. This study analyzed the equilibrium data using Langmuir and Freundlich isotherm models. These are generally related to the type of coverage, the possibility of interaction between the adsorbent and adsorbate species, and the heterogeneity and homogeneity of the adsorbent. Isotherms models relate adsorbate per unit weight of adsorbent (q_e) to the equilibrium adsorbate concentration in the bulk fluid phase (C_e) (Adane et al., 2015).

4.2.2.1. Langmuir adsorption isotherm model

The experimental data was analyzed according to the linear form of the Langmuir isotherm as described in Equation 2. The value of q_m and K_L of linear expression of Langmuir adsorption isotherm were calculated from the slope and intercept of the linear plot of C_e versus C_e/q_e shown in Figure 4.11.

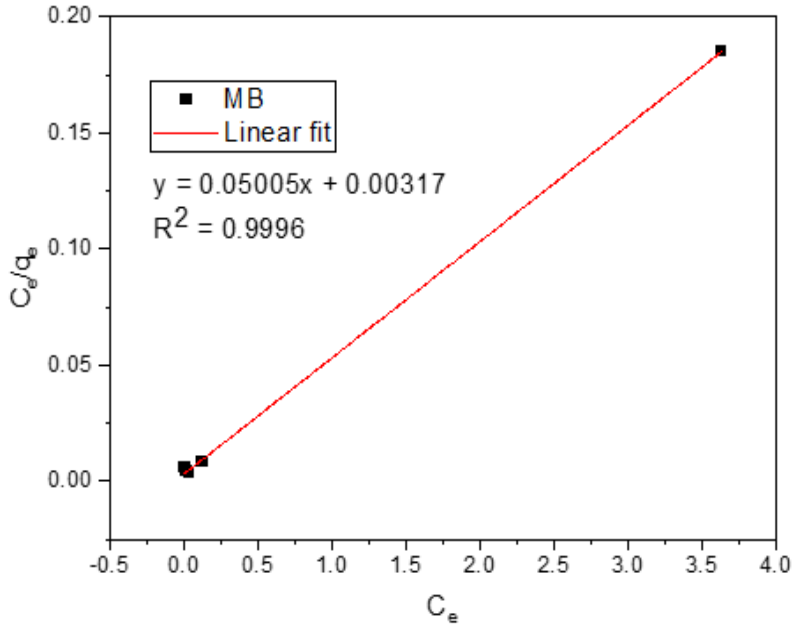

Figure 4. 11: Langmuir adsorption isotherm model.

The calculated values of isotherm parameters and the adsorption of MB on SSBC-AlS shows high correlation coefficients for the Langmuir isotherm model. Langmuir's adsorption isotherm model result shows a more excellent R^2 (0.9996) value than Freundlich's adsorption isotherm (discussed later). This explains the monolayer adsorption in MB's adsorption process and the presence of homogenous sites on the SSBC-AlS surface. The Langmuir isotherm is effective for the adsorption of a solute from a liquid solution as monolayer adsorption on a surface containing a fixed number of identical sites. The Langmuir isotherm often applies to a homogeneous adsorption surface with the entire adsorption site having equal adsorbate affinity (Adane et al., 2015). The value of the separation factor (R_L), called the equilibrium parameter, can be estimated by the Langmuir isotherm. The obtained R_L value was greater than 0 but less than 1, as shown in Table 4.2, indicating that the adsorption processes of MB on SSBC-AlS were favorable. Among the isotherm models commonly used for describing dye adsorption, the Langmuir adsorption isotherm model is the best known and has been successfully applied to various adsorption processes. For MB adsorption, the Langmuir adsorption isotherm model better fitted the adsorption isotherm (Azari et al., 2015).

Table 4. 2: Summary table for the line fit graph of Langmuir adsorption isotherm model.

Parameters	Results
C_i (mg/L)	100
q_e (mg/g)	7.11
Intercept	0.00317
Slope	0.05005
q_m (mg/g)	19.98
K_L	15.79
R_L	0.00063
R^2	0.9996

4.2.2.2. Freundlich adsorption isotherm model

The Freundlich adsorption isotherm model is the second most often used model to describe the adsorption data of MB. The Freundlich isotherm describes that during the adsorption process, different sites of the adsorbate are involved with several adsorption energy, an empirical relation for adsorption over heterogeneous surfaces. The applicability of the Freundlich adsorption isotherm was also analyzed (Equation 3), using the same set of experimental data as for the Langmuir model. To determine whether Freundlich adsorption isotherm model fit to the experimental value or not, the graph of log q_e and log C_e was plotted (Figure 4.12) . From linear equation the Freundlich constant K_F ($mg.g^{-1}$), and n is characteristic constants related to the relative adsorption capacity of the adsorbent and the intensity of adsorption, respectively. The K_F and 1/n can be obtained from the intercept and slope of the linear plot of log q_e versus log C_e.

The value of n was larger than one (Table 4.3), indicating that MB's adsorption onto SSBC-AlS was favorable. The Freundlich plot between log q_e versus log C_e for the adsorption of MB is shown in Figure 4.9. The K_F and 1/n were 19.2703 and 0.39569, respectively. The factor “1/n” in the Freundlich isotherm model can reflects the

heterogeneity factor, the heterogeneity of site energies, and the adsorption intensity. Values of 1/n smaller than 0.5 indicate that the adsorbate is easily adsorbed; values of 1/n larger than 2 indicates the adsorbate is hardly adsorbed (Uddin et al., 2009). In the present study, the value for 1/n of MB adsorption onto SSBC-AlS was less than 0.5. This is in agreement with the result obtained by Fan et al. (2017).

Compared with the Freundlich model, the correlation coefficient of the Langmuir model was more consistent with the adsorption process of MB on SSBC-AlS. Not only is its R^2, but the q_e value of the Langmuir model (7.11) is also closer to 9.99 than Freundlich's q_e value (5.11). Based on the literature, the Langmuir model is the most common model used to describe monolayer adsorption processes (Yao et al., 2011; Zhang et al., 2013). The model has been used to describe the sorption of chemical compounds on composited materials, including MB, onto BC-Al oxide composite material (Zeng et al., 2019).

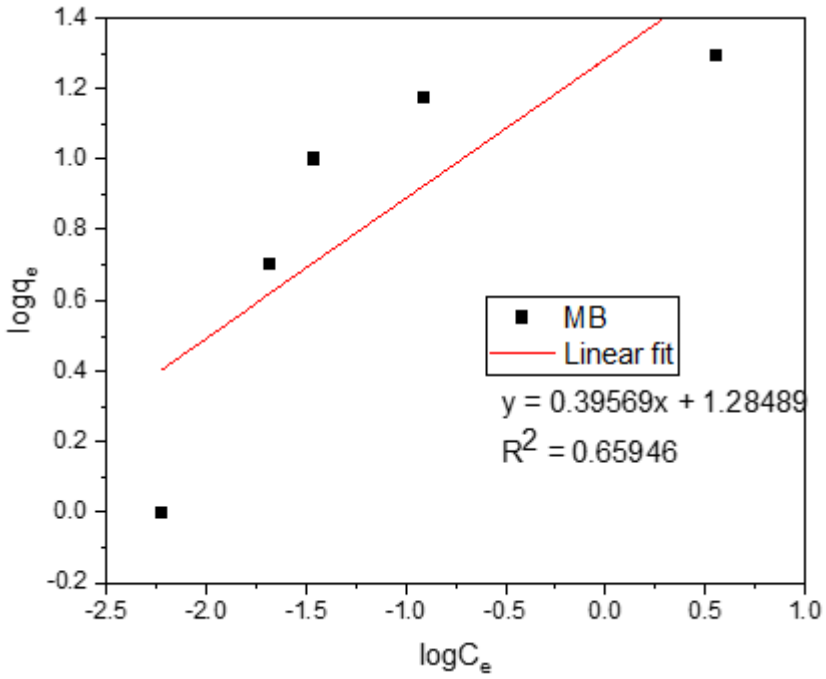

Figure 4. 12: Freundlich adsorption isotherm model.

Table 4. 3: Results of the line fit graph of Freundlich adsorption isotherm model.

Parameters	Results
C_i (mg/L)	100
q_e (mg/g)	5.11
Intercept	1.28489
Slope	0.39569
1/n	0.39569
K_F	19.2703
R^2	0.65946

4.2.3. Kinetics study

Kinetics studies help to select optimum operating conditions for the full-scale batch process, which have been applicable to investigate the mechanism of adsorption and potential rate-controlling steps. To further understand the characteristics of the adsorption process, the pseudo-first and second-order kinetics order kinetic models were applied to fit experimental data obtained from batch experiments. The conformity between experimental data and the model-predicted values was expressed using the correlation coefficient significance. The relative greater is the more applicable model to the kinetic study.

4.2.3.1. Pseudo-first order kinetic model

To determine whether the adsorption process fits with the pseudo-first-order model, the experimental data was introduced to Equation 4 (Figure 4.13).

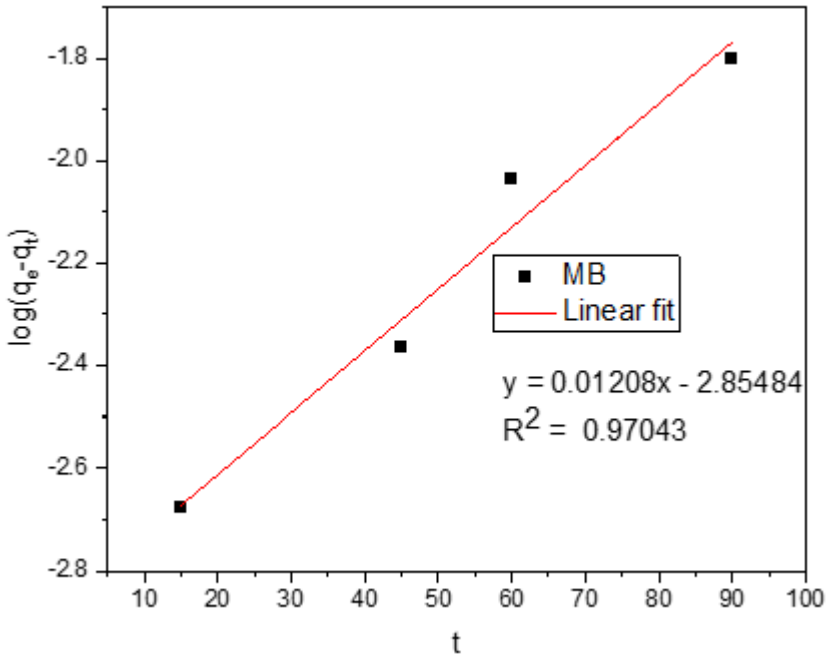

Figure 4. 13: Pseudo-first order kinetic plots for the adsorption of MB onto SSBC-AlS.

The straight-line plot of log (q_e–q_t) against t (Figure 4.13) gives a linear relationship from which the pseudo-first-order rate constant (K_1) and equilibrium adsorption capacity (q_e) were calculated from the slope and intercept, respectively, as shown in Table 4.4. The rate constant and q_e (cal) were calculated from the slope and intercepts of the graph log (q_e-q_t) against time (Adane et al., 2015). The pseudo-first-order kinetics model did not predict the adsorption kinetics of MB removal using SSBC-AlS (Figure 4.13) since the correlation factor was low (0.97043).

Table 4. 4: Results of line fit model of pseudo-first order kinetics.

Parameters	Results
C_i (mg/L)	100
Intercept	-2.85484
q_e (exp) (mg/g)	9.99
q_e (cal) (mg/g)	0.001397
Slope	0.01208
K_1	-0.0278
R^2	0.97043

4.2.3.2. Pseudo-second order kinetic model

In addition to the first-order kinetics model, the linearized form of the kinetic rate expression for a pseudo-second-order model was applied to the experimental data. Calculated equilibrium adsorption capacity q_e(cal) and pseudo-second-order rate constant (K_2) were obtained from the model using Equation 5. The linear plots of t/q_t against t are shown in Figure 4.14 for MB adsorbed on SSBC-AlS. Figure 4.14 and Table 4.5 showed the values of R^2 on pseudo-second-order for MB are higher than on first-order kinetics. Since the calculated adsorption capacity q_e (cal) was closer to the experimental adsorption capacity q_e (exp), and since the regression coefficient, R^2 of the pseudo-second-order kinetic model is 1, which is greater than that of the pseudo-first-order kinetic model (0.97043) indicates that the pseudo-second-order kinetic model describes the adsorption process of MB by SSBC-AlS perfectly. Also, the chemisorption process is the rate-controlling step for the adsorption of MB by SSBC-AlS. Liu et al. (2013) reported a similar fit to this model for MB adsorption.

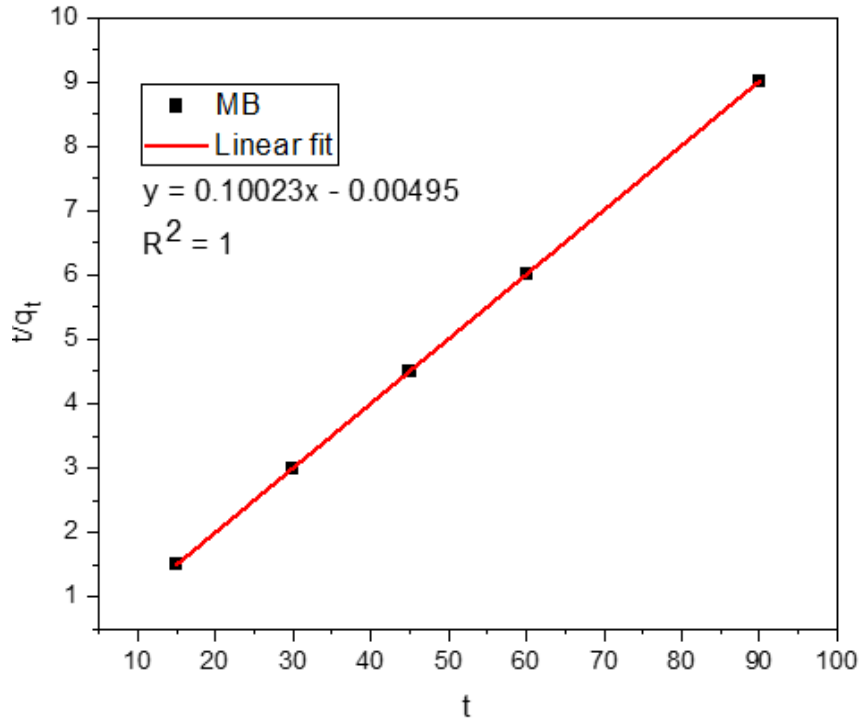

Figure 4. 14: Pseudo-second order kinetic plots for the adsorption of MB onto SSBC-AlS.

Table 4. 5: Results of line fit model of pseudo-second order kinetics.

Parameters	Results
C_i (mg/L)	100
Intercept	-0.00495
q_e (exp) (mg/g)	9.9925
q_e (cal) (mg/g)	9.97
Slope	0.10023
K_2	-2.0323
R^2	1

4.3. Adsorption of Real Textile Industry Wastewater Sample Onto Composite Adsorbent

Evaluation of the real textile industrial wastewater sample physicochemical properties is significant to apply SSBC-AlS composite adsorbent as an adsorbent for industrial wastewater sample. As it is mentioned in material and method chapter, the industrial wastewater sample was collected from the discharge point of Dongfang Spinning, Printing and Dyeing PLC. The results of the Physicochemical parameters of the wastewater sample studied in this study are presented in Table 4.6.

Table 4. 6: Some physicochemical characteristics of textile industrial wastewater sample.

Characteristics	Textile effluent
Color	Blue
pH	7.5
Temperature	27.1 ^{0}C
Electrical conductivity (mS cm^{-1})	3.8
MB (mg/L)	61

EPA recommends a limit value of 0.2 mg/L of MB in wastewater (Environmental Protection Agency, 2001). The textile industry wastewater sample was first determined for its initial MB dye concentration by using UV-Vis spectrophotometer at λmax 665nm (Utomo et al., 2015). As shown in Table 4.6, the results revealed that the MB concentration in the real textile industry wastewater sample was found above the permissible level. So, the amount of MB found in the real wastewater sample could seriously threaten human health and the natural environment.

To study the application of SSBC-AlS as composite adsorbent for MB removal from industrial wastewater, the sample was treated under optimized experimental parameters at pH 7, contact time 30 min, adsorbent dose 1 g per 100 mL of volume, and at room

temperature with an initial concentration of MB dye 61 mg/L. The filtrate obtained after treatment was analyzed by UV-Vis spectrophotometer. The composite adsorbent SSBC-AlS effectively removed the MB from real textile industry wastewater sample with 96.9% adsorption efficiency.

The % R of SSBC-AlS for synthetic MB aqueous solution was higher than that of the real textile industry wastewater sample. This may be because the real textile industry wastewater sample has a different matrix that competes with the MB dye. Different matrix competing pollutants reduce the adsorption efficiency of the adsorbent material in real textile industry wastewater samples by occupying the adsorbent surfaces.

4.4. Regeneration Study of Composite Adsorbent

To discuss the application prospect of the material in the actual situation, the regeneration and reuse of adsorbent was further studied. The desorption processes are significant for the regeneration of adsorbents for reuse in other adsorption processes. MB is a cationic dye, and the isoelectric point (pH_{pzc}) of SSBC-AlS was measured as 6.5 (Figure 4.5). When pH > pH_{pzc}, the surface of the material was negatively charged, which is conducive to the completion of adsorption. Therefore, the material prepared in this experiment had poor adsorption effect under low pH, so it should be regenerated under acidic conditions. The sample SSBC-AlS was eluted with 0.1 N HCl, and the adsorption after regeneration was shown in Figure 4.15 and Table 4.7. The regeneration experiment was conducted for six cycles. It is shown in Figure 4.15 and Table 4.7 that the uptake capacity for MB of SSBC-AlS decreased gradually with the regeneration times increasing, but the MB removal rate was kept at about 82.04% after six cycles of regeneration, indicating that the adsorbent has a good reproducibility. Comparable result was obtained by Zeng et al. (2021). But the decreased removal rate as the number of regeneration cycle increment was due to the effect of the prior desorption process, which solubilized some parts of the adsorbent, changed superficial structures and subsequently led to loss or blockage of adsorption sites (Wang et al., 2015).

Table 4. 7: Recyclability of SSBC-AlS for MB removal.

No. of cycle	% R of MB
1	98.37%
2	96.08%
3	93.44%
4	89.7%
5	85.24%
6	82.04%

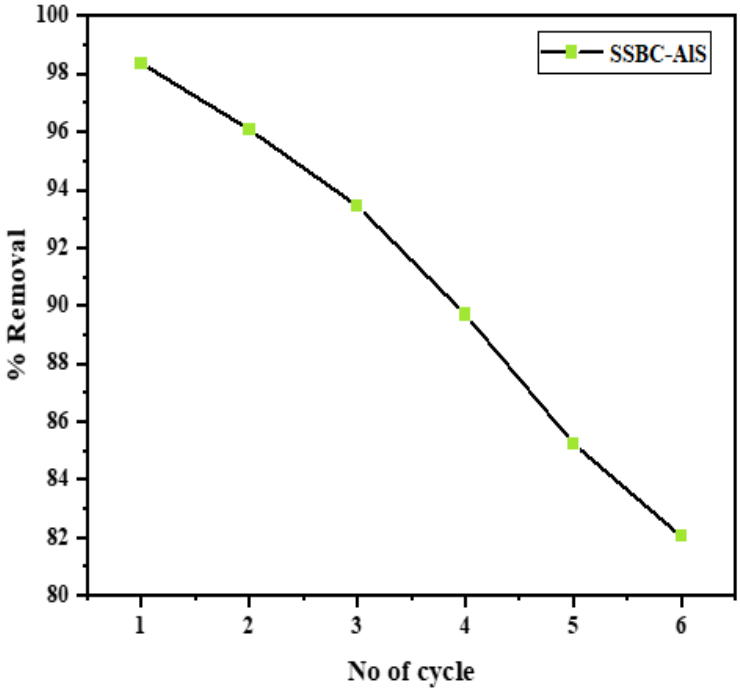

Figure 4.15: Recyclability of SSBC-AlS.

5. CONCLUSION AND RECOMMENDATIONS

5.1. Conclusion

The restoration of dye polluted wastewater using byproduct wastes from water treatment activities is a promising approach to transform the waste to treasure and to ensure the environmental sustainability. Moreover, future existence of the manufacturing industry such as textile industry in developing countries depend the development and use of locally available low cost materials that substitute imported ones. Dye like MB, is organic pollutant of water that cause a health risk on animals, plants, and humans because of its environmental persistence, toxicity and non-biodegradable nature, as well as bioaccumulation. Therefore, it is significant to remove MB from wastewater using a cost-effective and efficient method. To this end, this study investigates the possibility of developing composite from sewage sludge based biochar and dewatered alum sludge to be used as efficient adsorbent for removal of MB from wastewater in a batch mode at optimized condition. Accordingly:

- The different physicochemical and surface characteristics of the SS pyrolyzed at temperatures of 350 °C, 450 °C and 550 °C and labeled (SSBC350, SSBC450, and SSBC550) confirmed the SSBC550 have better potential to form composite adsorbent with AlS and used for MB dye decontamination. Moreover, the different physicochemical, mineralogical, and surface characteristics of SSBC, and AlS adsorbents as well as sewage sludge-based biochar-alum sludge (SSBC-AlS) composite adsorbent revealed the presence of suitable functional groups for MB adsorption like (-OH), (C-N), (C-O), and (Si-O), and (Si-O-Si), honeycomb-like rough structure, and highly porous surface characteristics that influence its adsorption efficiency.

- The pre-test performed prior to batch adsorption experiment on five different SSBC-AlS composite adsorbent compositions confirmed the composite comprised of 75w% SSBC and 25w% AlS, showed a superior removal efficiency to be further investigated for its application to effectively remove MB dye from aqueous solution and wastewater.

- Except solution temperature, adsorption parameters such as solution pH, contact time, initial concentration of MB and adsorbent dose significantly influence removal efficiency of the composite adsorbent and needs to be optimized for its effective use.

- The composite adsorbent (SSBC-AlS) has maximum removal capacity of 19.98 mg/g with removal efficiency of 99.96% at optimized contact time of 30 minutes, initial MB dye concentration of 100 mg/L, and 1g of SSBC-AlS composite dose at room temperature with stirring rate of 100 rpm. In which, its efficiency were not significantly dropped before six (6) consecutive usages, indicated the prepared composite has excellent properties for removal of MB from textile industry wastewater with good regeneration and reusability potential.

- The adsorption process of this study is well described by the Langmuir model with a high R^2 value of 0.9996 than Freundlich model, which indicated the adsorption mechanism is monolayer adsorption processes and the presence of homogenous sites on the SSBC-AlS surface. The data from kinetic experiments was found to fit well with the pseudo-second-order kinetic model with a high R^2 value of 1, which indicates the presence of chemisorption.

- In general, the composite synthesized from SSBC and AlS can be used as low cost, and environmentally friendly adsorbent with good thermal stability and rough porous surface for the removal of MB dye from textile industry wastewater.

5.2. Recommendations

- However, forthcoming study should consider the applicability of SSBC-AlS composite for different cations adsorption from industrial wastewater and simultaneous removal of heavy metals and mixed dyes.

- It is also recommended to study the desorption using different eluent to get a full picture of the adsorption-desorption science of the SSBC-AlS for MB as well as other contaminant removal from different types of wastewater.

6. REFERENCE

Abidi, N., Cabrales, L., & Haigler, C. H. (2014). Changes in the cell wall and cellulose content of developing cotton fibers investigated by FTIR spectroscopy. *Carbohydrate Polymers*, 100, 9-16. https://doi.org/10.1016/j.carbpol.2013.01.074.

Ackah, L. A., R. Guru, M. Peiravi, M. Mohanty, X. M. Ma, S. Kumar, & J. Liu. (2018). Characterization of Southern Illinois Water Treatment Residues for Sustainable Applications. E*nvironmental Science and Pollution Research,* 10(5):14. https://doi.org/10.3390/su10051374.

Agarwal, S., I. Tyagi, Gupta V. K, N. Ghasemi, M. Shahivand, & M. Ghasemi. (2016). Kinetics, Equilibrium Studies and Thermodynamics of Methylene Blue Adsorption on Ephedra Strobilacea Sawdust and Modified Using Phosphoric Acid and Zinc Chloride. *Journal of Molecular Liquids,* 218:208-18. https://doi.org/10.1016/j.molliq.2016.02.073.

Aghapour, A. A., H. Khorsandi, A. Dehghani, & Karimzade. (2018). Preparation and Characterization and Application of Activated Alumina (AA) from Alum Sludge for the Adsorption of Fluoride from Aqueous Solutions: New Approach to Alum Sludge Recycling. *Water Sci. Technol.Water Supply,* 18(5):1825-31. https://doi.org/10.2166/ws.2018.006.

Agrafioti, E., Bouras, G., Kalderis, D. & Diamadopoulos, E. (2013). Biochar production by sewage sludge pyrolysis. *Journal of Analytical and Applied Pyrolysis*, 101, 72-78. https://doi.org/10.1016/j. jaap.2013.02.010.

Ahmed, M. B., J. L. Zhou, H. H. Ngo, M. A. H. Johir, L. Sun, M. Asadullah, & D. Belhaj. (2018). Sorption of hydrophobic organic contaminants on functionalized biochar: protagonist role of π-π electron-donor-acceptor interactions and hydrogen bonds. *J. Hazard. Mater,* 360:270-78. https://doi.org/10.1016/j.jhazmat.2018.08.005.

Ahmad, T., Ahmad, K., & Alam, M. (2016). Characterization of water treatment plant's sludge and its safe disposal options. *Procedia Environmental Sciences*, *35*, 950-955. https://doi.org/10.1016/j.proenv.2016.07.088.

Ahmad, T., K. Ahmad, & M. Alam. (2017). Sludge Quantification at Water Treatment Plant and Its Management Scenario. *Environ. Monit. Assess,* 189:453-63. https://doi.org/10.1007/s10661-017-6166-1.

Ahmad, T., K. Ahmad, & M. C. D. Alam. (2016). Sustainable Management of Water Treatment Sludge through 3 'R' Concept. *J. Clean. Prod,* 124:1-13. https://doi.org/10.1016/J.JCLEPRO.2016.02.073.

Ak, N., & H. Dumrul. (2017). Wastewater Treatment Unit Operations and Processes. *Energy Educ. Sci. Tech-C,* 9:1-12. https://doi.org/10.5714/CL.2017.23.030.

Al Juboury, Maad F., Musa H. Alshammari, Mohammed R. Al-Juhaishi, Laith A. Naji, Ayad A. H. Faisal, Mu Naushad, & Eder C. Lima. (2020). Synthesis of Composite Sorbent for the Treatment of Aqueous Solutions Contaminated with Methylene Blue Dye. *Water Science and Technology,* 81(7):1494-1506. https://doi.org/10.2166/wst.2020.241.

Alatalo, S. M.; Repo, E.; Makila, E.; Salonen, J.; Vakkilainen, E.; & Sillanpaa, M. (2013). Adsorption behavior of hydrothermally treated municipal sludge & pulp and paper industry sludge. *Bioresour. Technol*., 147, 71-76. https://doi.org/10.1016/j.biortech.2013.08.034.

Ali, I. (2012). New generation adsorbents for water treatment. *Chem. Rev*. . https://doi.org/10.1021/cr300133d.

Ali, L., Palamanit, A., Techato, K., Chowdhury, Md. S., & Phoungthong, K. (2021). Characteristics and agrarian properties of biochar derived from pyrolysis and co-pyrolysis of rubberwood sawdust and sewage sludge for further application to soil improvement. *Journal of Water Reuse and Desalination.* https://doi.org/10.21203/rs.3.rs-830242/v1.

Alssgeer, H. M. A., M. B. Gasim, M. M. Hanafiah, E. R. A. Abdulhadi, & A. Azid. (2018). GIS-Based Analysis of Water Quality Deterioration in the Nerus River, Kuala Terengganu, Malaysia. *Desalination Water Treat,* 112:334–43. https://doi.org/10.5004/dwt.2018.22335.

Ambroz, F., Macdonald, T. J., Martis, V., & Parkin, I. P. (2018). Evaluation of the BET theory for the characterization of meso and microporous MOFs. *Small Methods*, *2*(11), 1-17. https://doi.org/10.1002/smtd.201800173.

Ameri, B., S. Hanini, & M. Boumahdi. (2020). Influence of drying methods on the thermo-dynamic parameters, effective moisture diffusion and drying rate of wastewater sewage sludge. *Renewable Energy*, 147:1107–19. https://doi:10.1016/j.renene.2019.09.072.

Antal, M. J., Mochidzuki, K. H. & Paredes, L. S. (2003). Flash carbonization of biomass. *Ind. Eng. Chem. Res*., 42, 3690–3699. https://doi.org/10.1038/s41598-019-40634-2.

Ataei-Germi, T., & A. Nematollahzadeh. (2016). Bimodal Porous Silica Microspheres Decorated with Polydopamine Nano-Particles for the Adsorption of Methylene Blue in Fixed-Bed Columns. *Journal of Colloid and Interface Science,* 470:172–82. https://doi.org/10.1016/j.jcis.2016.02.057.

Awab Kourtan. (2012). Properties and chemical composition of Water Treatment Sludge. *Malaysian Journal of Fundamental & Applied Sciences,* 251-255. https://doi.org/10.1007/s13201-019-0927-7.

Babatunde, A. O., & Y. Q. Zhao. (2007). Constructive Approaches toward Water Treatment Works Sludge Management: An International Review of Beneficial Reuses. *Crit. Rev. Environ. Sci. Technol,* 37:99-164. https://doi.org/10.1080/10643380600776239.

Babatunde, A. O., Y. Q. Zhao, M. O'Neill, & B. O'Sullivan. (2008). Constructed Wetlands for Environmental Pollution Control: A Review of Developments, Research and Practice in Ireland. *Environ. Int.* https://doi.org/10.1016/j.envint.2007.06.013.

Bagreev, A., & Bandosz, T.J., (2004). Efficient hydrogen sulfide adsorbents obtained by pyrolysis of sewage sludge derived fertilizer modified with spent mineral oil. *Environ. Sci. Technol*. 38, 345-351. https://doi.org/10.1021/es0303438.

Bahiru, D. B., Teju, E., Kebede, T., & Demissie, N. (2019). Levels of some toxic heavy metals (Cr , Cd and Pb) in selected vegetables and soil around eastern industry zone, central Ethiopia. *Journal of Sustainable Development of Energy, Water and Environment Systems14*(2), 92–101. https://doi.org/10.5897/AJAR2018.13324.

Bartolomeu, M., M. Neves, M. Faustino, & A. Almeida. (2018). Wastewater Chemical Contaminants: Remediation by Advanced Oxidation Processes. *Photochem. Photobiol. Sci* 17:1573–98. https://doi.org/10.1039/C8PP00249E.

Basri M, Don N, Kasmuri N, Hamzah N, Alias S, & Azizan FA. (2019). Aluminium recovery from water treatment sludge under different dosage of sulphuric acid. *J Phys: Conf Series IOP Publ, 1349*:012005. https://doi.org/10.1088/1742-6596/1349/1/012005.

Bayuo, J., Abukari, M. A., & Pelig-Ba, K. B. (2020). Desorption of chromium (VI) and lead (II) ions and regeneration of the exhausted adsorbent. *Applied Water Science*, *10*(7), 1–6. https://doi.org/10.1007/s13201-020-01250.

Bharathiraja, B., D. Yogendran, R. Ranjith Kumar, M. Chakravarthy, & S. Palani. (2014). Biofuels from Sewage Sludge- A Review. *Int. J. Chem. Tech. Res,* 6:4417–4427. https://doi.org/10.1016/j.talanta.2006.05.094.

Bhatnagar, A. & Sillanpaa, M. (2010). Utilization of agro-industrial and municipal waste materials as potential adsorbents for water treatment- A review. *Chem. Eng. J*., 157, 277–296. https://doi.org/10.2202/1542-6580.2413.

Bilgic, A. (2019). Removal of chromium (VI) from polluted wastewater by chemical modification of silica gel. *RSC Advances, 9(64),* 37403–37414. https://doi.org/10.1039/c9ra05810a.

Bonfiglioli, L., Bianchini, A., Pellegrini, M., & Saccani, C. (2014). Sewage sludge: characterstics and recovery options. *Wastewater Treatment Engineering*. https://doi.org/10.6092/unibo/amsacta/ 4027.

Boyer, T. H., A. Persaud, P. Banerjee, & P. Palomino. (2011). Comparison of Low-Cost and Engineered Materials for Phosphorus Removal from Organic-Rich Surface Water. *Water Res*. https://doi.org/10.1016/j.watres.2011.06.020.

Breulmann, M., Schulz, E., van Afferden, M., Müller, R.A., & Fuhren, C. (2018). Hydrochars derived from sewage sludge: effects of pre-treatment with water on char properties, phytotoxicity and chemical structure. *Arch. Agron Soil Sci*. 64, 860e872. https://doi.org/10.1080/03650340.2017.1396318.

Bulgariu, L., L. B. Escudero, O. S. Bello, M. Iqbal, J. Nisar, K. A. Adegoke, F. Alakhras, M. Kornaros, & I. Anastopoulos. (2019). The Utilization of Leaf-Based Adsorbents for Dyes Removal: A Review. *J. Mol. Liq,* 276:728–47. https://doi.org/10.1016/j.molliq.2018.12.001.

Bullen, J. C., Saleesongsom, S., Gallagher, K., & Weiss, D. J. (2021). A Revised Pseudo-Second-Order Kinetic Model for Adsorption, Sensitive to Changes in Adsorbate and

Adsorbent Concentrations. *Langmuir*, *37*(10), 3189–3201. https://doi.org/10.1021/acs.langmuir.1c00142.

Callegari, A., & Capodaglio, A.G. (2018). Properties and Beneficial Uses of (Bio) Chars, with Special Attention to Products from Sewage Sludge Pyrolysis. *Indian Journal of Pharmacology*, **7**, 20. https://doi.org/10.3390/resources7010020.

Capodaglio, A.G., Callegari, A., & Dondi, D. (2016). Microwave-induced pyrolysis for production of sustainable biodiesel from waste sludges. *Waste Biomass Valoriz.* 7(4), 703–709. https://doi.org/10.1007/s12649-016-9496-2.

Capodaglio, A.G., & Callegari, A. (2017). Properties and beneficial uses of biochar from sewage sludge pyrolysis. In 5th International Conference on Sustainable Solid Waste Management (Athens). https://doi.org/10.2166/wqrj.2009.019.

Ceini, G., & E. Lichtfouse. (2019). Advantages and disadvantages of techniques used for wastewater treatment. *Environ. Chem. Lett*, 17:145–55. https://doi.org/10.1007/s10311-018-0785-9.

Chen D., Yin L., Wang H., & He P. (2014). Pyrolysis technologies for municipal solid waste: A review. *Waste Manage.*, 34 , pp. 2466-2486. https://doi.org/10.1016/j.wasman.2014.08.004.

Chen, S., Qin, C., Wang, T., Chen, F., Li, X., Hou, H., & Zhou, M. (2019). Study on the adsorption of dyestuffs with different properties by sludge-rice husk biochar: Adsorption capacity, isotherm, kinetic, thermodynamics and mechanism. *J. Mol. Liq.* 285, 62-74. https://doi.org/10.1016/j.molliq.2019.04.035.

Chen, Q., Liu, H., Ko, J.H., Wu, H., & Xu, Q. (2019). Structure characteristics of biochar generated from co-pyrolysis of wooden waste and wet municipal sewage sludge. *Fuel Process. Technol.*, 183, 48–54. https://doi.org/10.1016/j.fuproc.2018.11.005.

Chen, T., Zhou, Z., Han, R., Meng, R.,Wang, H., & Lu, W. (2015). Adsorption of cadmium by biochar derived from municipal sewage sludge: impact factors and adsorption mechanism. *Chemosphere,* 134, 286e293. https://doi.org/10.1016/j.chemosphere.2015.04.052.

Chen, W., Gao, X., Xu, H., Wang, K., & Chen, T. (2017). Preparation of modified water-works sludge particles as adsorbent to enhance coagulation of slightly polluted source water. *Environmental Science and Pollution Research*, *24*(23), 19393-19401. https://doi.org/10.1007/s11356-017-9563-7.

Chiang, K. Y., Chou, P. H., Hua, C. R., Chien, K. L., & Cheeseman C. (2009). Lightweight bricks manufactured from water treatment sludge and rice husks. J. Hazard. Mater. 171, 76-82. https://doi.org/10.1016/j.jhazmat.2009.05.144.

Chittoo, V. S., & C. Sutherland. (2014). Adsorption of Phosphorus Using Water Treatment Sludges (Alum, Lime, Lime-Iron). *J. Appl. Sci*. https://doi.org/10.3923/jas.2014.3455.3463.

Chowdhary, P., A. Raj, & R. N. Bharagava. (2018). Environmental Pollution and Health Hazards from Distillery Wastewater and Treatment Approaches to Combat the Environmental Threats. *Chemosphere*, 194:229-46. https://doi.org/10.1016/j.chemosphere.2017.11.163.

Contescu, C., Adhikari, S., Gallego, N., Evans, N., & Biss, B. (2018). Activated carbons derived from high-temperature pyrolysis of lignocellulosic biomass. *J. Carbon Res*. 4, 51. https://doi.org/10.3390/c4030051.

Crombie K, Masek O, Sohi SP, Brownsort P, & Cross A. (2013). The effect of pyrolysis conditions on biochar stability as determined by three methods. *Glob Chang Biol Bioenergy*, 5:122–131. https://doi.org/10.1111/gcbb.12030.

Dagne, B. B. (2020). Determination of Heavy Metals in Wastewater and Their Toxicological Implications around Eastern Industrial Zone, Central Ethiopia. *Journal of Environmental Chemistry and Ecotoxicology*, *12*(2), 72–79. https://doi.org/10.5897/jece2019.0453.

Danner T, Norden G & Justnes H. (2018). Characterization of calcined raw clays suitable as supplementary cementitious materials. *Appl. Clay Sci.* 162 391–402. https://doi.org/10.1016/j.clay.2018.06.030.

Dassanayake, K. B., G. Y. Jayasinghe, A. Surapaneni, & C. Hetherington. (2015). A Review on Alum Sludge Reuse with Special Reference to Agricultural Applications and Future

Challenges. *Waste Management*, 38:321–35. https://doi.org/10.1016/j.wasman.2014.11.025.

De Gisi, S., Lofrano, G., Grassi, M., & Notarnicola, M. (2016). Characteristics and adsorption capacities of low-cost sorbents for wastewater treatment: A review. *Sustain. Mater. Technol*. 9, 10-40. https://doi.org/10.1016/j.susmat.2016.06.002.

Demirbas, A., O. Taylan, & D. Kaya. (2016). Biogas production from municipal sewage sludge. MSS. *Energy Sour. Part A*, 34:3027–33. https://doi.org/10.1080/15567036.2015.1124944.

Desore, A., & S. A. Narula. (2018). An Overview on Corporate Response towards Sustainability Issues in Textile Industry. *Environ. Dev. Sustain*, 20:1439–59. https://doi.org/10.1007/s10668-017-9949-1.

Devi, P., & A. K. Saroha. (2017). Utilization of Sludge Based Adsorbents for the Removal of Various Pollutants: A Review. *Sci. Total Environ*, 578:16-33. https://doi.org/10.1016/j.scitotenv.2016.10.220.

Dias, R., D. Sousa, M. Bernardo, I. Matos, I. Fonseca, V. V. Cardoso, R. N. Carneiro, S. Silva, P. Fontes, & M. A. Daam. (2021). Study of the Potential of Water Treatment Sludges in the Removal of Emerging Pollutants. *Molecules*, 26:1010. https://doi.org/10.3390/molecules26041010.

Dube, S., P. Muchaonyerwa, F. Mapanda, & J. Hughes. 2018. Effects of Sludge Water from a Water Treatment Works on Soil Properties and the Yield and Elemental Uptake of Brachiaria Decumbens and Lucerne. *Agric. Water Manage*, 208:335–43. https://doi.org/10.1016/j.agwat.2018.06.015.

El-Tokhy, T., Ahmed, M., ElGamma, M., & Ibrahim, M. (2020). Improvement and characterization of alum sludge by nano-iron oxide and rice husk for removal of methylene blue dye from aqueous solution. *Journal of Egyptian Academic Society for Environmental Development. and Environmental Studies*, *21*(1), 25–59. https://doi.org/10.21608/jades.2020.145445.

Emongor, V., E. Nkegbe, B. Kealotswe, I. Koorapetse, S. Sankwasa, & S. Keikanetswe. (2015). Pollution Indicators in Gaborone Industrial Effluent. *J Appl Sci*, 5(1). https://doi.jas.2005.147.150kw.

Enders, A. & Lehmann, J. (2017). Proximate analyses for characterizing biochars. In Biochar: A Guide to Analytical Methods. https://doi.org/10.1007/s13201-019-0927-7.

F. Mashkoor, A. Nasar, & Magsorbents. (2020). Potential candidates in wastewater treatment technology – a review on the removal of methylene blue dye. *J. Magn. Magn. Mater.*, 500, 166408. https://doi.org/10.1016/j.jmmm.2020.166408.

Fan, S., Tang, Jie, Wang, Y., Li, H., Zhang, H., Tang, Jun, Wang, Z., & Li, X. (2016). Biochar prepared from co-pyrolysis of municipal sewage sludge and tea waste for the adsorption of methylene blue from aqueous solutions: kinetics, isotherm, thermodynamic and mechanism. *J. Mol. Liq.* 220, 432-441. https://doi.org/ 10.1016/j.molliq.2016.04.107.

Fan, S. S., Y. Wang, Z. Wang, J. Tang, J. Tang, X. & D. Li. (2017). Removal of Methylene Blue from Aqueous Solution by Sewage Sludge-Derived Biochar: Adsorption Kinetics, Equilibrium, Thermodynamics and Mechanism. *J. Environ. Chem. Eng*, 5:601–11. https://doi:10.1016/j.jece.2016.12.019 JECE 1378.

Faria, W.M., Figueiredo, C., Coser, T.R., Vale, A.T., & Schneider, B.G. (2018). Is sewage sludge biochar capable of replacing inorganic fertilizers for corn production? Evidence from a two-year field experiment. *Arch. Agron Soil* Sci. 64, 505-519. https://doi.org/10.1080/03650340.2017.1360488.

Figueiredo, C., Lopes, H., Coser, T., Vale, A., Busato, J., Aguiar, N., Novotny, E., & Canellas, L. (2018). Influence of pyrolysis temperature on chemical and physical properties of biochar from sewage sludge. *Arch. Agron Soil Sci.* 64, 881-889. https://doi.org/10.1080/03650340.2017.1407870.

Gao, N., Li, J., Qi, B., Li, A., Duan, Y., & Wang, Z. (2014). Thermal analysis and products distribution of dried sewage sludge pyrolysis. *J. Anal. Appl. Pyrolysis*, 105, 43-48. https://doi.org/10.1016/j.jaap.2013.10.002.

Gao, N., Quan, C., Liu, B., Li, Z., Wu, C., & Li, A. (2017). Continuous pyrolysis of sewage sludge in a screw-feeding reactor: products characterization and ecological risk assessment

of heavy metals. *Energy Fuels,* 31, 5063-5072. https://doi.org/10.1021/acs.energyfuels.6b03112.

Gao, S., C. Wang, & Y. Pei. (2013). Comparison of Different Phosphate Species Adsorption by Ferric and Alum Water Treatment Residuals. *J. Environ. Sci,* 25(5):986–92. https://doi.org/10.1016/S1001-0742(12)60113-2.

Geng, Yani, Jun Zhang, Jinhong Zhou, & Ji Lei. (2018). Study on Adsorption of Methylene Blue by a Novel Composite Material of TiO_2 and Alum Sludge. *RSC Advances,* 8(57). https://doi.org/10.1039/C8RA05946B.

Gomez-Pacheco, C.V., Rivera-Utrilla, J., Sanchez-Polo, M., & Lopez-Penalver, J.J. (2012). Optimization of the preparation process of biological sludge adsorbents for application in water treatment. *J. Hazard Mater,* 217-218, 76-84. https://doi.org/10.1016/j.jhazmat.2012.02.067.

Gong, Z. Q., A. X. Du, Z. B. Wang, P. W. Fang, & X. Y. Li. (2018). Experimental study on pyrolysis characteristics of oil sludge with a tube furnace reactor. *Energy and Fuels,* 31:8102–08. https://doi.org/10.1021/acs.energyfuels.7b01363.

Gopinath, A., Divyapriya, G., Srivastava, V., Laiju, A. R., Nidheesh, P. V., & Kumar, M. S. (2021). Conversion of sewage sludge into biochar: A potential resource in water and wastewater treatment. *Environmental Research*, *194*, 110656. https://doi.org/10.1016/j.envres.2020.110656.

Gregorio Crini, Eric Lichtfouse, & Lee Wilson, N. M. C. (2018). Adsorption-oriented processes using conventional and non-conventional adsorbents for wastewater treatment. In *Environmental Chemistry Letters* (Vol. 17, Issue 1). https://doi.org/10.1007/s10311-018-0786-8.

Grosser, A., M. Worwag, E. Neczaj, & T. Kamizela. (2013). Co-digestion of Organic Fraction of Municipal Solid Waste with Different Organic Wastes: A Review. in *Environmental Engineering IV—Proceedings of the Conference on Environmental Engineering IV*. https://doi.org/10.1201/b14894-38.

Guo, K., B. Gao, R. Li, W. Wang, Q. Yue, & Y. Wang. (2017). Flocculation Performance of Lignin-Based Flocculant during Reactive Blue Dye Removal: Comparison with

Commercial Flocculants. *Frontiers in Environmental Science.* https://doi.org/10.1007/s11356-017-0835-z.

H. Zazou, H. Afanga, & S. Akhouairi. (2019). Treatment of textile industry wastewater by electrocoagulation coupled with electrochemical advanced oxidation process. Journal of *Water Process Enginerring*, vol. 28, pp. 214-221. https://doi.org/10.1016/j.jwpe.2019.02.006.

H. Zeng, T. Qiao, L. Zhai, J. & Zhang, D. Li. (2019). Fe_3O_4@C particles synthesized with iron-containing water treatment residuals and its potential for methylene blue removal. *J. Chem. Technol. Biotechnol*., 94, 3970–3980. https://doi.org/10.1002/jctb.6202.

H. Zhu, Z. Wang, W. Xing, & X. Shu. (2018). Process optimization and adsorption performance of biochar's prepared by co-pyrolysis of sludge and biomasses. *Chem. Ind. Eng. Prog*., 37, 199–204. https://doi.org/10.1016/j.heliyon.2020.e05049.

Hadi, P., Xu, M., Ning, C., Sze Ki Lin, C., & McKay, G. (2015). A critical review on preparation, characterization and utilization of sludge-derived activated carbons for wastewater treatment. *Chem. Eng. J*., 260, 895-906. https://doi.org/10.1016/ j.cej.2014.08.088.

Hassan, M. A., & A. El-Nemr. (2017). Health and environmental impacts of dyes: Mini review. *AJESE,* 1:64–67. https://doi.org/10.11648/j.ajese.20170103.11.

Haynes, R. J. (2015). Use of Industrial Wastes as Media in Constructed Wetlands and Filter Beds - Prospects for Removal of Phosphate and Metals from Wastewater Streams. *Crit. Rev. Environ. Sci. Technol*., https://doi.org/10.1080/10643389.

He, C., Giannis, A., & Wang, J.Y. (2013). Conversion of sewage sludge to clean solid fuel using hydrothermal carbonization: hydrochar fuel characteristics and combustion behavior. *Appl. Energy, 111*, 257-266. https://doi.org/10.1016/ j.apenergy.2013.04.084.

Hidalgo, A. M., M. D. Murcia, M. Gomez, E. Gomez, C. Garcia-Izquierdo, & C. Solano. (2017). Possible Uses for Sludge from Drinking Water Treatment Plants. *Journal of Environmental Engineering,* 143(3):04016088. https://doi.org/10.1061/(ASCE)EE.1943-7870.0001176.

Ho, S. H., Y. D. Chen, Z. K. Yang, D. Nagarajan, J. S. Chang, & N. Q. Ren. (2017). High-efficiency removal of lead from wastewater by biochar derived from anaerobic digestion sludge. *Bioresource Technology*, 246:142–49. https://doi.org/10.1016/j.biortech.2017.08.025.

Ho, Y. S., T. H. Chiang, & Y. M. Hsueh. (2005). Removal of Basic Dye from Aqueous Solution Using Tree Fern as a Biosorbent. *Process Biochem*, 40:119–24. https://doi.org/10.1016/j.procbio.2003.11.035.

Hossain, M.K., Strezov Vladimir, V., Chan, K.Y., Ziolkowski, A., & Nelson, P.F. (2011). Influence of pyrolysis temperature on production and nutrient properties of wastewater sludge biochar. *J. Environ. Manag*., 92, 223–228. https://doi.org/ 10.1016/j.jenvman.2010.09.008.

Hua, T., R. J. Haynes, & Y. F. Zhou. (2018). Competitive Adsorption and Desorption of Arsenate, Vanadate, and Molybdate onto the Low-Cost Adsorbent Materials Alum Water Treatment Sludge and Bauxite. *Environ. Sci. Pollut. Res.*, 25:34053 34062. https://doi.org/10.1007/s11356-018-3301-7.

Hugo Perazzini FBF, Fabio Bentes Freire & Jose Teixeira Freire. (2016). Thermal Treatment of Solid Wastes Using Drying Technologies: A Review. *Drying Technology*., Vol 34, No 1, 39–52. https://doi.org/10.1080/07373937.2014.995803.

Ippolito, J. A. (2015). Aluminum-Based Water Treatment Residual Use in a Constructed Wetland for Capturing Urban Runoff Phosphorus: Column Study. *Water Air Soil Poll.*, 226:1–8. https://doi.org/10.1007/s11270-015-2604-2.

Ippolito, J. A., K. A. Barbarick, & H. A. Elliott. (2011). Drinking Water Treatment Residuals: A Review of Recent Uses. *J. Environ. Qual.*, 2:1–12. https://doi.org/10.2134/jeq2010.0242.

J. Qi, Y. Hou, J. Hu, W. Ruan, Y. Xiang, & X. Wei. (2020). Decontamination of methylene Blue from simulated wastewater by the mesoporous GO/Fe/Co nanohybrids: artificial intelligence modeling and optimization. *Mater. Today Commun*., 24. https://doi.org/10.1016/j.mtcomm.2019.100709.

Jae Gon Kim, Jung Hyun Kim, Hi-Soo Moon, Chul-Min Chon & Joo Sung Ahn. (2002). Removal capacity of water plant alum sludge for phosphorus in aqueous solutions, Chemical Speciation & Bioavailability. *Critical Reviews in Environmental Science and Technology,* 14:1-4, 67-73. https://doi.org/10.3184/095422902782775344.

Jafari, M., & Botte, G.G. (2021). Electrochemical treatment of sewage sludge and pathogen inactivation. *J. Appl. Electrochem*., 51 119–130. https://doi.org/10.1007/s10800-020-01481-6.

Ji, H., X. Song, & Z. Shi. (2018). Reinforced-Concrete Structured Hydrogel Microspheres with Ultrahigh Mechanical Strength, Restricted Water Uptake, and Superior Adsorption Capacity. *ACS Sustainable Chem Eng.,* 6:5950–58. https://doi.org/10.1021/acssuschemeng.7b04323.

Jin J., Li Y., Zhang J., Wu S., Cao Y., Liang P., Zhang J., Wong M., Wang M., Shan S., & Christie P. (2016). Influence of pyrolysis temperature on properties and environmental safety of heavy metals in biochars derived from municipal sewage sludge. *J. Hazards Mater*., 320. pp. 417-426, https://doi.org/10.1016/j.jhazmat.2016.08.050.

K. Mao, H. Chen, T. Chen, X. Xia, Z. Cao, & Y. Zhao. (2020). Adsorption effects of sludge biochar of different particale sizes on Zn contamination in water. *Acta Sci. Circumst*., 40 536–545. https://doi.org/10.1016/j.biteb.2020.100466.

Kaczmarski, K., & J. C. Bellot. (2013). Effect of Particle-Size Distribution and Particle Porosity Changes on Mass-Transfer Kinetics. *Acta Chromatograph,* 13:22–37. https://doi.org/10.1016/j.cej.2018.09.202.

Kalderis, D., Kotti, M. S., Mendez, A., & Gasco, G. (2014). Characterization of hydrochars produced by hydrothermal carbonization of rice husk. *Solid Earth,* 5, 477–483. https://doi.org/10.1080/03650340.2017.1407870.

Karaer, H., & I. Kaya. 2016. Synthesis, Characterization of Magnetic Chitosan/Active Charcoal Composite and Using at the Adsorption of Methylene Blue and Reactive Blue 4. *Microporous Mesoporous Mater,* 232:26–38. https://doi.org/10.1016/j.micromeso.2016.06.006.

Khalid Z. Elwakeel, Ahmed M. Elgarahy, Ziya A. Khan, Muath S. & Almughamisi A. (2020). Perspectives regarding metals/minerals-incorporated materials for water purification: with special focus on Cr removal. *Russian Journal of General Chemistry*, *79*(6), 1141–1145. https://doi.org/10.1039/D0MA00153H.

Khatri, A., M. H. Peerzada, M. Mohsin, & M. White. (2015). A Review on Developments in Dyeing Cotton Fabrics with Reactive Dyes for Reducing Effluent Pollution. *J. Cleaner* Prod., 87:50–57. https://doi.org/10.1016/J.JCLEPRO.2014.09.017.

Kim, J. G., H. Bin Kim, G. S. Yoon, S. H. Kim, S. J. Min, D. C. W. Tsang, & K. Baek. (2020). Simultaneous Oxidation and Adsorption of Arsenic by One-Step Fabrication of Alum Sludge and Graphitic Carbon Nitride. *J. Hazard Mater.,* 383:121138. https://doi.org/10.1016/j.jhazmat.2019.121138.

Kim KH, Kim JY, Cho TS, & Choi JW. (2012). Influence of pyrolysis temperature on physicochemical properties of biochar obtained from the fast pyrolysis of pitch pine (Pinus rigida). *Bioresour Technol.,* 118, 158–62. https://doi.org/10.1016/j.biortech.2012.04.094.

Konczak, M., Oleszczuk, P., & Rozylo, K. (2019). Application of different carrying gases and ratio between sewage sludge and willow for engineered (smart) biochar production. *J. CO_2 Util*., 29, 20–28. https://doi.org/10.1016/j.jcou.2018.10.019.

L.Xiong, Y.Yang, J.Mai, W. Sun, C.Zhang, D. Wei, Q. Chen, & J.Ni. (2010). Adsorption behavior of methylene blue onto titanate nanotubes. *Chem. Eng. J*., 156, 313-320. https://doi.org/10.1142/S1793292018501424.

Lasaridi, K.-E., Manios, T., Stamatiadis, S., Chroni, C., & Kyriacou, A. (2018). The evaluation of hazards to man and the environment during the composting of sewage sludge. *Sustainability 10*, 2618. https://doi.org/10.3390/su10082618.

Launay, M. A., U. Dittmer, & H. Steinmetz. (2016). Organic Micropollutants Discharged by Combined Sewer Overflows-Characterization of Pollutant Sources and Stormwater-Related Processes. *Water Res.,* 104:82–92. https://doi.org/10.1016/j.watres.07.068.

Lehmann J, Rillig MC, & Thies J. (2011). Biochar effects on soil biota – A review. *Soil Biol Biochem*., 43:1812–1836. https://doi.org/10.1016/j.soilbio.2011.04.022.

Leng, L., Yuan, X., Huang, H., Shao, J., Wang, H., Chen, X., & Zeng, G. (2015). Bio-char derived from sewage sludge by liquefaction: characterization and application for dye adsorption. *Appl. Surf. Sci*., 346, 223-231. https://doi.org/10.1016/j.apsusc.

Li, X., J. Cui, & Y. Pei. (2018). Granulation of Drinking Water Treatment Residuals as Applicable Media for Phosphorus Removal. *J. Environ. Manag.*, 213:36–46. https://doi.org/10.1016/j.jenvman.2018.02.056.

Lin, Yan, Liao, Y., Yu, Z., Fang, S., Lin, Yousheng, Fan, Y., Peng, X., & Ma, X. (2016). Co-pyrolysis kinetics of sewage sludge and oil shale thermal decomposition using TGA-FTIR analysis. *Energy Convers. Manag*., 118, 345-352. https://doi.org/ 10.1016/j.enconman.2016.04.004.

Litaor, M. I., S. Schechter, I. Zohar, M. S. Massey, & J. A. Ippolito. (2019). Making Phosphorus Fertilizer from Dairy Wastewater with Aluminum Water Treatment Residuals. *Soil Sci. Soc. Am. J*. https://doi.org/10.2136/sssaj2018.07.0278.

Liu, G.H.; Chen, J.H.; Wang, Y.Y.; Qi, L.; & Wang, H.C. (2020). Study on advanced treatment of organic matter in effluent by modified sludge based adsorbent. *Acta Sci. Circumstantiae*., 40, 1196–1203. https://doi.org/http://dx.doi.org/10.4314/bcse.v27i1.4.

Liu, L. H., Y. Lin, Y. Y. Liu, H. Zhu, & Q. He. (2013). Removal of Methylene Blue from Aqueous Solutions by Sewage Sludge Based Granular Activated Carbon: Adsorption Equilibrium, Kinetics, and Thermodynamics. *J. Chem. Eng. Data*, 58:2248–53. https://doi.org/10.1021/je4003543.

Liu, Y., Chen, J., Chen, M., Zhang, B., Wu, D., & Cheng, Q., 2015. Adsorption characteristics and mechanism of sewage sludge-derived adsorbent for removing sulfonated methyl phenol resin in wastewater. *RSC Adv*., 5, 76160-76169. https://doi.org/10.1039/c5ra17125c.

Lu, H., Zhang, W., Wang, S., Zhuang, L., Yang, Y., & Qiu, R. (2013). Characterization of sewage sludge-derived biochars from different feedstocks and pyrolysis temperatures. *Journal of Analytical and Applied Pyrolysis*, 102, 137-143. https://doi.org/10.1016/j.jaap.2013.03.004.

Lu, Qin, Zhenli L. He, & Peter J. Stoffella. (2012). Land Application of Biosolids in the USA: A Review. *Applied and Environmental Soil Science*, 1–11. https://doi.org/10.1155/2012/201462.

Lucia Ivanova TM, Roman Grabic, Oksana Golovko, Olga Kob, Andrea Vojs Stanova, Petra Szabova, Anna Grencikova, & Igor Bodik. (2018). Pharmaceuticals and illicit drugs – A new threat to the application of sewage sludge in agriculture. *Science of the Total Environment*, 634 606–615. https://doi.org/10.3390/ijerph110100249.

M.T. Uddin, M.A. Islam, S. Mahmud, & M. Rukanuzzaman. (2009). Adsorptive removal of methylene blue by tea waste. *J. Hazard. Mater*., 164, 53-60. https://doi.org/10.1016/j.jhazmat.2008.07.131.

M. Zhang, & B. Gao. (2013). Removal of arsenic, methylene blue, and phosphate by biochar/ AlOOH nanocomposite. *Chem. Eng. J*., 226, 286–292. https://doi.org/10.1016/J.CEJ.2013.04.077.

Magdziarz, A., & Wilk, M. (2013). Thermogravimetric Study of Biomass, Sewage Sludge and Coal Combustion. *Energy Conversion and Management*, 75, 425-430. https://doi.org/10.1016/j.enconman.2013.06.016.

Markandeya, T., S. P. Shukla, & D. Mohan. (2017). Toxicity of Desperse Dyes and Its Removal from Wastewater Using Various Adsorbents: A Review. *Res. J. Environ. Toxicol.,* 11:72–89. https://doi.org/10.3923/rjet.2017.72.89.

Masresha B, & Enyew A. (2017). Synthesis of magnetic nano composite adsorbent by co-precipitation method for wastewater treatment. *Ethiop J Sci Sustain Dev*., 4:33–48. https://doi.org/10.1155/2021/6678588.

Mateo-Sagasta, J., Raschid-Sally, L., & Thebo, A. (2019). Global wastewater and sludge production, treatment and use. In: Wastewater: Economic Asset in an Urbanizing World. *Springer Netherlands*. https://doi.org/10.1007/978-94-017-9545-62.

Mehta, C.M., Khunjar, W.O., Nguyen, V., Tait, S., & Batstone, D.J. (2015). Technologies to recover nutrients from waste streams: A critical review. *Crit. Rev. Environ. Sci. Technol*., 45, 385-427. https://doi.org/10.1080/10643389.2013.866621.

Mendez, A., Barriga, S., Fidalgo, J.M., & Gasco, G. (2009). Adsorbent materials from paper industry waste materials and their use in Cu (II) removal from water. *J. Hazard Mater*., 165, 736-743. https://doi.org/10.1016/j.jhazmat.2008.10.055.

Menya, E., P. Olupot, H. Storz, M. Lubwama, & Y. Kiros. (2018). Production and Performance of Activated Carbon from Rice Husks for Removal of Natural Organic Matter from Water: A Review. *Chemical Engineering Research and Design*, 129:271–96. https://doi.org/10.1016/j.cherd.2017.11.008.

Mian, M.M., & Liu, G. (2018). Sewage sludge-derived TiO_2/Fe/Fe_3C-biochar composite as an efficient heterogeneous catalyst for degradation of methylene blue. *Chemosphere.* https://doi.org/10.1016/j.chemosphere.10.027.

Mimmo, T., Panzacchi, P., Baratieri, M., Davies C. A., & Tonon, G. (2014). Effect of pyrolysis temperature on miscanthus (Miscanthus xgiganteus) biochar physical, chemical and functional properties. *Biomass Bioenerg.,* 62, 149–157. https://doi.org/10.1016/j.micromeso.2016.06.006.

Miraboutalebi, S. M., S. K. Nikouzad, M. Peydayesh, N. Allahgholi, L. Vafajoo, & G. Mckay. (2017). Methylene Blue Adsorption via Maize Silk Powder: Kinetic, Equilibrium, Thermodynamic Studies and Residual Error Analysis. *Process Safety and Environmental Protection,* 106:191–202. https://doi.org/10.1016/j.psep.2017.01.010.

Mironyuk, I., T. Tatarchuk, M. Naushad, H. Vasylyeva, & I. Mykytyn. (2019). Highly Efficient Adsorption of Strontium Ions by Carbonated Mesoporous TiO_2. *J Mol Liq,* 285:742–53. https://doi.org/10.1016/j.molliq.2019.04.111.

Mohamed, B.; Rachid, H.; Mohammed, K.; Mohammed, A.; Nasser, H.S.; Emad, M.M.E.; Riyad, M.E. & Adel, A. (2017). Rice husk template water treatment sludge as low cost dye and metal adsorbent. *J. Egypt. J. Petrol*, 26: 661–668. https://doi.org/10.1016/j.ejpe.2016.10.006.

Mohan, D., Sarswat, A., Ok, Y.S., & Pittman, C.U. (2014). Organic and inorganic contaminants removal from water with biochar, a renewable, low cost and sustainable adsorbent - A critical review. *Bioresour. Technol*., 160, 191-202. https://doi.org/10.1016/j.biortech.2014.01.120.

Mohanty P, Nanda S, & Pant K. (2013). Evaluation of the physiochemical development of biochars obtained from pyrolysis of wheat straw, timothy grass and pinewood: Effects of heating rate. *J Anal Appl Pyrolysis*, 104:485–493. https://doi.org/10.1016/j.jaap.2013.05.022.

Monama, G. R., S. B. Mdluli, & G. Mashao. (2018). Palladium Deposition on Copper(II) Phthalocyanine/Metal Organic Framework Composite and Electrocatalytic Activity of the Modified Electrode towards the Hydrogen Evolution Reaction. *Renew Energy*, 119:62–72. https://doi.org/10.1016/j.renene.2017.11.084.

Montoya, J.I., Chejne-Janna, F., & Garcia-Perez, M. (2015). Fast pyrolysis of biomass: A review of relevant aspects. Part I: parametric study. *Dyna* 82, 239-248. https://doi.org/10.15446/dyna.v82n192.44701.

N.B. Singh, G. Nagpal, & S. Agrawal. (2018). Water purification by using adsorbents: A review. *Environ. Technol. Innov*., 11 187–240, https://doi.org/10.1016/j.eti.2018.05.006.

Nair, A. T., & M. M. Ahammed. (2015). Water Treatment Sludge for Phosphate Removal from the Effluent of UASB Reactor Treating Municipal Wastewater. *Process Saf. Environ. Prot.*, 94:105-112,. https://doi.org/10.1016/j.psep.2015.01.004.

Nanda, Sonil, Ajay K. Dalai, Iskender Gokalp, & Janusz A. Kozinski. (2016). Valorization of Horse Manure through Catalytic Supercritical Water Gasification. *Waste Management*, 52:147–58. https://doi.org/10.1016/j.wasman.2016.03.049.

Nasr, J. B., Hamdi, N., & Elhalouani, F. (2017). Characterization of activated carbon Prepared from sludge paper for methylene blue adsorption. *JMES, 8,* 1960-1967. https://doi.org/10.1016/j.talanta.2006.05.094.

Ncibi, M.C., Jeanne-Rose, V., Mahjoub, B., Jean-Marius, C., Lambert, J., Ehrhardt, J.J., Bercion, Y., Seffen, M., & Gaspard, S. (2009). Preparation and characterisation of raw chars and physically activated carbons derived from marine Posidonia oceanica (L.) fibres. *J. Hazard Mater.*, 165, 240-249. https://doi.org/10.1016/j.jhazmat.2008.09.126.

Odimegwu, T. C., I. Zakaria, M. M. Abood, C. B. K. Nketsiah, & M. Ahmad. (2018). Review on Different Beneficial Ways of Applying Alum Sludge in a Sustainable Disposal Manner. *Civ. Eng, J.-Tehran*, 4(9):2230–41. https://doi.org/10.28991/cej-03091153.

Oja V, Hajaligol MR, & Waymack BE. (2006). The vaporization of semi-volatile compounds during tobacco pyrolysis. *J Anal Appl Pyrolysis*, 76:117–123. https://doi.org/10.1016/j.jaap.2005.08.005.

Pathania, D.; Sharma, S.; & Singh, P. (2017). Removal of methylene blue by adsorption onto activated carbon developed from Ficus carica bast. *Arab. J. Chem*., 10, S1445–S1451. https://doi.org/10.1016/J.ARABJC.2013.04.021.

Paula Arbelaez FB, Rosa Maria Marce, & Eva Pocurull. (2015). Trace-level determination of sweeteners in sewage sludge using selective pressurized liquid extraction and liquid chromatography–tandem mass spectrometry. *Journal of Chromatography*, A, 1408. 15–21. https://doi.org/10.3390/molecules26082392.

Petrova, P., Karadjova, I., Chochkova, M., Dakova, I., & Karadjov, M. (2017). New amino acid modified silica gel sorbents for solid phase extraction of Au. *Journal of Saudi Chemical Society*. http://dx.doi.org/10.1016/j.chroma.2015.07.001.

Pokorna, E., Postelmans, N., Jenicek, P., Schreurs, S., Carleer, R., & Yperman, J. (2009). Study of bio-oils and solids from flash pyrolysis of sewage sludges. *Fuel*, 88, 1344-1350. https://doi.org/10.1016/j.fuel.2009.02.020.

Poormand, Hamid, Mostafa Leili, & Marzieh Khazaei. (2017). Adsorption of Methylene Blue from Aqueous Solutions Using Water Treatment Sludge Modified with Sodium Alginate as a Low Cost Adsorbent. *Water Science & Technology Water Supply*, 75. https://doi.org/10.2166/wst.2016.510.

Putra, R.S., & Tanaka, S. (2011). Aluminum drinking water treatment residuals as an entrapping zone for lead in soil by electrokinetic remediation. *Purif. Technol*., 79, 208–215. https://doi.org/10.1016/j.seppur.2011.02.015.

Qiao Xiong MZ, Mengjia Liu, Shijie Jiang, & Haobo Hou. (2018). The transformation behaviors of heavy metals and dewaterability of sewage sludge during the dual conditioning with Fe_2-sodium persulfate oxidation and rice husk. *Chemosphere*, 208, 93-100. https://doi.org/10.1007/s13201-020-01233-z.

Qiu, H., Lv, L., Pan, B. C., Zhang, Q. J., Zhang, W. M., & Zhang, Q. X. (2009). Critical review in adsorption kinetic models. *Journal of Zhejiang University: Science A*, 10(5), 716–724. https://doi.org/10.1631/jzus.A0820524.

Qiu, Y., Z. Zheng, Z. Zhou, & G. D. Sheng. (2009). Effectiveness and Mechanisms of Dye Adsorption on a Straw-Based Biochar. *Bioresource Technology*, 100 (21):5348–51. https://doi.org/10.1016/j.biortech.2009.05.054.

Quinones, K. D., A. Hovsepyan, A. Oppong-Anane, & J. C. J. Bonzongo. (2016). Insights into the Mechanisms of Mercury Sorption onto Aluminum Based Drinking Water Treatment Residuals. *J. Hazard. Mater,* 307:184–92. https://doi.org/10.1016/j.jhazmat.2016.01.001.

Racek J, Sevcik J, Chorazy T, Kucerik J, & Hlavinek P. (2020). Biochar - recovery material from pyrolysis of sewage sludge: A review. *Waste Biomass Valor*, 11:3677–3709. https://doi.org/10.1007/ s12649- 019- 00679.

Radi, S., El Abiad, C., Carvalho, A. P., Santos, S. M., Faustino, M. A. F., Neves, M. G. P. M. S., & Moura, N. M. M. (2018). An efficient hybrid adsorbent based on silica-supported amino penta-carboxylic acid for water purification. *Journal of Materials Chemistry, A, 6* (27), 13096–13109. https://doi.org/10.1039/c8ta02560f.

Rahman, M. A., S. R. Amin, & A. S. Alam. (2012). Removal of Methylene Blue from Waste Water Using Activated Carbon Prepared from Rice Husk. *Dhaka University Journal of Science,* 60(2):185–89. https://doi.org/10.3329/dujs.v60i2.11491.

Rajasulochana, P., & Preethy, V. (2016). Comparison on efficiency of various techniques in treatment of waste and sewage water - A comprehensive review. *Resour. Technol.*, 2, 175-184. https://doi.org/10.1016/j.reffit.2016.09.004.

Ran, C. M., Y. Liu, A. R. Siddiqui, A. A. Siyal, X. Mao, Q. H. Kang, J. Fu, W. Y. Ao, & J. J. Dai. (2019). Pyrolysis of textile dyeing sludge in fluidized bed: Analysis of products, and migration and distribution of heavy metals. *Journal of Cleaner Production*, 241:118308. https://doi.org/10.1016/j.jclepro.2019.118308.

Raposo, F., De La Rubia, M., & Borja, R. (2009). Methylene blue number as useful indicator to evaluate the adsorptive capacity of granular activated carbon in batch mode: Influence of

adsorbate/adsorbent mass ratio and particle size. *Journal of hazardous materials*, 165(1-3), 291-299. https://doi.org/10.1155/2018/8972549.

Rashed, M. N., M. E. D. El Taher, & S. M. Fadlalla. (2016). Adsorption of Methylene Blue Using Modified Adsorbents from Drinking Water Treatment Sludge. *Water Science and Technology*, 74(8):1885–98. https://doi.org/10.2166/wst.2016.377.

Ravulapalli, S., & Kunta, R. (2018). Enhanced removal of chromium (VI) from wastewater using active carbon derived from Lantana camara plant as adsorbent. *Water Science and Technology*, *78*(6), 1377-1389. https://doi.org/10.2166/wst.2018.413.

Reddy, P. M. K., P. Verma, & C. Subrahmanyam. (2016). Bio-Waste Derived Adsorbent Material for Methylene Blue Adsorption. *Journal of the Taiwan Institute of Chemical Engineers*, 58:500–508. https://doi.org/10.1016/j.jtice.2015.07.006.

Rehman, R.A., Rizwan, M., Qayyum, M.F., Ali, S., Ziaur-Rehman, M., Zafarul, M., Hafeez, F., & Iqbal, M.F. (2018). Efficiency of various sewage sludges and their biochars in improving selected soil properties and growth of wheat (Triticum aestivum). *J. Environ. Manag*., 223, 607–613. https://doi.org/10.1016/j.jenvman.2018.06.081.

Rio, S., Faur-Brasquet, C., Le Coq, L., & Le Cloirec, P. (2005). Structure characterization and adsorption properties of pyrolyzed sewage sludge. *Environ. Sci. Technol*., 39, 4249-4257. https://doi.org/10.1021/es0497532.

Rodriguez N H, Ramirez S M, Varela M T B, Guillem M, Puig J, Larrotcha E & Flores J. (2010). Re-use of drinking water treatment plant (DWTP) sludge: Characterization and technological behaviour of cement mortars with atomized sludge additions. *Cem. Concr. Res.*, 40, 778–86. http://dx.doi.org/10.1016/j.cemconres.2009.11.012.

Rorat A, Courtois P, Vandenbulcke F, & Lemiere S. (2019). Sanitary and environmental aspects of sewage sludge management in Industrial and Municipal Sludge. *Butterworth-Heinemann, Oxford*, pp 155–180. https://doi.org/10.1016/B978-0.

Roy, A.; Chakraborty, S.; Kundu, S. P.; Adhikari, B.; & Majumder, S. B. (2012). Adsorption of Anionic-Azo Dye from Aqueous Solution by Lignocellulose-Biomass Jute Fiber: Equilibrium, Kinetics, and Thermodynamics Study. *Ind. Eng. Chem. Res*., 51, 12095−12106. https://doi.org/10.1021/ie301708e.

Rudi, N. N., M. S. Muhamad, L. Te Chuan, J. Alipal, S. Omar, N. Hamidon, N. H. A. Hamid, N. M. Sunar, R. Ali, & H. Harun. (2020). Evolution of Adsorption Process for Manganese Removal in Water via Agricultural Waste Adsorbents. *International Journal of Environmental Research and Public Health.* https://doi.org/10.1016/j.heliyon.2020.e05049.

Russo, I., Confente, I., Scarpi, D., & Hazen, B. (2019). From trash to treasure: The impact of consumer perception of bio-waste products in closed-loop supply chains. *J. Clean. Prod.* 218, 966-974. https://doi.org/10.1016/j.jclepro.2019.02.044.

Sahoo, J. K., S. K. Paikra, M. Mishra, & H. Sahoo. (2019). Amine functionalized magnetic iron oxide nanoparticles: synthesis, antibacterial activity and rapid removal of Congo Red dye. *J Mol Liq.*, 282 (15):428–40. https://doi.org/10.1021/acsanm.9b01305.

Sales, A., F. R. De Souza, & F. R. Almeida. (2011). Mechanical Properties of Concrete Produced with a Composite of Water Treatment Sludge and Sawdust. *Constr. Build. Mater.*, 25:2793–98. https://doi.org/10.1016/j.conbuildmat.2010.12.057.

S. Ben-Ali, I. Jaouali, S. Souissi-Najar, & A. Ouederni. (2017). Characterization and adsorption capacity of raw pome-granate peel biosorbent for copper removal. *Journal of Cleaner Production*, vol. 142, pp. 3809–3821. https://doi.org/10.1016/j.jclepro.2016.10.081.

S. Y. Wang, Y. K. Tang, C. Chen, J. T. Wu, Z. Huang, Y. Y. Mo, K.X. Zhang, & J. B. Chen, Regeneration of magnetic biochar derived from eucalyptus leaf residue for lead (II) removal. *Bioresour. Technol*., 186 (2015) 360-364. https://doi.org/10.1016/j.biortech.2015.03.139.

Salleh, M.A.M.; Mahmoud, D.K.; Karim, W.A.W.A.; & Idris, A. (2011). Cationic and anionic dye adsorption by agricultural solid wastes: A comprehensive review. *Desalination*, 280, 1–13. https://doi.org/10.1016/J.DESAL.2011.07.019.

Sarioglu, M., & Atay U. A. (2006). Removal of Methylene blue by using biosolid. *Global NEST Journal*, 8(2):113–20. https://doi.org/10.1155/2021/5556940.

Sarkar, A., & Paul, B. (2016). The global menace of arsenic and its conventional remediation - A critical review. *Chemosphere*, 158, 37–49. https://doi.org/10.1016/j.chemosphere.2016.05.043.

Sembiring S, Simanjuntak W, Manurung P, & Asmi D. (2014). Synthesis and characterisation of gel-derived mullite precursors from rice husk silica. *Ceram. Int.*, 40, 7067–674, 72. https://doi.org/10.1016/j.ceramint.2013.12.038.

Shaaban A, Se S-M, Dimin MF, Juoi JM, Husin MH, & Mitan N. (2014). Influence of heating temperature and holding time on biochars derived from rubber wood sawdust via slow pyrolysis. *J Anal Appl Pyrol.*, 107:31–39. https://doi.org/10.1016/j.jaap.2014.01.021.

Shakya, A. K., R. Bhande, & P. K. Ghosh. (2019). A Practical Approach on Reuse of Drinking Water Treatment Plant Residuals for Fluoride Removal. *Environ. Technol.*, 41:2907–19. https://doi.org/10.1080/09593330.2019.1588383.

Sham, A. Y. W., & S. M. Notley. (2018). Adsorption of Organic Dyes from Aqueous Solutions Using Surfactant Exfoliated Grapheme. *Journal of Environmental Chemical Engineering*, 6(1):495–504. https://doi.org/10.1016/j.jece.2017.12.028.

Shang, J.J. (2019). Research on the preparation method of activated carbon from sludge coal ash and activated carbon's adsorption property. *Adhesion*, 40, 61–65. https://doi.org/10.1038/s41545-021-00127-0.

Shen, C., Y. Q. Zhao, W. Li, Y. Yang, R. Liu, & D. Morgen. (2019). Global Profile of Heavy Metals and Semimetals Adsorption Using Drinking Water Treatment Residual. *Chem. Eng. J*, 372:1019–27. https://doi.org/10.1016/j.cej.2019.04.219.

Sierra, I., Iriarte-Velasco, U., Gamero, M., & Aguayo, A. T. (2017). Upgrading of sewage sludge by demineralization and physical activation with CO_2: Application for methylene blue and phenol removal. *Microporous and Mesoporous Materials*, 250, 88–99. https://doi.org/10.1016/j.micromeso.2017.05.020.

Silgado, K. J., Marrugo, G. D. & Puello, J. (2014). Adsorption of Chromium (VI) by Activated Carbon Produced from Oil Palm Endocarp. *Chemical Engineering Transactions*, 37: pp 721-726. https://doi.org/10.3303/CET1437121.

Singh, N. B. (2018). Water Purification by Using Adsorbents: A Review. *Environmental Technology and Innovation*, 11:187–240. https://doi.org/10.1016/J.ETI.2018.05.006.

Singh, Simranjeet; Kumar, Vijay; Dhanjal, Daljeet Singh; Datta, Shivika; Bhatia, Deepika; Dhiman, Jaskaran; Samuel, Jastin; Prasad, Ram; & Singh, Joginder. (2020). A sustainable paradigm of sewage sludge biochar: Valorization, opportunities, challenges and future prospects. *Journal of Cleaner Production*. https://doi.org/10.1016/j.jclepro.2020.122259.

Smith, K.M., Fowler, G.D., Pullket, S., & Graham, N. J. (2009). Sewage sludge-based adsorbents: A review of their production, properties and use in water treatment applications. *Water Res*. 43, 2569-2594. https://doi.org/10.1016/ j.watres.2009.02.038.

Sonal, S., A. Singh, & B. K. Mishra. (2018). Decolorization of Reactive Dye Remazol Brilliant Blue R by Zirconium Oxychloride as a Novel Coagulant: Optimization through Response Surface Methodology. *Water Sci Technol.,* 78(2):379–89. https://doi.org/10.2166/wst.2018.307.

Song X., Xue X.Y., Chen D., He P., & Dai X. Application of biochar from sewage sludge to plant cultivation: Influence of pyrolysis temperature and biochar-to-soil ratio on yield and heavy metal accumulation. *Chemosphere,* 109 (2014), pp. 213-220. https://doi.org/10.1016/j.chemosphere.2014.01.070.

Srinivasan, P., Sarmah, A.K., Smernik, R., Das, O., Farid, M., & Gao, W. (2015). A feasibility study of agricultural and sewage biomass as biochar, bioenergy and biocomposite feedstock: production, characterization and potential applications. *Sci. Total Environ*., 512 (513), 495–505. https://doi.org/10.1016/j.scitotenv.2015.01.068.

Stella Mary, G., Sugumaran, P., Niveditha, S., Ramalakshmi, B., Ravichandran, P., & Seshadri, S. (2016). Production, characterization and evaluation of biochar from pod (Pisum sativum), leaf (Brassica oleracea) and peel (Citrus sinensis) wastes. *Int. J. Recycl. Org. Waste Agric*., 5, 43–53. https://doi.org/10.1007/s40093-016-0116-8.

Subramaniam, R., & S. K. Ponnusamy. (2015). Novel Adsorbent from Agricultural Waste (Cashew NUT Shell) for Methylene Blue Dye Removal: Optimization by Response Surface Methodology. *Water Resources and Industry,* 11:64–70. https://doi.org/10.1016/j.wri.2015.07.002.

Tag AT, Duman G, Ucar S, & Yanik J. (2016). Effects of feedstock type and pyrolysis temperature on potential applications of biochar. *J Anal Appl Pyrol.,* 120:200–206. https://doi.org/10.1016/j.jaap.2016.05.006.

Tan, Xiaofei; Liu, Yunguo; Zeng, Guangming; Wang, Xin; Hu, Xinjiang; Gu, Yanling; & Yang, Zhongzhu. (2015). Application of biochar for the removal of pollutants from aqueous solutions. *Chemosphere,* volume 125. https://doi.org/10.1016/j.chemosphere.2014.12.058.

Tang, L., J. F. Yu, Y. P. Pang, G. M. Zeng, Y. C. Deng, J. J. Wang, X. Y. Ren, S. J. Ye, B. Peng, & H. P. Feng. (2018). Sustainable efficient adsorbent: Alkali-acid modified magnetic biochar derived from sewage sludge for aqueous organic contaminant removal. *Chemical Engineering Journal,* 336:160–69. https://doi.org/10.1016/j.cej.2017.11.048.

Tang, Y., Alam, M.S., Konhauser, K.O., Alessi, D.S., Xu, S., Tian, W.J., & Liu, Y. (2019). Influence of pyrolysis temperature on production of digested sludge biochar and its application for ammonium removal from municipal wastewater. *J. Clean. Prod*., 209, 927–936. https://doi.org/10.1016/j.jclepro.2018.10.268.

Tatarchuk, T., N. Paliychuk, R. B. Bitra, A. Shyichuk, M. Naushad, I. Mironyuk, & D. Ziolkowska. (2019). Adsorptive Removal of Toxic Methylene Blue and Acid Orange 7 Dyes from Aqueous Medium Using Cobalt-Zinc Ferrite Nano adsorbents. *Desalin Water Treat.,* 150:374–85. https://doi.org/10.5004/DWT.2019.23751.

Thangarajan, R., Bolan, N., Mandal, S., Kunhikrishnan, A., Choppala, G., Karunanithi, R., & Qi, F. (2016). Biochar for Inorganic Contaminant Management in Soil: Production, Characterization and Applications. *CRC Press Taylor and Francis Group, Boca Raton*. https://doi.org/10.1051/e3sconf/20183402049.

Trinh, T.N., Jensen, P.A., Kim, D.J., Knudsen, N.O., & Sorensen, H.R. (2013). Influence of the pyrolysis temperature on sewage sludge product distribution, bio-oil, and char properties. *Energy Fuels*, 27, 1419-1427. https://doi.org/10.1021/ef301944r.

Tripathi, M., Sahu, J.N., & Ganesan, P. (2016). Effect of process parameters on production of biochar from biomass waste through pyrolysis: A review. *Renew. Sustain. Energy Rev.* 55, 467–481. https://doi.org/10.1016/j.rser.2015.10.122.

Tronsmo, A., T. Gjoen, H. Sørum, J. Godfroid, S. P. Yazdankhah, A. Jelmert, & I. Skaar. (2016). Antimicrobial Resistance Due to the Use of Biocides and Heavy Metals: A Literature Review. https://doi.org/10.1080/16512235.2018.1548248.

V. Kumar, A. K. Chopra, & A. Kumar. (2017). A review on sewage sludge (Biosolids) a resource for sustainable agriculture. *Archives of Agriculture and Environmental Science*, vol. 2, no. 4, pp. 340–347. https://doi.org/10.26832/24566632.2017.020417.

V.S. Chittoo, & C. Sutherland. (2014). Adsorption of phosphorus using water treatment sludges (alum, lime, lime-iron). *Pdf, J. Appl. Sci*. https://doi.org/10.3923/jas.2014.3455.3463.

Wakkel, M., Khiari, B., & Zagrouba, F. (2019). Textile wastewater treatment by agro-industrial waste: equilibrium modelling, thermodynamics and mass transfer mechanisms of cationic dyes adsorption onto low-cost lignocellulosic adsorbent. *Journal of the Taiwan Institute of Chemical Engineers, 96*, 439-452. https://doi.org/10.1016/j.jtice.2018.12.014.

Wang J, & Wang S. (2019). Preparation, modification and environmental application of biochar: A review. *J Clean Prod*, 227:1002–1022. https://doi.org/10.1016/j.jclep.

Wang, S., Guo, W., Gao, F., & Yang, R. (2017). Characterization and Pb(II) removal potential of corn straw- and municipal sludge-derived biochars. *R. Soc. Open Sci*., https://doi.org/10.1098/rsos.170402, 170402.

Wang, X., Chang, V. W. C., Li, Z., Chen, Z., & Wang, Y. (2021). Co-pyrolysis of sewage sludge and organic fractions of municipal solid waste: Synergistic effects on biochar properties and the environmental risk of heavy metals. *Journal of Hazardous Materials*, 412, 125200. https://doi.org/10.1016/j.jhazmat.2021.125200.

Wang, X., & Jia, J. (2012). Effect of heating rate on the municipal sewage sludge pyrolysis character. *Energy Procedia. Elsevier*. https://doi.org/10.1016/j.egypro.2011.12.11460.

Wang X., Li C., Li Z., Yu G., & Wang Y. (2019). Effect of pyrolysis temperature on characteristics, chemical speciation and risk evaluation of heavy metals in biochar derived from textile dyeing sludge. *Ecotoxicol. Environ. Saf*., 168. https://doi.org/10.1016/j.ecoenv.2018.10.022.

Wei, J., Liu, Y., Li, J., Yu, H., & Peng, Y. (2018). Removal of organic contaminant by municipal sewage sludge-derived hydrochar: kinetics, thermodynamics and mechanisms. *Water Sci. Technol*., 78, 947-956. https://doi.org/10.2166/wst.2018.373.

Werle, S., & M. Dudziak. (2014). Analysis of Organic and Inorganic Contaminants in Dried Sewage Sludge and Byproducts of Dried Sewage Sludge Gasification. *Energies,* 7:462–76. https://doi.org/10.0.1201/b19983-9.

Wolowiec, M., A. Pruss, M. Komorowska-Kaufman, I. Lasocka-Gomuła, G. Rzepa, & T. Bajda. (2019). The Properties of Sludge Formed as a Result of Coagulation of Backwash Water from Filters Removing Iron and Manganese from Groundwater. *SN Appl. Sci.,* 1:639. https://doi.org/10.1007/s42452-019-0653-7.

Wu, D. Q., P. Y. Ma, & S. Hu. (2018). Preparation of activated carbon from sludge and sawdust with $ZnCl_2$ as activator. *The Chinese Journal of Process Engineering*, 18 (4):792–98. https://doi.org/10.1007/s10450-010-9214-5.

Xu, D., L. Y. Lee, F. Y. Lim, Z. Lyu, H. Zhu, S. L. Ong, & Hu, J. (2020). Water Treatment Residual: A Critical Review of Its Applications on Pollutant Removal from Stormwater Runoff and Future Perspectives. *J. Environ. Manag.*, 259:109649. https://doi.org/10.1016/j.jenvman.2019.109649.

Xu, G., Yang, X., & Spinosa, L. (2015). Development of sludge-based adsorbents: preparation, characterization, utilization and its feasibility assessment. *J. Environ. Manag*., 151, 221-232. https://doi.org/10.1016/j.jenvman.2014.08.001.

Xu, G., Zhang, Z., & Deng, L. (2018). Adsorption behaviors and removal efficiencies of inorganic, polymeric and organic phosphates from aqueous solution on biochar derived from sewage sludge of chemically enhanced primary treatment process. *Water 10,* 869. https://doi.org/10.3390/w10070869.

Y. Yao, B. Gao, M. Inyang, A.R. Zimmerman, X. Cao, P., & L. Yang. (2011). Removal of phosphate from aqueous solution by biochar derived from anaerobically digested sugar beet tailings. *J. Hazard. Mater*., 190, 501–507. https://doi.org/10.1016/j.jhazmat.2011.03.083.

Yan, F., Y. Chu, & K. Zhang. (2015). Determination of Adsorption Isotherm Parameters with Correlated Errors by Measurement Error Models. *Chem Eng J,* 281:921–30. https://doi.org/10.1016/j.cej.2015.07.021.

Yang, G., Y. Hu, & J. Wang. (2019). Biohydrogen production from co-fermentation of fallen leaves and sewage sludge. *Bioresource Technology,* 285:121342. https://doi.org/10.1016/j.biortech.2019.121342.

Yang, Y., Tomlinson, D., Kennedy, S., & Zhao. Y.Q. (2006). Dewatered alum sludge: A potential adsorbent for phosphorus removal. *Water Sci. Technol*., 54, 207–213. https://doi.org/10.2166/wst.2006.564.

Yang, Y., Y. Zhao, R. Liu, & D. Morgan. (2018). Global Development of Various Emerged Substrates Utilized in Constructed Wetlands. *Bioresour. Technol.,* 261:441-452. https://doi.org/10.1016/j.biortech.2018.03.085.

Yang, Y. Zhao, Y.Q., & Kearney P. (2008). Influence of ageing on the structure and phosphate adsorption capacity of dewatered alum sludge. *Chem. Eng. J*., 145, 276–284. http://dx.doi.org/10.1016/j.cej.2008.04.026.

Yi Deng , Qing Huang , Weihua Gu & Shuyuan Li. (2020). Application of sludge based biochar generated by pyrolysis: A mini review, Energy Sources, Part A: Recovery, Utilization and Environmental Effects. *Journal of Environmental Chemical Engineering*, *2*(3), 1467-1473. https://doi.org/10.1080/15567036.2020.1826602.

Yin, R., Guo, W., Wang, H., Du, J., Wu, Q., Chang, J.S., & Ren, N. (2019). Singlet oxygen-dominated peroxydisulfate activation by sludge-derived biochar for sulfamethoxazole degradation through a nonradical oxidation pathway: performance and mechanism. *Chem. Eng. J.*, 357, 589–599. https://doi.org/10.1016/j.cej.2018.09.184.

Yusuff, S. M., Ong, K. K., Yunus, W. M. Z. W., Fitrianto, A., & Ahmad, M. B. (2018). Removal of methylene blue from aqueous solutions using alum Sludge: Sorption optimization by response surface methodology. *Journal of Fundamental and Applied Sciences, 9*(3S), 532. https://doi.org/10.4314/jfas.v9i3s.4.

Zaghbani, N., A. Hafiane, & M. Dhahbi. (2007). Separation of Methylene Blue from Aqueous Solution by Micellar Enhanced Ultrafiltration. *Separation and Purification Technology*, 55(1):117–24. https://doi:10.1016/j.seppur.2006.11.008.

Zaker, A., Z. Chen, X. L. Wang, & Q. Zhang. (2019). Microwave-assisted pyrolysis of sewage sludge: A review. *Fuel Processing Technology,* 187:84–104. https://doi:10.1016/j.fuproc.2018.12.011.

Zeng, H., Qi, W., Zhai, L., Wang, F., Zhang, J., & Li, D. (2021). Magnetic biochar synthesized with waterworks sludge and sewage sludge and its potential for methylene blue removal. *Journal of Environmental Chemical Engineering*, *9*(5), 105951. https://doi.org/10.1016/j.jece.2021.105951.

Zielinska, A., & Oleszczuk, P. (2015). The conversion of sewage sludge into biochar reduces polycyclic aromatic hydrocarbon content and ecotoxicity but increases trace metal content. *Biomass Bioenerg,* 75, 235–244. https://doi.org/10.1016/j. biombioe.2015.02.019.

Zhai, Y., Chen, H., Xu, B.B., Xiang, B., Chen, Z., Li, C., & Zeng, G. (2014). Influence of sewage sludge-based activated carbon and temperature on the liquefaction of sewage sludge: yield and composition of bio-oil, immobilization and risk assessment of heavy metals. *Bioresour. Technol*., 159, 72-79. https://doi.org/10.1016/j.biortech.2014.02.049.

Zhang, J. (2013). Nitrogen conversion and control of nitrogen-containing compounds during microwave pyrolysis of sewage sludge. *China, Harbin, Harbin Institute of Technology*. https://doi.org/10.1021/es304248j.

Zhang, J. H., Lin, Q. M., & Zhao, X. R. (2014). The hydrochar characters of municipal sewage sludge under different hydrothermal temperatures and durations. *Journal of Integrative Agriculture*, 13(3), 471-482. https://doi.org/10.1016/S2095-3119(13)60702-9.

Zhang, J., Shao, J., Jin, Q., Li, Z., Zhang, X., Chen, Y., Zhang, S., & Chen, H. (2019). Sludge-based biochar activation to enhance Pb(II) adsorption. *Fuel*, 252, 101–108. https:// doi.org/10.1016/j.fuel.2019.04.096.

Zhao S-X, Na T, & Wang X D. (2017). Effect of temperature on the structural and physico-chemical properties of biochar with apple tree branches as feedstock material. *Energies*, 10:1293. https://doi.org/10.3390/en10091293.

Zhao, X. H., H. L. Luo, T. Tao, & Y. Q. Zhao. (2015). Immobilization of Arsenic in Aqueous Solution by Waterworks Alum Sludge Prospects in China. *Int. J. Environ. Stud.*, 72:989–1001. https://doi.org/10.1080/00207233.2015.1071522.

Zhao, Y., Feng, D., Zhang, Y., Huang, Y., & Sun, S. (2016). Effect of pyrolysis temperature on char structure and chemical speciation of alkali and alkaline earth metallic species in biochar. *Fuel Processing Technology*, 141, 54-60. https://doi.org/10.1016/j.fuproc.2015.06.029.

Zhao, Y., R. Liu, O. W. Awe, Y. Yang, & C. Shen. (2018). Acceptability of Land Application of Alum Based Water Treatment Residuals – An Explicit and Comprehensive Review. *Chemical Engineering Journal*, 353:717–26. https://doi: 10.1016/j.cej.2018.07.143.

Zheng H., Wang Z., Deng X., Zhao J., & Xing B. (2012). Characteristics and nutrient values of biochars produced from giant reed at different temperatures. *Bioresour. Technol*., 130, pp. 463-471. https://doi.org/10.1016/j.biortech.2012.12.044.

Zhou, D., Liu, D., Gao, F., Li, M., & Luo, X. (2017). Effects of biochar-derived sewage sludge on heavy metal adsorption and immobilization in soils. *Int. J. Environ. Res. Publ. Health*. https://doi.org/10.3390/ijerph14070681.

Zhu, X. F., L. Zhao, F. Y. Fu, Z. B. Yang, W. Y. Yuan, M. Y. Zhou, W. Fang, G. Y. Zhen, X. Q. Lu, & X. D. Zhang. (2019). Pyrolysis of pre-dried dewatered sewage sludge under different heating rates: Characteristics and kinetics study. *Fuel*, 255:115591. https://doi:10.1016/j.fuel.2019.05.174.

Appendix

Appendix 1. Pre-test for Selection of the Best SSBC-AlS Composite Adsorbent

Pre-test was performed for the selection of the best SSBC and AlS proportion to prepare SSBC-AlS composite adsorbent from the precursor materials. Five different SSBC and AlS proportions (100:0, 75:25, 50:50, 25:75, 0:100, respectively) were synthesized and MB removal efficiency of them from synthetic MB wastewater (aqueous MB solution) was evaluated using adsorbent dose of 0.5 g/100 ml, initial MB concentration of 100 mg/L, contact time of 60 minutes, shaking speed of 100 rpm and pH of 7. The Pre-test result is shown below.

A. Pre-test results

Proportion (SSBC:AlS)	% Removal
100:0	52.46 %
75:25	99.86 %
50:50	98.33 %
25:75	98.06 %
0:100	98.03 %

Appendix 2. Result for BET Analysis

A. BET result for SSBC-AlS adsorbent characterization.

Horiba Instruments, Inc.
SA-9600 Series Surface Area Analyzer

Analysis Report
Jun/09/2022

Customer	: Tsedeniya	Operator ID	: SARA
Description	: Different Experiment	Analysis Date	: Jun/09/2022
Filename	: TSE.sa2	Analysis Time	: 13:23:13

Condition Settings

Room Temp	: 28.0 (°C)	Atm. Pres	: 700.0 (mm)
Gas Used	: Nitrogen	Gas Conc	: 0.100, 0.000, 0.000 %

	Channel: 1	Channel: 2	Channel: 3
Sample Name	AlS SSBC		
Tube Number	1	0	0
Tare Weight	10.1100 (gm)	0.0000 (gm)	0.0000 (gm)
Sample Weight	10.1670 (gm)	1.0000 (gm)	1.0000 (gm)
Degas Temp.	150 (°C)	0 (°C)	0 (°C)
Degas Time	60 (min)	0 (min)	0 (min)
Surface Area (M²/gm)	55.977	-1.#IO	-1.#IO
Slope	1079.611	-1.#IO	-1.#IO
Intercept	11.051	-1.#IO	-1.#IO
Vm	0.001	-1.#IO	-1.#IO
BET Const	98.696	-1.#IO	-1.#IO
Pearson Coef	0.999	0.000	0.000
X[1] - 0.090	107.231	1.#IO	1.#IO
X[2] - 0.045	61.382	1.#IO	1.#IO
X[3] - 0.018	29.249	1.#IO	1.#IO